TALLINN UNIVERSITY OF TECHNOLOGY
DOCTORAL THESIS
43/2018

Experimental Analysis of Combustion Characteristics of Estonian Oil Shale in Regular and Oxy-Fuel Atmospheres

LAURI LOO

TTÜ PRESS

TALLINN UNIVERSITY OF TECHNOLOGY
School of Engineering
Department of Energy Technology

This dissertation was accepted for the defence of the degree of Doctor of Philosophy in Engineering 03/07/2018

Supervisor:	Professor Alar Konist School of Engineering Tallinn University of Technology Tallinn, Estonia
Co-supervisor:	Professor Andres Siirde School of Engineering Tallinn University of Technology Tallinn, Estonia
Opponents:	Professor Ben Anthony Centre for Power Engineering Cranfield University Ants Martins, PhD

Defence of the thesis: 22/08/2018, Tallinn

Declaration:
Hereby I declare that this doctoral thesis, my original investigation and achievement, submitted for the doctoral degree at Tallinn University of Technology, has not been previously submitted for doctoral or equivalent academic degree.

Lauri Loo

----
signature

European Union
European Social Fund

Investing in your future

ISSN 2585-6898 (publication)
ISBN 978-9949-83-300-9 (publication)
ISSN 2585-6901 (PDF)
ISBN 978-9949-83-301-6 (PDF)

TALLINNA TEHNIKAÜLIKOOL
DOKTORITÖÖ
43/2018

Eesti põlevkivi põlemiskarakteristikute eksperimentaalne analüüs tavalises ja oxy-fuel keskkonnas

LAURI LOO

TTÜ
KIRJASTUS

Contents

List of Publications

I Alar Konist, **Lauri Loo**, Aleksandr Valtsev, Birgit Maaten, Andres Siirde, Dmitri Neshumayev, and Tõnu Pihu. 'Calculation of the Amount of Estonian Oil Shale Products from Combustion in Regular and Oxy-Fuel Mode in a CFB Boiler'. Oil Shale 31, no. 3 (July 2014): 211–224. doi:10.3176/oil.2014.3.02.

II **Lauri Loo**, Birgit Maaten, Andres Siirde, Tõnu Pihu, and Alar Konist. 'Experimental Analysis of the Combustion Characteristics of Estonian Oil Shale in Air and Oxy-Fuel Atmospheres'. Fuel Processing Technology 134 (June 2015): 317–324. doi:10.1016/j.fuproc.2014.12.051.

III Alar Konist, Aleksandr Valtsev, **Lauri Loo**, Tõnu Pihu, Martin Liira, and Kalle Kirsimäe. 'Influence of Oxy-Fuel Combustion of Ca-Rich Oil Shale Fuel on Carbonate Stability and Ash Composition'. Fuel 139 (January 1, 2015): 671–677. doi:10.1016/j.fuel.2014.09.050.

IV **Lauri Loo**, Alar Konist, Dmitri Neshumayev, Tõnu Pihu, Birgit Maaten, Andres Siirde. 'Ash and Flue Gas from Oil Shale Oxy-Fuel Circulating Fluidized Bed Combustion'. Energies 11, no. 5 (May 10, 2018): 1218. https://doi.org/10.3390/en11051218.

V **Lauri Loo**, Birgit Maaten, Alar Konist, Andres Siirde, Dmitri Neshumayev, Tõnu Pihu. 'Carbon Dioxide Emission Factors for Oxy-fuel CFBC and Aqueous Carbonation of the Ca-rich Oil Shale Ash'. Energy Procedia 128 (International Scientific Conference 'Environmental and Climate Technologies', CONECT 2017, 10–12 May 2017, Riga, Latvia): 144–149. doi:10.1016/j.egypro.2017.09.034.

Author’s Contribution to the Publications

The author’s contributions to the publications in this thesis are as follows:

I The author contributed in the development of the calculation model and in the interpretation of results.

II The author was the first and corresponding author. Moreover, the author designed the experiments, interpreted the results, and had the leading role in writing the paper.

III The author designed and performed the experiments and contributed to the interpretation of results.

IV The author was the first and corresponding author and was a member of the experiment design and implementation team. The author also interpreted the results and had the leading role in writing the paper.

V The author was the first and corresponding author and was a member of the experiment design and implementation team. The author also interpreted the results and had the leading role in writing the paper.

Introduction

The increasing global population and improving living standards result in a growing demand for energy. The main energy source during the last century has been fossil fuels. This results in large emissions of carbon dioxide (CO_2), which is believed to be the main cause of climate change and global warming. Decreasing the CO_2 emission has been set on high priority internationally. There are various methods of decreasing the CO_2 emission (Figure 1). According to International Energy Agency predictions of primary energy supply for the next century, a combination of different CO_2 emission reduction methods could be used to limit the global warming to 2 °C by 2050. Increase in efficiency, renewables, and carbon capture and storage (CCS) are highlighted as solutions with the highest impact.

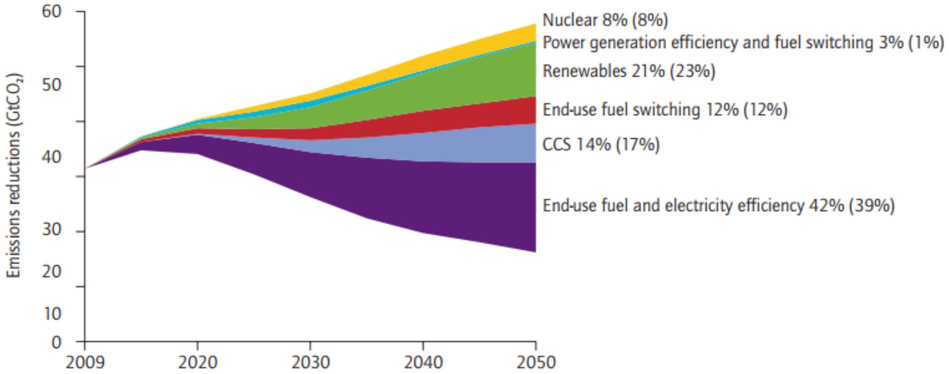

Figure 1. CCS contributes 14% of total emission reduction through 2050 in decreasing global warming pace to 2 °C compared to predicted 6 °C (business as usual scenario) [1].

CCS refers to a number of technologies that capture CO_2 at some stage from processes such as combustion or gasification. There are various CCS solutions proposed. CO_2 could be removed before or after combustion, but the most energy- and cost-effective CCS technology considered is the oxy-fuel technology [2]. The concept of oxy-fuel technology involves removing nitrogen (N_2) from the combustion process: combustion will occur in oxygen (O_2) and recycled flue gas. As a result, the formed flue gas mainly consists of CO_2 and water vapour. Oxy-fuel technology avoids the costly CO_2 separation from N_2; however, it entails additional expenditure on O_2 production. It is possible to retrofit existing combustors to oxy-fuel combustors, which avoids the cost of redesigning and building new facilities and allows faster transition to zero carbon emissions.

Estonia is a part of the European Union and all global trends, including the encountered challenges, are also valid here. The main energy provider and as well the largest CO_2 emitter in Estonia has been the oil shale industry [3]. In the light of climate change and decline of old equipment, new solutions for energy supply are required. It is even more alarming that not only Estonia, but also the entire Baltic Sea region is facing energy deficit: the old power units have been exhausted and new investments are not made due to uncertainties in regulatory policies [4], [5]. Despite concentrated research on different renewable solutions, none is ready to cover the base load of a developed cold and plain country. Appling CCS technology on oil shale combustion would enable a CO_2 emission-free power production.

The main difference of oxy-fuel combustion from regular firing is that the combustion occurs in a CO_2-based environment instead of N_2. This affects combustion of organic matter and reactions of mineral matter [6]. The pollutant content in flue gas may increase and cause difficulties in further processing the CO_2. The changes in properties of produced ash, particularly because Estonian oil shale has high content of mineral matter, may ease the use of waste. The most altered processes may require different designs of equipment to reach a complete burnout of fuel. To estimate the listed changes, theoretical calculations and a number of experiments were conducted, beginning from thermogravimetric analysis (TGA) using a few milligrams of sample per experiment, up to circulating fluidised bed combustion (CFBC) experiments firing 24 kg fuel per hour.

The ultimate goal of this research was to acquire base knowledge for oil shale oxy-fuel CFBC, i.e. to find and examine possible technological bottlenecks caused by peculiarities of Estonian oil shale. The objective set for this work was to investigate possible changes in Estonian oil shale CFBC in oxy-fuel mode compared to conventional CFB firing. To be more precise, this work aimed to analyse the following:

- combustion process of a particle,
- mineral matter behaviour,
- produced flue gas pollutant content, and
- CO_2 formation and emission.

In order to achieve the above goals, extensive experimental work was conducted on a thermogravimetric analyser, a batch reactor, and a CFB combustor.

This dissertation is based on five papers and consists of four chapters. Chapter 1 includes a literature overview of CCS and oxy-fuel combustion research as well as hypothesis applicable for Estonian oil shale utilisation. Chapter 2 describes the materials and details of experiments including devices, applied conditions, boundaries, and simplifications. Chapter 3 summarises the results of experiments and highlights the most important ones: at first, predictions from a theoretical study [Paper I]; then a research of reactions in mineral matter and combustion products [Paper II-III]; an investigation of ash properties, i.e. experimental work on a batch reactor [Paper III]; and combustion experiments on a circulating fluidised bed (CFB) combustor—acquiring data about real combustion, ash formation, and potential emissions [Paper IV–V]. Chapter 4 concludes the results of this research. The papers presented offered new information about oil shale oxy-fuel combustion, and for the first time, the results of oil shale oxy-fuel CFBC products.

Further studies concerning oxy-fuel combustion of oil shale should explore the possibilities of increasing O_2 content in combustion gas. This may decrease the measurements in the combustor and therefore lead to smaller capital cost. Oil shale ash and oxy-fuel environment influence sediment formation on heating surfaces and corrosion. Another interesting topic is oil shale and biomass co-firing in oxy-fuel CFB. This solution can lead to negative CO_2 net emissions, because CO_2 from biomass is considered neutral.

Abbreviations

A	Ash content
ar	As-received basis
CCS	Carbon capture and storage
CFB	Circulating fluidised bed
CFBC	Circulating fluidised bed combustion
CO_2	Carbon dioxide
D	Dry basis
DSC	Differential scanning calorimetry
ELPI+	Electrical low-pressure impactor
FC	Fixed carbon
LHV	Lower heating value
m/z	Mass-to-charge ratio
N_2	Nitrogen
NO_x	Nitric oxide and nitrogen dioxide as nitrogen dioxide
O_2	Oxygen
PC	Pulverised combustion
QMS	Quadrupole mass spectrometry
RFG	Recycled flue gas
SO_x	Sulfur oxides as sulfur dioxide
TGA	Thermogravimetric analysis
W	Moisture content
XRD	X-ray diffraction
XRF	X-ray fluorescence spectrometer

1 LITERATURE REVIEW

1.1 CO_2 emissions

The world primary energy supply relies on three fossil fuels: oil, coal, and natural gas [7]. During the period from 1990 to 2015, the world's primary energy supply increased by 60%. Renewable energy sources comprised a considerable part of the total supply, but replacing them with fossil fuels requires more time and breakthrough in technology.

To meet future targets for the reduction of greenhouse gas emissions, a number of simultaneous actions are necessary. Arrangements for reducing greenhouse gas emissions often reduce co-emitted air pollutants, bringing benefits to air quality and human health. Improvements in air quality and health benefits, especially as they are mainly local and near-term, provide strong additional motivation for transitioning to a low-carbon future [8]. To attain the set objective, fuel and energy efficiency has to be increased and new renewable energy sources must be applied. Wind and solar energy are periodic and need energy storage solutions to maintain constant power. Fossil fuel power stations are able to vary their output in response to changes in demand, and thus, CCS reduces the need for large-scale energy storage that are still to be developed [1], [9]. CCS is a way of reducing CO_2 emissions from existing sources and coping with changing power demand.

According to the International Energy Agency [10], global CO_2 emissions reached 32.3 Gt_{CO2} in 2015, which is 0.1% less than that in 2014. The decrease was achieved by changes in fuel mix. In the USA and EU, the share of coal in energy mixture decreased: it was replaced by natural gas. Over 40% of the global anthropogenic CO_2 emissions were caused by power and heat generation. Most of the world's electricity is produced in pulverised coal combustion plants [11]. Coal combustion was responsible for approximately 45% of CO_2 emissions, with 31% emitted from coal-fired power plants [7]. Coal will remain a major energy resource for the next few decades, especially in China and India.

For pulverised combustion (PC), the solid fuel is ground below 70 µm and fired in the furnace at temperatures of 1300–1400 °C. Such high temperatures promote formation of nitrogen oxides (NO_x), and due to ash slagging and fouling, deposits form on heat exchangers; hence, active methods are required to maintain heat transmission. For pollution control, sulfur oxide (SO_x), NO_x, and particulate matter removal equipment is required. When firing solid fuel in a CFB boiler, the fuel has to be ground to 3–6 mm. Circulating solid matter allows reaching burnout at considerably lower temperatures (760 to 930 °C) [12]. The lower temperatures and circulating solid matter result in decreased pollutant generation, and thus, the investments into pollutant control equipment are smaller. Regardless of the combustion technology, CO_2 emissions will continue to be a major environmental concern.

1.2 Solid fuel combustion in Estonia

Power in Estonia is mainly produced from oil shale [3], [13]. Combustion of Estonian oil shale is challenging [14], [15]. The combustion technologies applied for Estonian oil shale have been following the development of solid fuel combustion systems. Oil shale firing in Estonia started with grate firing in the 1920s, when grate firing was the only known industrial combustion technology. Large-scale industrial firing of Estonian oil shale in PC boilers started in 1959. An advantage of PC is higher heat flux (MW/m^2), which leads to reduced dimensions and higher efficiency [16]. The first oil shale power plants with high steam parameters were utilising PC technology. The power plants had consistent problems with deposits formation. The calcium-rich ash melts at relatively low temperatures and forms bound sediments on heating surfaces. High alkali and chlorine content of oil shale ash caused significant corrosion and fouling problems in the PC units [17]. SO_2 and particulate matter emission were high (2100 mg/Nm^3 @ 6% O_2) [18]. The high ash content of the fuel (over 50%) is an environmental and technical challenge [19], [20]. Even today, most of the alkali ash is still landfilled, but on the positive side, the ash at the landfills sequestrates up to 10% of previously emitted CO_2 from the atmosphere [21], [22].

The introduction of CFB boilers for oil shale combustion has resolved many of the oil shale firing problems. No significant fouling or corrosion of convective heat exchangers has occurred during the more than ten-year exploitation period. Due to the inherent lime content of oil shale and suitable temperature in the CFB furnace, SO_2 emission was reduced considerably (the concentration was nearly zero) [23], [24]. Moreover, because of the relatively low furnace temperatures and low N_2 content in Estonian oil shale, no deNOx facilities are required. The improved efficiency, decreased carbonate decomposition, and improved steam turbines in CFB power units have decreased the specific CO_2 emission of power production by nearly 24% [23].

For power production from Estonian oil shale, two different combustion technologies are still in use: PC and the newer CFBC. In addition, a new 300 MW$_{el}$ CFB unit is under commissioning. The new boiler will be fuel flexible by design: it will be capable of burning 10% of oil shale retort gas, 50% of biomass, and 20% of peat in oil shale blend [25]. In addition, there are areas reserved for future installation of CCS solution for the new power plant.

1.3 Carbon capture and storage

CCS involves three main steps [6], [26]–[28]: CO_2 capture; compression and transport by pipeline or tankers; and storage or utilisation. Capture is possible either before combustion or after combustion using different processes (see Figure 2).

Pre-combustion capture from coal and gas and CO_2 separation by physical absorption are options that could be applied to integrated coal gasification combined cycle and natural gas combined cycle plants.

Post-combustion capture options include CO_2 chemical absorption from flue gas and oxy-fuel combustion. The issues concerning oxy-fuel combustion will be discussed later. Other separation methods such as using membranes are being considered as a potential longer-term option for both pre-/post-combustion capture, alone or in combination with other absorption techniques.

After capture or separation, CO_2 must be compressed and transported by pipeline or tankers. CO_2 storage, or sequestration, can be accomplished through geologic storage, ocean storage, industrial use, or mineral sequestration [29]. The options for storage and utilisation of CO_2 will be introduced later. Several CCS technologies are likely to co-exist in the future, but all the options require further research and development to improve efficiency and reduce cost.

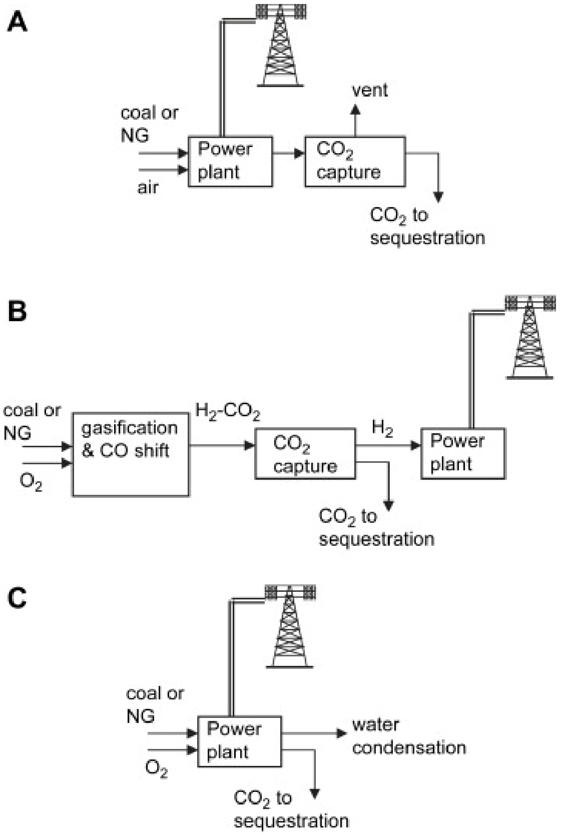

Figure 2. Fossil decarbonisation strategies: (A) post-combustion, (B) pre-combustion, and (C) oxy-fuel combustion decarbonisation [28].

1.4 Oxy-fuel combustion

Designs of oxy-fuel CO_2 recovery power plants for pulverised coal were already proposed by a number of authors in the 80s [30], [31]. It was found that the process is more economical than other CO_2 recovery techniques [32]. The recovered CO_2 can be sequestered into deep ocean [33] or underground [34], [35]. More feasible options would be using the CO_2 for enhanced oil recovery [36] or utilising for other solutions explained briefly in section 1.5 on page 17.

Extensive overviews of oxy-fuel combustion and oxy-fuel CFBC development and status are available [6], [26], [27], [37], [38]. The concept of oxy-fuel technology involves the removal of N_2 from the combustion process. Air is replaced with a mixture of O_2 and recycled flue gas. The O_2 is supplied by a cryogenic air separation process, which is the only commercially available mature technology. The general flowsheet of the oxy-fuel technology power generation is shown in Figure 3. O_2 is produced in an air separation unit (ASU). The combustion occurs in a boiler where O_2 and recycled flue gas are used for combustion. The flue gas is cleaned and part of it is recycled into the boiler. As a result, the formed flue gas mainly consists of CO_2 and water vapour, and the volume of flue gas decreases considerably. This makes it easier to compress and transport CO_2 to the storage or utilisation site [39], [40].

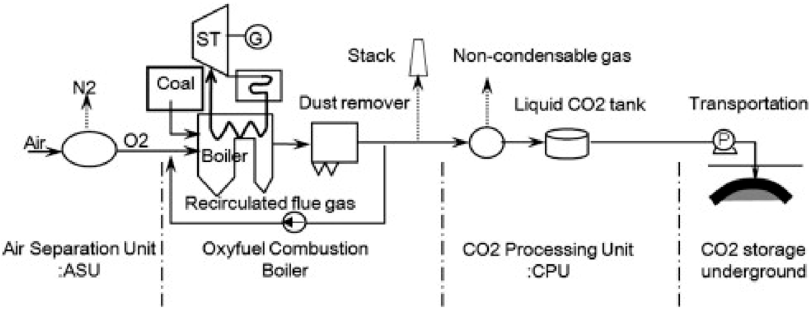

Figure 3. Schematics of entire oxy-fuel combustion power plant for carbon capture and storage [41].

Because the CFBC technology is relatively young and the majority of world power plants are using PC, most of research projects in oxy-fuel combustion are associated with pulverised coal combustion [6], [27]. Fluidised bed or CFB combustion could be an alternate technology to PC, when employing oxy-fuel technology. The synergy of the technologies allows controlling combustion temperatures despite relatively low flue gas recycle ratios. Fans and blowers consume less power because the draft system handles higher molecular weight gas. O_2 concentration in the recycled flue gas can be kept to a low and safe level, while additional O_2 can be introduced through O_2 nozzles separate from the burner or in the secondary gas inserting points. Transition from air to oxy-fuel combustion is potentially easier relative to oxy-fuel PC, because in a CFB, there is a large amount of inert bed material that helps to control the bed temperature [38].

Although functioning oxy-fuel CFB pilot plant units are still limited in number (see Figure 4), studies are being undertaken in many countries. To date, most test works have been performed at small scale (in < 100 kW range), and/or using bottled gases to supply the suitable combustion gas, instead of recycling flue gas, to achieve the necessary gas velocity and solid circulation rate in terms of heat transfer requirement [9].

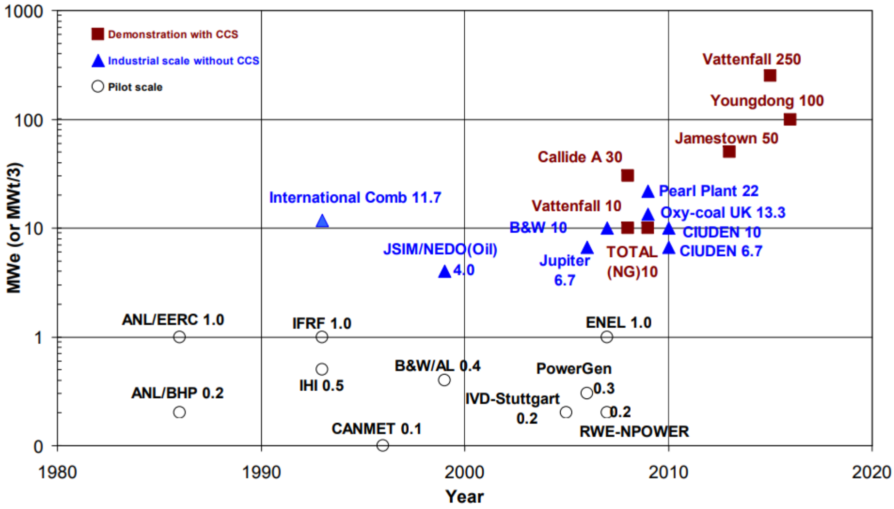

Figure 4. Historical progression of scale of oxy-fuel CFB pilot and demonstration plants [6].

1.4.1 Changes in combustion

The main causes of differences between conventional air and oxy-fuel combustion are the different physical properties of CO_2 and N_2: thermal conductivity, density, specific heat capacity, gas emissivity, and O_2 diffusivity. The solid fuel in combustion is usually investigated at first in small scale (TGA and different batch reactors) and then in laboratory scale combustors (10–200 kW_{th}). The results from laboratory experiments allows moving on with the industrial design. Oxy-fuel combustion experiments with coal have proved that the oxy-fuel atmosphere considerably changes the combustion process [42]–[47]. Compared to combustion in air, the particle burnout is reached later and ignition is delayed in oxy-fuel mode. Increasing the O_2 content decreases the difference. Niu et al. [42] suggested higher O_2 concentration to reach burnout in sufficient time. O_2 enrichment elevates temperatures and improves combustion efficiency [48], but experiments of Czakiert et al. [49] at elevated O_2 partial pressure (35%) resulted in increased pollutant formation. The N_2 and sulfur conversion ratios to oxides increased due to the considerably elevated temperature in the furnace. Generally, it is considered that the optimum flue gas recycle ratio is 0.7. This results in an oxidant environment that typically contains 25 to 30% O_2 and leads to similar heat transfer characteristics to those of air [9]. This allows obtaining ignition properties and combustor temperatures that are similar to those for conventional combustion in air [26], [39], [50].

1.4.2 Nitrogen oxides

Nitrogen oxides are considered to be formed by three pathways [51]: thermal, prompt, and fuel nitrogen-caused nitric oxide (NO). Thermal NO formation results from N_2 and O_2 reacting at high temperatures (above 1500 °C) to form NO. Prompt NO is formed when hydrocarbon radicals in fuel-rich zones attack molecular N_2 to form cyanide species, which subsequently form NO. Fuel NO is derived from N_2 in the fuel. The formed NO is later oxidised to NO_2; thus, the emissions are expressed as NO_x, i.e. nitrogen oxides as NO_2.

One advantage of oxy-fuel technology is its potentially lower NO_x production. Significant reduction in NO_x emission rate can be achieved with oxy-fuel combustion compared with air PC, as thermal and prompt NO_x formations are eliminated owing to the absence of air N_2 [40]. CFBC already offers low NO_x emissions due to low furnace temperature, which prevent thermal and prompt NO_x formations. Results from different oxy-fuel CFB experimental facilities are relatively diverse [52]–[57]. Overall, the results indicate that N_2 behaviour in oxy-fuel CFB will be similar to that of firing in regular CFB, and no drastic changes are expected in fuel N_2 conversion to oxides.

N_2 content in the Estonian oil shale is low: below 0.1% in dry fuel. Owing to this and the low temperatures in CFB combustor, no problems with excess NOx formation have been recorded in utility boilers [23]. Applying oxy-fuel CFBC on Estonian oil shale should result in similar pollutant formation as from conventional CFBC.

1.4.3 Sulfur oxides

SO_x is an important pollutant generated by combustion including oxy-fuel combustion. The flue gas of oxy-fuel combustion is meant for storage or utilisation, but SO_x in the flue gas causes problems in its further use [58, p. 2]. One of the advantages of CFBC is its in situ sulfur capture ability [59]. The SO_2 concentration can be reduced by injecting sorbents, such as limestone or dolomite, into the furnace. The calcination process depends on the CO_2 partial pressure and temperature (Figure 5). If the CO_2 partial pressure is lower than the equilibrium pressure, limestone decomposes and forms CaO and CO_2 (Eq. 1). CaO then reacts with SO_2 (Eq. 2). This process is called indirect sulfation.

$$CaCO_3(s) \leftrightarrow CaO(s) + CO_2(g) \qquad \text{(Eq. 1)}$$

$$CaO(s) + SO_2(g) + 0.5O_2 \leftrightarrow CaSO_4(s) \qquad \text{(Eq. 2)}$$

If the calcination process does not take place, then SO_2 may react directly with $CaCO_3$ (Eq. 3).

$$CaCO_3(s) + SO_2(g) + 0.5O_2 \leftrightarrow CaSO_4(s) + CO_2(g) \qquad \text{(Eq. 3)}$$

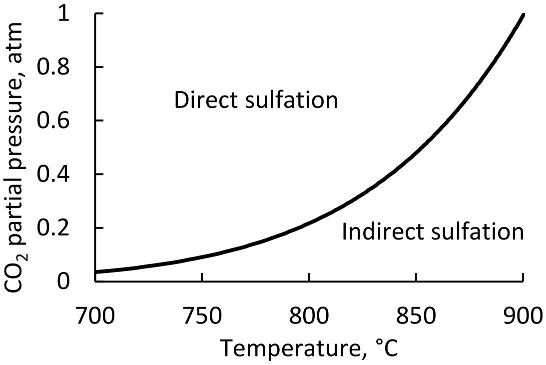

Figure 5. Equilibrium CO_2 pressure over limestone [60].

Estonian oil shale has a high content of carbonate minerals (mostly calcite and dolomite). In air-fired atmospheric units, sulfur capture occurs via relatively rapid calcination and much slower sulfation reactions. In oxy-fuel CFB combustors, sulfation can occur directly without the calcination step [61]. Theoretical calculations [38], [62]–[64] and experiments [65], [66] suggest that carbonate minerals do not fully decompose under oxy-fuel combustion environment and the sulfur binding rate decreases. On the contrary, some other experiments [52], [61], [67] show a decrease in sulfur emissions or increased sulfur capture efficiency when applying oxy-combustion. If the sulfur binding rate decreases, then an additional deSO$_x$ facility may be necessary.

1.4.4 Behaviour of mineral matter

When solid fuel is fired in a combustor, the mineral matter in the fuel forms ash, which separates into different ash flows with different particle size distributions and chemical-mineralogical compositions. The mineral matter in fuel is influenced by the temperature and gas composition in the furnace. In a CFB combustor, the temperatures are relatively low (< 900 °C) compared to PC furnaces, where temperatures may extend to 1400 °C. Due to lower temperatures, fewer reactions involving mineral matter occur. In a CFB combustor, absorbed and crystal water is released from minerals; carbonate minerals and marcasite decompose and sulfur is bound into anhydrite [16], [68]. When firing fuel in a PC boiler, the mineral matter is subjected to various reactions: thermal decomposition, volatilisation, and formation of novel minerals [69]–[71]. Estonian oil shale has a high ash content, and thus, the processes occurring in mineral matter become even more important.

As mentioned before, carbonate minerals (dolomite and limestone) have an important part in SO_2 binding from flue gas. Rahiala et al. [63] modelled the limestone particle behaviour in an oxy-fuel CFBC process. Limestone and dolomite calcination reaction in oxy-fuel atmosphere has been studied widely [72]–[76], but usually in contents of additive/sorbent for SO_2 binding. Estonian oil shale already contains a considerable amount of calcite and dolomite; thus, no additive is necessary.

In general, it has been noted that there are no major changes in ash composition, although the relative amount of mineral phases changes [77]–[79]. The results of different drop tube experiments indicate that the furnace temperature and fuel mineral part are the major factors affecting formation of gaseous compounds and ash rather than the main gas, which still seems to affect the fine ash (submicron) composition and the ash deposition mechanisms [80]. Mapping the ash produced is important in finding solutions to turn ash or part of it into products [81].

1.5 Carbon storage and utilisation

Carbon capture solutions are only one side of CCS: CO_2 needs to be utilised or stored safely and stably. Oxy-fuel combustion simplifies CO_2 transportation and utilisation by already creating a concentrated CO_2 flow.

CO_2 can be stored into depleted oil/gas reservoirs and coal seams, but the largest capacities and most widespread locations are offered by deep saline aquifers [35]. Storage of CO_2 with enhanced industrial production has great potential to enable large-scale CO_2 storage at reasonable cost. The solution can help in storing CO_2 and enhancing industrial production at the same time. CO_2 injection can enhance oil [82], natural gas [83], coal bed methane [84], and shale gas recovery [35]. Injecting CO_2 into the ground could also be used for improving geothermal power generation [85] and even for in situ uranium leaching [86]. Most of the technologies are still in the phase of research, except for enhanced oil recovery. This solution has been successfully used already for decades [87].

The goal of CO_2 mineralisation and industrial utilisation is to trap CO_2 permanently in stable minerals. CO_2 can be used as a feedstock for chemical engineering and various innovative construction materials can be manufactured. For example, concentrated CO_2 flow could be used for precipitated calcium carbonate production [88]–[90]. Overall, the carbonisation industry is still in a demonstration phase.

2 EXPERIMENTAL METHODS

This dissertation is based on five papers. The materials and methods used are described in detail in the papers, but an overview of the materials, experimental devices, and methods applied is presented here. First is a short description of the material used—the Estonian oil shale. This is followed by an overview of the methods and experiments conducted to investigate the oxy-fuel combustion: the theoretical study [Paper I], research on oil shale oxy-fuel combustion in TGA [Paper II], batch reactor experiments [Paper III], description of real combustion experiments in a CFB combustor [Paper IV–IV], and accelerated calcination experiments [Paper V].

2.1 Materials

2.1.1 Oil shale

Oil shale is generally rich in bituminous organic matter that is processed worldwide in few countries including China, Brazil, Jordan, and Estonia as an energy resource, although the large reserves are known also in the U.S.A., Australia, Russia, and elsewhere [91]. However, the increasing need for energy, depletion of easily accessible oil reserves, and concurrently increasing oil prices have significantly raised the interest in oil shale mining and processing in the last decades.

In this research, Estonian kukersite oil shale from Estonia and Ojamaa underground mines were used. The oil shale is a solid fuel and its organic matter has a relatively high H/C molecular ratio resulting in smaller CO_2 emission compared to coals. The oil shales worldwide are as diverse as coals. Estonian oil shale has a high content of mineral matter, which consists of carbonaceous, sandy-clay-carbonaceous, and sandy-clay parts [16]. The molar ratio of Ca/S is 7–10 in oil shale; this exceeds by over 2–3 times the ratio of Ca/S sufficient to complete the capture of SO_2 [24]. The thermal decomposition of carbonaceous minerals liberates CO_2. A higher CO_2 concentration during combustion may change the decomposition reactions of carbonates and decrease the CO_2 emission [76]. Therefore, implementation of oxy-fuel technology offers many benefits.

Estonian oil shale for the oxy-fuel experiments [Paper II and III] was sampled from crushed oil shale mined in Estonia underground mine. The sample was collected from fuel flow to utility power plants. The oil shale was dried and crushed by passing through a 2 mm sieve opening. The median size of the oil shale was 0.25 mm. In CFB experiments [Paper IV–V], oil shale from Ojamaa underground mine was used. The fuel was sieved to pass through 3 mm openings.

Table 1. Proximate and ultimate analysis of the underground mine Ojamaa oil shale.

LHV, MJ/kg	Proximate analysis, wt. %				Ultimate analysis, wt. %					
Q^{ar}_{net}	W^{ar}	$^*VM^{ar}$	FC^{ar}	A^{ar}	C^d	N^d	S^d	H^d	TOC^d	$(CO_2)^d_{mineral}$
8.56	0.5	47.5	1.3	50.7	27.4	0.1	1.6	2.7	21.8	20.6

** VM^{ar} includes mineral CO_2 from decomposition of carbonate minerals*

The CFBC experiments [Paper IV–V] were carried out with typical Estonian oil shale from Ojamaa underground mine. The fuel was dried, crushed, and sieved through 3 mm openings. The fuel ultimate and proximate analyses are listed in Table 1. The laboratory ash composition is presented in Table 2. The Ca/S molar ratio in the oil shale was 8.0.

Table 2. Chemical composition of oil shale laboratory ash, wt. %.

CaO	SiO_2	Al_2O_3	SO_3	MgO	Fe_2O_3	K_2O	Cl	Na_2O	Others
43.9	27.5	8.6	5.5	4.9	4.8	3.3	0.4	0.1	1.0

2.2 Equipment and methods

2.2.1 Calculation model for oil shale oxy-fuel CFBC

The calculations of the flue gas volumes in oxy-fuel CFBC of oil shale were performed under a steady-state regime, implementing a process for which the schematic is shown in Figure 6. The flue gas was recycled after a water vapour condenser [Paper I].

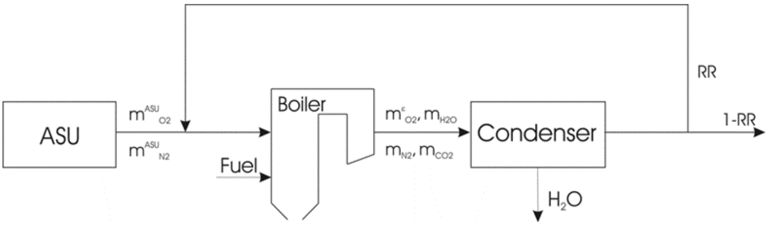

Figure 6. Schematic of the proposed oxy-fuel combustion process [Paper I].

The temperature in the CFB boiler furnace was presumed to be in the range of 750–850 °C. This ensures sufficient sulfur binding. The bed temperature in the CFB boiler was mainly controlled by adjusting the ash recirculating ratio and temperature. This feature can be used to reduce the recycled flue gas (RFG) ratio in the CFB when retrofitting to oxy-fuel combustion [92].

Based on an overview article [40], the O_2 content after the ASU was assumed to be $95\%_{vol}$ with $5\%_{vol}$ of N_2. The oil shale calculations were performed for an excess O_2 constant value of $5\%_{vol}$ at the boiler outlet. In the steady-state regime, the CO_2 content per kg fuel at the boiler outlet for different RFG ratios was calculated. The gas volume calculations for oil shale oxy-fuel CFBC for different oil shale LHVs and different recycled flue gas ratios were performed.

2.2.2 TGA, DSC, and QMS analyses

TGA, differential scanning calorimetry (DSC), and quadrupole mass spectrometry (QMS) were used to obtain data with high precision from different processes that occur in the oil shale during the thermal treatment [Paper II]. TGA is a common technique to rapidly investigate and compare thermal events and kinetics during the combustion and pyrolysis of a material. The gas environment in TGA was well controlled and even water vapour could be added to the gas mixture in the analyser. TGA measured the mass loss of the sample as a function of time and temperature. QMS improved the analyses of the processes by adding information about the evolving gases. The temperatures at which the mass changes occurred were viewed using TGA. DSC added thermal information about the processes that took place during the measurement.

The thermal analyses were performed on Netzsch STA 449 F3 Jupiter Simultaneous Thermal Analyser (TG-DSC/DTA Apparatus) coupled with a Netzsch QMS 403D Aeolos (mass 1–300 amu). The samples were analysed in Pt/Rh crucibles with lid and removable liner of thin walled Al_2O3 in the gas. A standard sample mass of 20±1 mg was used. The total gas flow during all the measurements was 60 ml/min. Different gas mixtures (see Figure 7) were used to simulate oxy-fuel and conventional combustion conditions in TGA. The samples were equilibrated at 40 °C for 45 min, and then heated at 10 °C/min up to 1240 °C. The temperature and enthalpy measurements were calibrated with In, Sn, Zn, Al, and Au standards. The evolved gas was analysed using QMS. Mass/charge (m/z) values from 8 to 150 were collected with a sampling rate of 0.2 s. All measurements were performed at least twice for sufficient reproducibility.

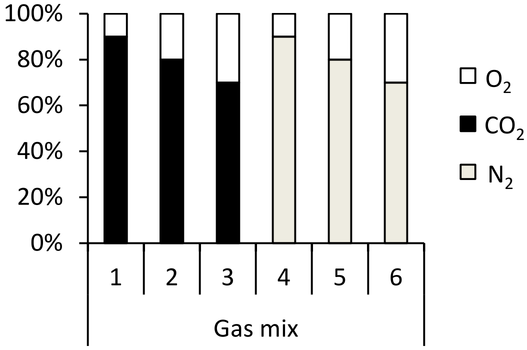

Figure 7. Gas mixtures used in TGA experiments [Paper II].

2.2.3 Batch reactor experiments

Experiments in simulated oxy and regular CFB furnace conditions were conducted in a batch reactor to investigate the produced ash [Paper III]. The batch reactor (Figure 8) was designed to burn up a portion of solid fuel in a controlled environment. The experimental facility consists of a reactor-heater, temperature control system, gas mixing-control system, steam generator-insertion system, flue gas analyser, and data acquisition and control system. The gas mixing-control system consisted of mass flow controllers, calibrated according to the gas to be used, with check valves. Water vapour of up to 25% was added to the gas mixture with the steam generator. To prevent water vapour condensation in the gas pipes, a heated supply channel was used. The batch reactor was designed to meet working temperatures of up to 950 °C.

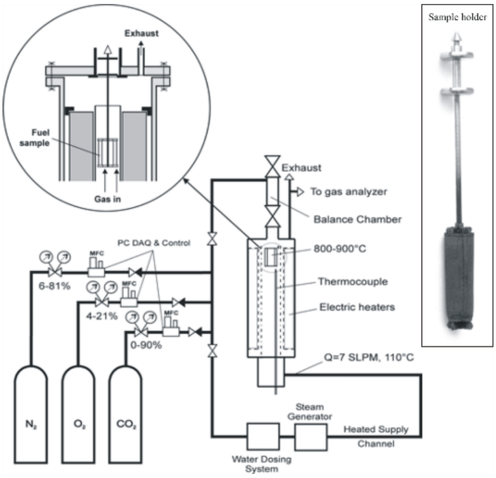

Figure 8. Schematic of batch reactor and a sample holder.

Combustion experiments were performed at temperatures of 800 °C, 850 °C, and 900 °C while varying N_2, O_2, and CO_2 ratios. In addition to different temperatures and air composition variation, the furnace was injected with water vapour to determine the moisture influence on formation of solid combustion products.

Approximately 5 g of oil shale was loaded to the sample holder (Figure 8) for each experiment. A stainless steel bound net sample holder was used. In each run, the sample holder with sample was loaded together into the balance chamber. The balance chamber was filled with gas mixture used in the experiment. Then the sample holder was dropped into the reactor. Because the combustion and reactions with oil shale mineral part and coke takes some time, the sample was removed from the reactor after 1.5 h. The holding time was selected according to earlier studies on the behaviour of oil shale carbonates [93].

The mineral composition of crystalline phases in ash and raw oil shale was determined using powder X-ray diffraction (XRD) method with a Bruker D8 diffractometer. The micromorphology of ash was investigated using scanning electron microscopy (SEM) imaging, and analysis of samples was performed on a variable pressure Zeiss EVO MA15 SEM equipped with Oxford X-MAX energy dispersive detector system and AZTEC software for element analysis.

2.2.4 Experimental oxy-fuel circulating fluidised bed (CFB) combustor

The combustion experiments [Paper IV] were conducted on a 60 kW_{th} CFB combustor, which was designed and constructed for fuels with high (up to 60 wt. %) ash content. The main components of the test facility are shown in Figure 9. The height of the riser was 4.90 m and the inner diameter was 0.12 m. The combustion chamber was isolated with ceramics and a high-temperature thermal isolation material. To minimise leaks, the combustor was enclosed by a stainless steel shell. The fuel was fed using a screw conveyer at a height of 0.49 m and the recirculated solids were fed back at a height of 0.86 m. The secondary and tertiary air inlet ports were located at heights of 0.49 m and 0.86 m respectively.

The combustion air was supplied by a compressor. The simulation of RFG was performed using bottled CO_2 and O_2. All gas lines, i.e. O_2, CO_2, and compressed air, were equipped with mass flow controllers for exact control of the mass flow rates and the ratio of O_2/CO_2. The oxidiser lines were equipped with electrical heaters to maintain the required gas temperature.

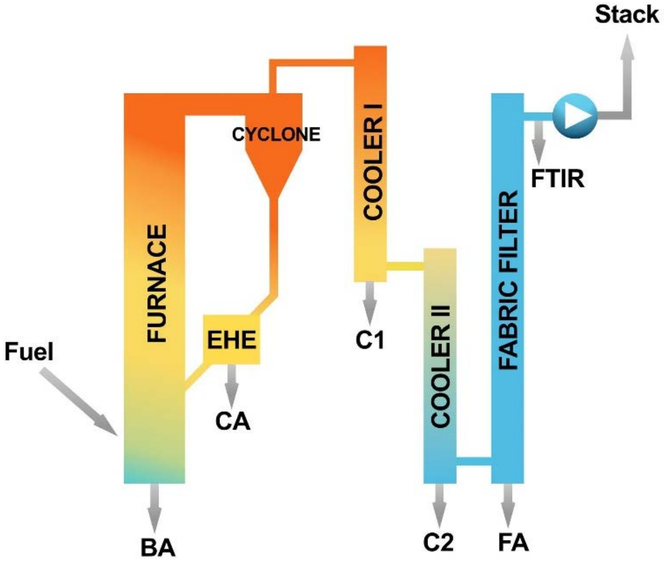

Figure 9. The circulating fluidised bed combustion test facility [Paper IV–V].

The test facility was equipped with three independent fuel/bed material feed silos and a gas burner. The main fuel silo was mounted on load cells, which enabled the determination of mass flow rates for solid materials and the calibration of fuel main screw feeder. The control and data acquisition of the test facility was fully automated and operated with a LabVIEW system.

The flue gas composition was simultaneously analysed using a Fourier transform infrared (FTIR) spectrometer. Ash samples were collected from five points: bottom ash (BA), cyclone ash (CA), cooler 1 ash (C1), cooler 2 ash (C2), and fabric filter ash (FA). The ash split of the CFB combustor used in the calculations is presented in Table 3. The chemical compositions of the ashes and fuel were measured using an X-ray fluorescence spectrometer (XRF) and elemental analyser. The particle size distributions in the flue gas [94] were measured using an electrical low-pressure impactor (ELPI+). It electrically charged the incoming particles and then classified them by aerodynamic size into 14 impactor stages.

Table 3. Ash split of CFB combustor.

Ash flow	BA	CA	C1	C2	FA
Wt. %	37	7	2	47	7

The oil shale combustion experiments were conducted using three different oxidiser mixtures: air (21% O_2 and 79% N_2), OXY21 (21% O_2 and 79% CO_2), and OXY30 (30% O_2 and 70% CO_2). The purpose of OXY21 was to highlight the differences caused by substituting N_2 with CO_2. Previous experiments [Paper II] had shown that combustion would be slower in a CO_2-based atmosphere; therefore, OXY30, with increased O_2 content, was chosen to ensure a similar temperature field in the furnace. During the experiments, the thermal load of the combustor was 24 ± 3 kW. The OXY30 experiment was conducted on a lower thermal load (12 kW) due to fuel feeder problems. The primary and secondary air ratio was 4:6, because the fuel has high volatile matter content.

2.2.5 Accelerated calcination experiments

In order to simulate natural carbonisation of calcium-rich ash on an ash field, accelerated carbonation experiments of oil shale ashes was conducted in the laboratory [Paper V]. Oil shale oxy-fuel CFBC ashes (OXY21) were mixed with distilled water with a solid to liquid ratio of 1:10. The solution pH increased rapidly to 12. To accelerate the natural carbonisation process, CO_2 was bubbled through the mixture. The mineral CO_2 amount was measured in the samples with an elemental analyser using the total inorganic carbon module. Based on the results, the extent of carbonate decomposition, specific emission of CO_2 from oil shale oxy-fuel combustion, and power production were estimated. The results of the experiments and calculations were compared with previous knowledge of oil shale PC [17] and CFBC [95], [96], and ash behaviour in natural conditions [21], [22].

3 RESULTS AND DISCUSSION

3.1 Predictions of CO_2 formation

Oxy-fuel combustion means that the fuel is fired in a mixture of O_2 and recycled flue gas. This alters the combustion environment and reactions occurring with mineral matter. The processes occurring in the mineral matter significantly affect the ash production and heat released in combustion. The main thermal effects in the oil shale ash are related to the decomposition of calcite and dolomite, pyrite oxidation, and sulfation. The extent of these reactions affects the amount of heat released, amount of ash and combustion products formed, and ultimately, the flue gas composition.

It was found that for Estonian oil shale combustion in CFB, the recycled flue gas ratio should be maintained higher than 70% to minimise the decomposition of carbonate minerals. This increases the partial pressure of CO_2 over the equilibrium state line of the calcite decomposition reaction at the bed temperature. The decrease in decomposition of carbonate minerals decreases CO_2 emissions (Figure 10) and leads to an additional increase in heat released during oil shale combustion. The effect depends on the carbonate content of the Estonian oil shale. The positive heat effect could be as high as 0.34 MJ/kg [Paper I].

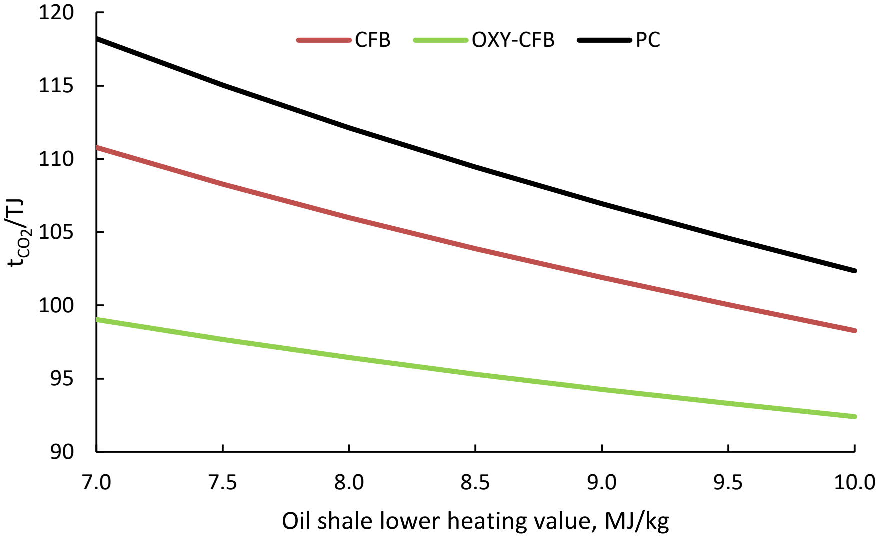

Figure 10. Theoretical oxy-fuel CFBC emissions compared to PC and regular CFBC. Extent of carbonate mineral decomposition in the model was 0.28 (minimum possible) for OXY-CFB, 0.7 for CFB, and 0.97 for PC [Paper I].

A comparison with bituminous and anthracite coals indicated that the specific emission of CO_2 per input fuel energy for oil shale could be expected to be even smaller than that of the considered coals [Paper I]. This is a strong positive impact that increases the competitiveness of Estonian oil shale compared to coals.

3.2 Oil shale combustion process

In order to investigate oil shale and its mineral matter behaviour in combustion, a number of TGA experiments were conducted. Data from the TGA, DSC, and QMS measurements are shown in Figure 11 and Figure 12. A more thorough description and analysis of the measurements are found in Paper II. During oil shale combustion in TGA, the following major reaction st0065ps occurred: water removal, decomposition of kerogen, dissociation of volatile matter into bitumen and gases, oxidation of volatile matter and fixed carbon (FC), and decomposition of carbonate minerals.

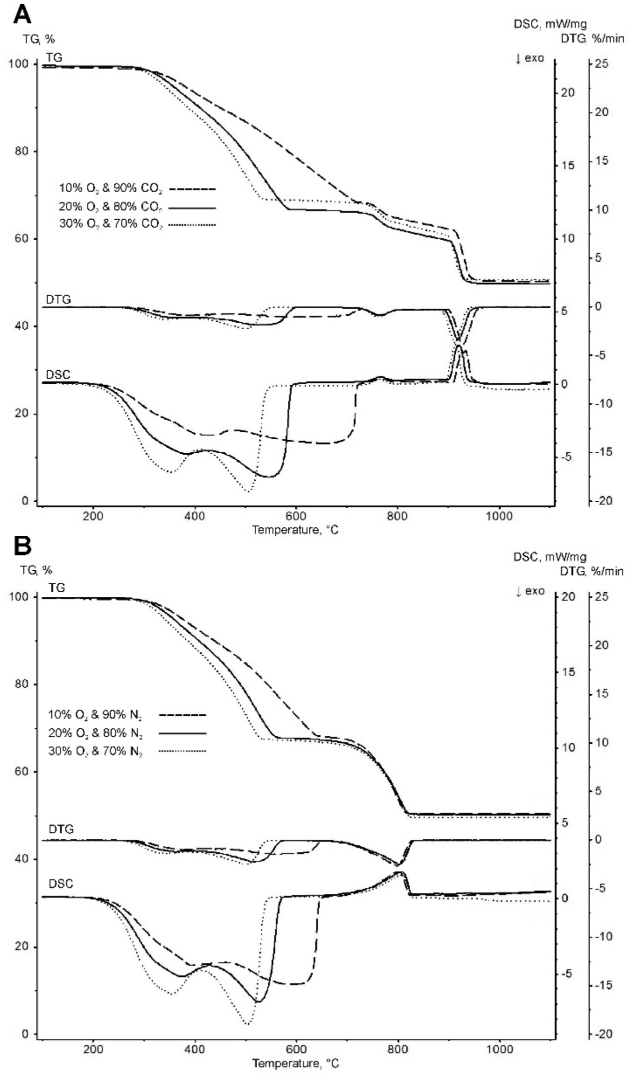

Figure 11. Oil shale combustion measurements in (A) oxy-fuel and (B) air atmospheres [Paper III]; the gas mixtures contained 10, 20, and 30% O_2 and were explained in Figure 7.

The first combustion step was the separation of water vapour. In addition to moisture, the oil shale contains crystal water (clay minerals, such as illite, chlorite, and kaolinite, which separate in the temperature range of 120–140 °C [16]). In the conducted measurements, only a minimal mass loss was observed in the water evaporation zone.

The kerogen volatilisation and char combustion (mass loss 31–33%) occurred in the temperature range of 300 to 715 °C. As visible in all the curves, two outstanding reaction rate peaks are recognised: the first one in the range of 340 to 440 °C and the second one between 500 and 660 °C. The QMS measurements indicate the separation of H_2O, CO, CO_2, and HCl at the first peak of combustion. The second peak of combustion matches the CO_2 and SO_2 peaks (see Figure 12). In this case, the H_2O reading was lower than that during the first phase of combustion, which indicated that hydrocarbons had already burned, and the combustion of aliphatic and aromatic compounds and char occurred during the second phase. The low readings of SO_2 during the first phase of combustion were caused by the combustion of organic sulfur. At 500 °C, marcasite (FeS_2) decomposes; thus, sulfur dioxide was formed, which causes the strong reading of SO_2 during the second combustion phase. This phase consists of the conversion of organic matter into volatiles and FC, oxidation of the formed volatiles, and finally, the combustion of carbon.

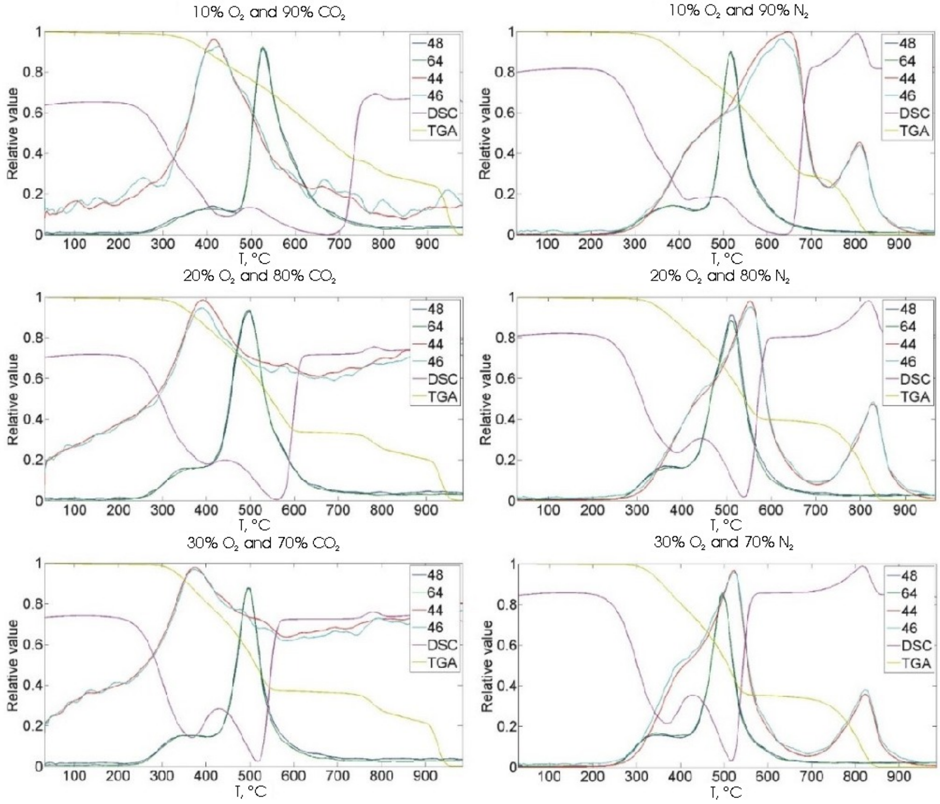

Figure 12. Evolved gas QMS measurements of SO_2 (m/z = 48 and 64) and CO_2 (m/z = 44 and 46) [Paper II].

Above 650 °C, all of the succeeding reactions were endothermic, which suggests that the organic compounds were already burned. The mass loss step(s) between 670 and 940 °C indicated the decomposition of carbonate minerals. The results improve the previous knowledge of Estonian oil shale combustion [16] and parallel researches done using TGA coupled with FTIR spectroscopy [47], [97].

3.3 Oil shale oxy-fuel combustion

The significant temperatures of oil shale combustion in TGA are plotted in Figure 13, based on Paper II findings. During all the experiments, the oil shale ignition temperature was similar, but the burnout temperature depended on the O_2 content and carrier gas. A lower O_2 content with CO_2 as a carrier gas leads to a slower burnout of the oil shale. When the O_2 content was increased to 30%, the burnout temperatures in N_2 and CO_2-based mixtures were identical. This indicates that increasing the O_2 content enables a similar combustion process in oxy-fuel mode as in conventional combustor.

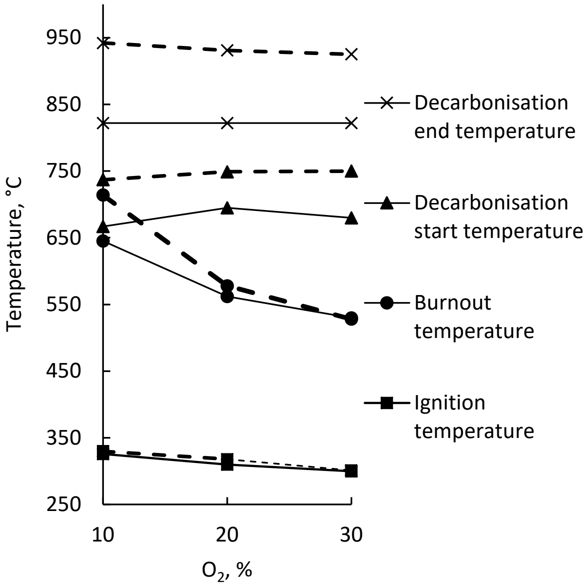

Figure 13. Oil shale combustion parameters measured using TGA. The solid lines represent measurements in air atmospheres whereas the dashed lines represent measurements in oxy-fuel atmospheres [Paper III].

The carbonate decomposition reactions occurred in similar temperature ranges in all air atmospheres (see Figure 11). The dolomite breakdown was merged into the larger calcite decomposition peak in the air atmosphere. In oxy-fuel combustion atmospheres, the start of decarbonisation shifts to higher temperatures (Figure 13) and the reactions occur in two separate parts: decomposition of dolomite ($CaMg(CO_3)_2$) and then decomposition of calcite ($CaCO_3$) [5], [10].

The experiments conducted at the batch reactor [Paper III] showed that the decomposition of Ca-Mg carbonate phase (dolomite) was completed in all temperature regimes in various combustion atmospheres. However, the decomposition of $CaCO_3$ phase (calcite) is significantly delayed at elevated CO_2 levels. It was noticed that Ca-Mg silicate phase formation was proportional to the firing temperature. The results in Paper III suggest that the elevated CO_2 levels and the inhibited calcite decomposition may have a noticeable effect on the SO_2 binding, and consequently, on the stable anhydrite formation in oil shale ash.

3.4 Oil shale oxy-fuel CFBC

After the small-scale laboratory experiments, considerably larger real combustion experiments were conducted in the CFB combustor. The CFBC experiments and results were described in Paper IV. The temperatures in the riser during air operation (Figure 14) were similar to the values used in the oil shale industrial CFB boilers (800 °C) [23]. During the OXY21 operation, the temperature in the riser dropped up to 100 °C, but the temperature in the cyclone exit remained similar. The reason behind the decreased temperatures in the riser might be the slight drop in primary air temperature from 284 to 250 °C together with decreased fuel reactivity [Paper II] and increased heat capacity of the CO_2 atmosphere [98]. When the O_2 concentration was increased to 30%, the temperature distribution in the CFB was similar to that of air mode. The observation confirmed that in order to achieve a similar temperature field in oxy-fuel mode, the O_2 concentration has to be increased [99].

Based on the unburnt carbon content of the ashes and on the flue gas analysis, the combustion efficiency was estimated [94]. Combustion efficiency considered losses due to incomplete combustion. The combustion efficiency of the oil shale fired CFB in air mode was 96.1% and 94.8% in OXY30 mode. Similar combustion efficiency values have been demonstrated by other CFBC test rigs [52]. Most of the losses in the oil shale combustion were attributed to unburnt carbon in ash. The average unburnt carbon content in regular CFBC ash was 1.5%. In the OXY30 mode, the unburnt carbon content in ash slightly increased to 2.2%. The oil shale had a high ash content of over 50% (Table 1). Thus, a slight increase in ash carbon content has a strong influence on the total combustion efficiency. The difference of unburnt carbon content in ash from different experiments was relatively small. During all the CFBC experiments, the unburnt carbon content in the bottom and cyclone ash was below 0.5%, but the fly ash contained almost 5% unburnt carbon. This indicates that the unburnt volatiles condensed and settled in the ash. This was caused by the design of the CFBC test rig. The flue gas was rapidly cooled down directly after the cyclone, and thus, the hot zone for combustion of volatiles was extremely short.

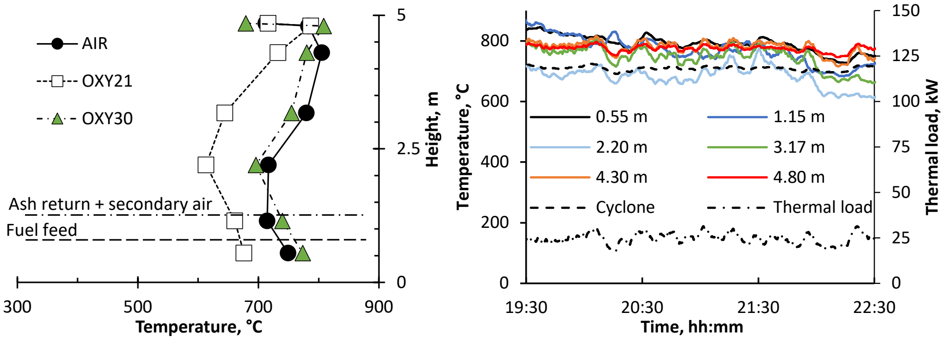

(a) (b)

Figure 14. (a) Temperature distribution along the CFB combustor riser and in the cyclone. (b) Temperatures in the CFB combustor riser and thermal load during steady-state operation when using air [Paper IV].

3.4.1 Emissions of oil shale oxy-fuel CFBC

The average pollutant concentrations during the CFBC experiments are presented in Table 4 and analysed in Paper IV. During all the CFBC experiments, the sulfur concentration in flue gas was at very low level (below 25 mg/Nm^3 @ 6% O_2). As noted before, during the OXY21 experiment, the temperature in the riser decreased up to 100 °C (Figure 14). Despite the temperature drop, the SO_2 concentration in flue gas remained similar. Even if the higher CO_2 partial pressure and lower temperature in the system inhibited the decomposition of $CaCO_3$ [Paper III], the calcium content in the oil shale was high enough to achieve an almost complete sulfur binding.

During the CFBC in air, sulfation reaction is indirect. The calcite and dolomite (carbonate minerals) decompose and form lime, which binds sulfur from flue gas and forms anhydrite. Because the regular CFBC ash [Paper IV and V] did not contain considerable amounts of carbonate (Figure 15), it indicates that the sulfur binding occurred via indirect reaction. However, during oxy-fuel CFB experiments, the sulfation occurred probably via direct reaction, because the ashes contained considerable amounts of carbonate, indicating decreased decomposition of carbonate minerals. At the same time, the SO_2 concentration in the flue gas remained at ultra-low levels. Our results suggest that the elevated CO_2 levels and the inhibited carbonate decomposition extent in the ashes do not have a noticeable effect on the SO_2 binding, when oxy-firing Estonian oil shale in CFB.

Table 4. Average emissions of oil shale firing in CFB combustor [Paper IV].

Item	Unit	Air-mode	OXY21	OXY30
O_2	$\%_{dry}$	10.0	8.5	13
NO_x	mg/Nm^3 @ 6% O_2	141	156	130
SO_2	mg/Nm^3 @ 6% O_2	< 15	23	< 15
CO	mg/Nm^3 @ 6% O_2	943	2361	337
Desulfurisation efficiency	%	99	99	99
SO_2 emission	mg/MJ	<8	9	<4
NO_x emission	mg/MJ	34	40	33
Fuel N_2 conversion ratio	%	20	24	20

The other acidic pollutant content that was measured in the flue gas was NO_x. The NO_x concentration in flue gas was below 160 mg/Nm^3 during all the CFBC experiments (Table 4). The N_2 conversion ratio into NO_x was up to 24%. A similar value (20–25%) was measured by Jankowska et al. [56] in experiments with bituminous coal. However, Pikkarainen et al. [57] measured higher N_2 conversion ratios (28–50%). Higher N_2 conversion ratios to oxides (> 25%) are expected when firing fuels with low N_2 content. From our experiments [Paper IV and V] and the literature [51], [56], [100], it seems that switching to oxy-fuel combustion did not alter the NO_x formation, but it is still possible to alter the pollutant formation by secondary air injection and load of a combustor.

Particle matter is a mixture of extremely small particles and droplets that may have harmful health effects. The emissions of such fine matter are under strict control. To evaluate oxy-fuel combustion influence on the formation of such particulates, short measurements were conducted using an ELPI+ [94]. The results showed that the flue gas contained nanoparticles. The median diameter of the particulates increased from 20 to 40 nm, when the combustion mode was changed from regular air to OXY30. At the same time, the particle count decreased from 13 600 in air mode to 11 100 particles/cm^3 in OXY30 mode. This indicates that the particles were present during both experiments in Aitken mode (10–50 nm). These type of particles were probably freshly formed during the condensation of volatiles. The lifetime of such particles is short (minutes to an hour). During the CFBC experiments, the particle concentration in flue gas was stable. It seems that the shift to oxy-fuel mode did not have a considerable effect on particle emissions.

3.4.2 Oil shale oxy-fuel CFBC ash and carbonation

During the experiments, samples were collected from all the ash flows (Figure 9). The results of chemical analysis of the ashes are displayed and analysed in Paper IV. The unburnt carbon content of BA and CA was below 0.7% and was 0.3–4.7% for the fly ashes (Figure 15). Typically, for oil shale, the ash had a high calcium content, followed by silica, magnesium, and alumina. The chemical compositions of the ashes were similar during all the CFBC experiments.

The mineral CO_2 content of the oxy-fuel CFBC ashes was considerably higher than in the ashes obtained in air mode (Figure 15). The composition and percentage of ash flows depend on the type of boiler, load, and fuel. From the total carbon in the fuel, 20% was inorganic (see Table 1). It is theoretically possible to reduce the extent of decomposition of carbonate minerals to 28% in an oxy-CFB combustor firing Estonian oil shale [Paper I]. The minimum is defined by dolomite and sulfur content in the fuel [101]. A limited decomposition of the carbonate minerals during oxy-fuel combustion would decrease CO_2 formation from oil shale combustion.

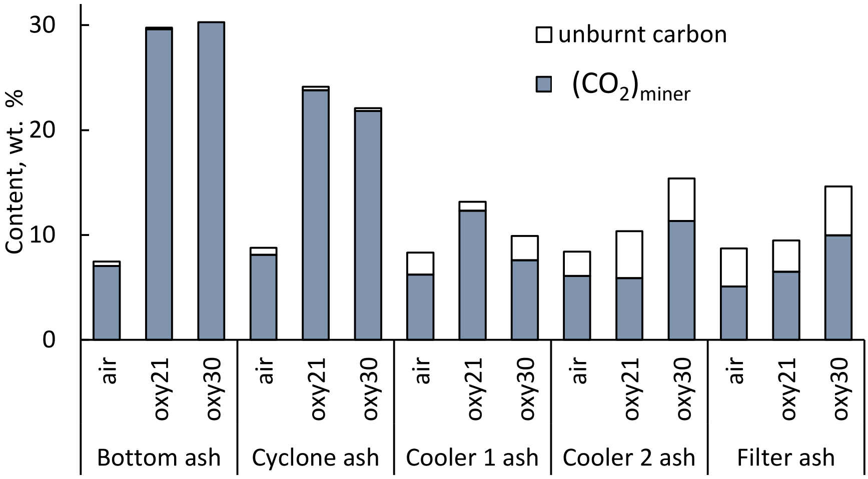

Figure 15. Mineral CO_2 ($[CO_2]_{mineral}$) and unburnt carbon content in CFBC ashes [Paper IV].

The Estonian oil shale combustion ash has considerable CO_2 sequestration potential [21]. The realised sequestration depends on many factors: oil shale ash properties, combustion mode, ash flow and ash removal, treatment, and stowing. For a first assessment of oil shale oxy-fuel combustion ashes CO_2 sequestration potential, fast calcination experiments were conducted [Paper V]. The results of experiments are presented in Table 5. The CO_2 content in all the ashes increased, but in the BA, CA, and C1 ashes, the change was small. The finest ashes (C2 and FA) sequestrated considerable amounts of CO_2.

Table 5. CO_2 sequestrated during simulated hydraulic transportation and landfilling [Paper V].

	BA	CA	C1	C2	FA	**AVERAGE**
CO_2 (%)	29.0	23.8	12.3	5.9	8.7	**16.1**
CO_2 after wet treatment (%)	31.3	26.3	15.6	18.8	11.7	**23.4**
CO_2 absorbed from the atmosphere, ΔCO_2 (t CO_2/t ash)	0.024	0.026	0.034	0.148	0.031	**0.079**

When oxy-fuel combustion of oil shale would be applied at utility scale, large amounts of CO_2 would be produced. To estimate the quantities, at first, CO_2 formation from combustion was estimated in Paper V. Based on the oxy-fuel CFBC ash analysis and assumed ash split (Table 3), the extent of carbonate decomposition and specific emission of CO_2 from oil shale oxy-fuel CFBC were estimated and compared with PC [17] and CFB [95] combustion (see Table 6). The CO_2 output from combustion decreases by 20% and 5%, respectively. The reason behind the decreased CO_2 formation was the decreased extent of decomposition of carbonate minerals. The flue gas from CFBC and PC contains up to 20% CO_2, but the oxy-fuel combustion residue contained up to 95% CO_2. This eases the reuse and/or transportation of the greenhouse gas.

Table 6. Laboratory oxy-fuel CFBC emissions compared to large scale CFBC [95] and PC [17].

		OXY21	CFBC	PC
Extent of carbonate decomposition (-)	k_{CO_2}	0.46	0.69	0.95
CO_2 absorbed from the atmosphere (t/TJ)	ΔCO_2	5.5	7.8	4.7
Specific emission of CO_2 for oil shale combustion (t/TJ)	qCO_2	100.0	106.7	122.4
Specific emission of CO_2 for oil shale combustion + landfilling (t/TJ)		94.6	98.9	117.7
Specific emission of CO_2 for oil shale combustion + landfilling compared to PC (%)		80	84	100

The CO_2 formation from combustion is only half the truth, because compared to regular CFBC, the oxy-fuel combustion has some extra energy consumption: O_2 is required, part of the flue gas has to be recycled, and the flue gas requires compression for further processing. According to a study by Escudero et al. [102], the net power production efficiency of a new CFB power unit is assumed as 43% and for a new corresponding oxy-fuel CFB power unit, the efficiency is 36%. This efficiency loss includes all the previously listed extras. If such efficiency would be reached for oil shale combustion (the designed efficiency of Auvere CFB power plant is 42% [25]), the specific emissions of CO_2 would be 819 kg/MWh_e; when oxy-fuel firing would be applied, 942 kg CO_2/MWh_e would be produced. It is more than that from CFB power production, but is still considerably less than that from PC (974 kg/MWh_e [17]). The results of Paper V suggest that despite the decreased decomposition of carbonates, the power production using new oxy-fuel CFB would produce more CO_2 than that by applying regular CFBC. Nevertheless, oxy-fuel combustion would decrease further CO_2 treatment cost and enable utilisation or storage of CO_2.

4 CONCLUSIONS

This thesis evaluated the suitability of oxy-fuel CFBC technology for Estonian oil shale. Theoretical analyses and different experiments were conducted on TGA, batch reactor, and CFB combustor. The conventional CFBC technology has been proved to be suitable for Estonian oil shale. The influence of oxy-fuel environment, substitution of N_2 with CO_2, and changes in O_2 concentration on the oil shale combustion were investigated. To simulate wet oil shale oxy-fuel CFBC ash landfilling, a short experiment was conducted. The oil shale oxy-fuel CFBC process, produced gases, and ash were analysed and the most important results are summarised here:

- The decomposition of calcite is inhibited when the CO_2 concentration in the combustor increases. The minimum extent of carbonate mineral decomposition when oxy-fuel CFBC is applied is 0.28. This leads to an additional increase in heat released and decreased CO_2 formation during oil shale CFBC. Depending on the carbonate content, the mean LHV value could be as high as 0.34 MJ/kg.
- The characteristic temperatures of the oil shale combustion in TGA differ in air and oxy-fuel environments: combustion was delayed in the oxy-fuel environment. A higher O_2 content decreases the differences of the air and oxy-fuel combustion parameters.
- When firing in air, the decomposition of carbonaceous minerals occurs in one step, but in the oxy-fuel atmosphere, the process occurs in two reaction steps: decomposition of dolomite ($CaMg(CO_3)_2$) and then decomposition of calcite ($CaCO_3$).
- The batch reactor experiment results suggest that the elevated CO_2 levels and the inhibited calcite decomposition extent have a noticeable effect on the SO_2 binding, and consequently, on the stable anhydrite formation in oil shale ash.
- When Estonian oil shale was oxy-fired in a CFB combustor using a gas mixture containing 21% O_2 and 79% CO_2, the temperatures in riser decreased as predicted by the TGA study. Increasing the oxidiser O_2 content to 30% ensured a similar temperature as in the air fired CFB combustor.
- Oil shale oxy-fuel CFBC flue gas and pollutant concentration remained at the same level in the regular and oxy-fuel combustion modes. No additional deSO_x or deNO_x is required before CO_2 compression for utilisation or transport.
- The chemical compositions of the oxy-fuel CFBC ashes were similar to the ashes produced in air mode, except for the carbonate content. When oxy-fuel CFBC was applied, the extent of carbonate mineral decomposition decreased considerably.
- Aqueous carbonisation experiments showed that oxy-fuel CFB ash still sequestrates some CO_2 even more than the Estonian oil shale ash from PC.
- When applying oxy-fuel combustion, some additional power is required for O_2 production, flue gas recirculation, and CO_2 compression. Calculations showed that when applying oxy-fuel CFBC, the specific CO_2 formation from combustion decreases, but the total specific CO_2 formation from oil shale CFB power production increases.

In oxy-fuel furnace carbonate mineral decomposition is inhibited, but direct sulfation of limestone will occur due the high partial pressure of CO_2 and the suitable conditions for sulfur capture. This ensures sulfur binding and reduces CO_2 formation. Combining CFBC and oxy-fuel technology would be most beneficial CCS technology for Estonian oil shale combustion.

List of Figures

List of Tables

References

[1] IEA, “Technology Roadmap: Carbon Capture and Storage 2013,” IEA, 2013.

[2] F. Châtel-Pélage *et al.*, “Applications of oxygen for NOx control and CO2 capture in coal-fired power plants,” *Therm. Sci.*, vol. 10, no. 3, pp. 119–142, Oct. 2006.

[3] I. Roos, S. Soosaar, A. Volkova, and D. Streimikene, “Greenhouse gas emission reduction perspectives in the Baltic States in frames of EU energy and climate policy,” *Renew. Sustain. Energy Rev.*, vol. 16, no. 4, pp. 2133–2146, May 2012.

[4] M. M. Sokolowski, “Energy markets in the Baltic Sea Region,” Gothenburg, 2013.

[5] “Eesti elektrisüsteemi varustuskindluse aruanne 2017,” Elering, Tallinn, 2017.

[6] H. I. Mathekga, B. O. Oboirien, and B. C. North, “A review of oxy-fuel combustion in fluidized bed reactors,” *Int. J. Energy Res.*, vol. 40, no. 7, pp. 878–902, Jun. 2016.

[7] J. G. J. Olivier, G. Janssens-Maenhout, M. Muntean, and J. A. H. W. Peters, “Trends in global CO2 emissions,” PBL Netherlands Environmental Assessment Agency, Jun. 2016.

[8] J. J. West *et al.*, “Co-benefits of mitigating global greenhouse gas emissions for future air quality and human health,” *Nat. Clim. Change*, vol. 3, no. 10, pp. 885–889, Oct. 2013.

[9] M. E. Boot-Handford *et al.*, “Carbon capture and storage update,” *Energy Environ. Sci.*, vol. 7, no. 1, pp. 130–189, 2014.

[10] “CO2 Emissions from Fuel Combustion,” INTERNATIONAL ENERGY AGENCY, 2017.

[11] S. Sen, “An Overview of Clean Coal Technologies II: Mitigating the Environmental Impacts by Continuous Improvement in Coal Combustion and CCS Technology,” *Energy Sources Part B Econ. Plan. Policy*, vol. 6, no. 2, pp. 118–125, Mar. 2011.

[12] J. Utt and R. Giglio, “Technology comparison of CFB versus pulverized fuel firing for utility power generation,” *J. South. Afr. Inst. Min. Metall.*, vol. 112, no. 6, pp. 449–454, Jun. 2012.

[13] “FE032: Capacity and production of power plants,” *Estonia Statistics*, 2017. [Online]. Available: www.stat.ee. [Accessed: 10-Feb-2017].

[14] T. Pihu, H. Arro, A. Prikk, R. Rootamm, and A. Konist, “Corrosion of Air Preheater Tubes of Oil Shale CFB Boiler. Part I. Dew Point of Flue Gas and Low-Temperature Corrosion,” *Oil Shale*, vol. 26, no. 1, pp. 5–12, 2009.

[15] T. Parve, A. Ots, B.-J. Skrifars, and M. Hupa, “The sintering of Estonian oil shale ashes,” *Oil Shale*, vol. 12, no. 4, pp. 341–356, 1995.

[16] A. Ots, *Oil Shale Fuel Combustion*. Estonia, Tallinn: Tallinna Raamatutrükikoda, 2006.

[17] A. Konist, T. Pihu, D. Neshumayev, and A. Siirde, “Oil Shale Pulverized Firing: Boiler Efficiency, Ash Balance and Flue Gas Composition,” *Oil Shale*, vol. 30, no. 1, pp. 6–18, 2013.

[18] R. Karolin, E. Latõšov, and J. Kleesmaa, “Primary Method for Reduction of SO2 Emission in Pulverized Oil Shale-Fired Boilers at Narva Power Plants: Test 1 - Water Injection After Superheater,” *Oil Shale*, vol. 34, no. 1, pp. 70–81, Jan. 2017.

[19] A. Konist, A. Valtsev, L. Loo, T. Pihu, M. Liira, and K. Kirsimäe, “Influence of oxy-fuel combustion of Ca-rich oil shale fuel on carbonate stability and ash composition,” *Fuel*, vol. 139, pp. 671–677, Jan. 2015.

[20] A. Paat, “About the mineralogical composition of Estonian oil shale ash,” *Oil Shale*, vol. 19, no. 3, pp. 321–333, 2002.

[21] A. Konist, B. Maaten, L. Loo, D. Neshumayev, and T. Pihu, “Mineral sequestration of CO2 by carbonation of Ca-rich oil shale ash in natural conditions,” *Oil Shale*, vol. 33, no. 3, pp. 248–259, Jul. 2016.

[22] H. Arro, A. Prikk, and T. Pihu, “Reducing the environmental impact of Baltic Power Plant ash fields,” *Oil Shale*, vol. 20, no. 3 SI, pp. 375–382, 2003.

[23] A. Hotta *et al.*, “Experience of Estonian oil shale combustion based on CFB technology at Narva Power Plants,” *Oil Shale*, vol. 22, no. 4, pp. 381–397, 2005.

[24] T. Kaljuvee, O. Trass, T. Pihu, A. Konist, and R. Kuusik, “Activation and reactivity of Estonian oil shale cyclone ash towards SO2 binding,” *J. Therm. Anal. Calorim.*, vol. 121, no. 1, pp. 19–28, Dec. 2014.

[25] R. Attikas, “Co-combustion of different fuels in Enefit´s power plants,” in *International Oil Shale Symposium 2016*, Tallinn, Estonia, 2016.

[26] R. Stanger *et al.*, “Oxyfuel combustion for CO2 capture in power plants,” *Int. J. Greenh. Gas Control*, vol. 40, pp. 55–125, Sep. 2015.

[27] E. J. Anthony, “Oxyfuel CFBC: status and anticipated development,” *Greenh. Gases Sci. Technol.*, vol. 3, no. 2, pp. 116–123, Apr. 2013.

[28] N. Z. Muradov and T. N. Veziroğlu, “‘Green’ path from fossil-based to hydrogen economy: An overview of carbon-neutral technologies,” *Int. J. Hydrog. Energy*, vol. 33, no. 23, pp. 6804–6839, Dec. 2008.

[29] E. R. Bobicki, Q. Liu, Z. Xu, and H. Zeng, “Carbon capture and storage using alkaline industrial wastes,” *Prog. Energy Combust. Sci.*, vol. 38, no. 2, pp. 302–320, Apr. 2012.

[30] M. Okawa, N. Kimura, T. Kiga, S. Takano, K. Arai, and M. Kato, “Trial design for a CO2 recovery power plant by burning pulverized coal in O2CO2,” *Energy Convers. Manag.*, vol. 38, pp. S123–S127, Jan. 1997.

[31] F. L. Horn and M. Steinberg, “Control of carbon dioxide emissions from a power plant (and use in enhanced oil recovery),” *Fuel*, vol. 61, no. 5, pp. 415–422, May 1982.

[32] S. Nakayama *et al.*, “Pulverized coal combustion in O2/CO2 mixtures on a power plant for CO2 recovery,” *Energy Convers. Manag.*, vol. 33, no. 5, pp. 379–386, May 1992.

[33] H. Herzog, D. Golomb, and S. Zemba, “Feasibility, modeling and economics of sequestering power plant CO2 emissions in the deep ocean,” *Environ. Prog.*, vol. 10, no. 1, pp. 64–74, Feb. 1991.

[34] D. Y. C. Leung, G. Caramanna, and M. M. Maroto-Valer, “An overview of current status of carbon dioxide capture and storage technologies,” *Renew. Sustain. Energy Rev.*, vol. 39, pp. 426–443, Nov. 2014.

[35] Z. Zhang and D. Huisingh, “Carbon dioxide storage schemes: Technology, assessment and deployment,” *J. Clean. Prod.*, vol. 142, pp. 1055–1064, Jan. 2017.

[36] B. M. Abraham, J. G. Asbury, E. P. Lynch, and A. P. S. Teotia, “Coal-oxygen process provides CO2 for enhanced recovery,” *Oil Gas J.*, vol. 80, no. 11, pp. 68–70, 75, 1982.

[37] G. Scheffknecht, L. Al-Makhadmeh, U. Schnell, and J. Maier, “Oxy-fuel coal combustion—A review of the current state-of-the-art,” *Int. J. Greenh. Gas Control*, vol. 5, no. Supplement 1, pp. S16–S35, Jul. 2011.

[38] B. Leckner and A. Gómez-Barea, “Oxy-fuel combustion in circulating fluidized bed boilers,” *Appl. Energy*, vol. 125, pp. 308–318, Jul. 2014.

[39] Y. Tan, E. Croiset, M. A. Douglas, and K. V. Thambimuthu, “Combustion characteristics of coal in a mixture of oxygen and recycled flue gas,” *Fuel*, vol. 85, no. 4, pp. 507–512, Mar. 2006.

[40] M. B. Toftegaard, J. Brix, P. A. Jensen, P. Glarborg, and A. D. Jensen, “Oxy-fuel combustion of solid fuels,” *Prog. Energy Combust. Sci.*, vol. 36, no. 5, pp. 581–625, Oct. 2010.

[41] T. Fujimori and T. Yamada, “Realization of oxyfuel combustion for near zero emission power generation,” *Proc. Combust. Inst.*, vol. 34, no. 2, pp. 2111–2130, Jan. 2013.

[42] S. Niu, C. Lu, K. Han, and J. Zhao, “Thermogravimetric analysis of combustion characteristics and kinetic parameters of pulverized coals in oxy-fuel atmosphere,” *J. Therm. Anal. Calorim.*, vol. 98, no. 1, pp. 267–274, Oct. 2009.

[43] O. Senneca and L. Cortese, “Kinetics of coal oxy-combustion by means of different experimental techniques,” *Fuel*, vol. 102, pp. 751–759, Dec. 2012.

[44] S. Niu, K. Han, and C. Lu, “Characteristic of coal combustion in oxygen/carbon dioxide atmosphere and nitric oxide release during this process,” *Energy Convers. Manag.*, vol. 52, no. 1, pp. 532–537, Jan. 2011.

[45] A. A. Raeva, N. Dongari, A. A. Artemyeva, E. I. Kozliak, D. T. Pierce, and W. S. Seames, “Experimental simulation of trace element evolution from the excluded mineral fraction during coal combustion using GFAAS and TGA–DSC,” *Fuel*, vol. 124, pp. 28–40, May 2014.

[46] Q. Li, C. Zhao, X. Chen, W. Wu, and Y. Li, “Comparison of pulverized coal combustion in air and in O2/CO2 mixtures by thermo-gravimetric analysis,” *J. Anal. Appl. Pyrolysis*, vol. 85, no. 1–2, pp. 521–528, May 2009.

[47] T. Meriste, C. Yörük, A. Trikkel, T. Kaljuvee, and R. Kuusik, "TG-FTIR analysis of oxidation kinetics of some solid fuels under oxy-fuel conditions," *J. Therm. Anal. Calorim.*, vol. 114, no. 2, pp. 483–489, Nov. 2013.

[48] L. Duan, C. Zhao, W. Zhou, C. Qu, and X. Chen, "O2/CO2 coal combustion characteristics in a 50kWth circulating fluidized bed," *Int. J. Greenh. Gas Control*, vol. 5, no. 4, pp. 770–776, Jul. 2011.

[49] T. Czakiert, K. Sztekler, S. Karski, D. Markiewicz, and W. Nowak, "Oxy-fuel circulating fluidized bed combustion in a small pilot-scale test rig," *Fuel Process. Technol.*, vol. 91, no. 11, pp. 1617–1623, Nov. 2010.

[50] T. Wall *et al.*, "An overview on oxyfuel coal combustion—State of the art research and technology development," *Chem. Eng. Res. Des.*, vol. 87, no. 8, pp. 1003–1016, Aug. 2009.

[51] P. Glarborg, A. D. Jensen, and J. E. Johnsson, "Fuel nitrogen conversion in solid fuel fired systems," *Prog. Energy Combust. Sci.*, vol. 29, no. 2, pp. 89–113, Jan. 2003.

[52] L. Duan, H. Sun, C. Zhao, W. Zhou, and X. Chen, "Coal combustion characteristics on an oxy-fuel circulating fluidized bed combustor with warm flue gas recycle," *Fuel*, vol. 127, pp. 47–51, Jul. 2014.

[53] X. Mingxin, L. Shiyuan, L. Wei, and L. Qinggang, "Effects of Gas Staging on the NO Emission during O2/CO2 Combustion with High Oxygen Concentration in Circulating Fluidized Bed," *Energy Fuels*, vol. 29, no. 5, pp. 3302–3311, May 2015.

[54] G. Hofbauer, T. Beisheim, H. Dieter, and G. Scheffknecht, "Experiences from Oxy-fuel Combustion of Bituminous Coal in a 150 kWth Circulating Fluidized Bed Pilot Facility," *Energy Procedia*, vol. 51, pp. 24–30, Jan. 2014.

[55] L. Duan, C. Zhao, W. Zhou, C. Qu, and X. Chen, "Effects of operation parameters on NO emission in an oxy-fired CFB combustor," *Fuel Process. Technol.*, vol. 92, no. 3, pp. 379–384, Mar. 2011.

[56] S. Jankowska, T. Czakiert, G. Krawczyk, P. Borecki, Ł. Jesionowski, and W. Nowak, "The Effect of Oxygen Staging on Nitrogen Conversion in Oxy-Fuel CFB Environment," *Chem. Process Eng.*, vol. 35, no. 4, pp. 489–496, 2014.

[57] T. Pikkarainen, J. Saastamoinen, H. Saastamoinen, T. Leino, and A. Tourunen, "Development of 2nd Generation Oxyfuel CFB Technology – Small Scale Combustion Experiments and Model Development Under High Oxygen Concentrations," *Energy Procedia*, vol. 63, pp. 372–385, Jan. 2014.

[58] V. White, L. Torrente-Murciano, D. Sturgeon, and D. Chadwick, "Purification of oxyfuel-derived CO2," *Int. J. Greenh. Gas Control*, vol. 4, no. 2, pp. 137–142, Mar. 2010.

[59] P. Basu, "Combustion of coal in circulating fluidized-bed boilers: a review," *Chem. Eng. Sci.*, vol. 54, no. 22, pp. 5547–5557, Nov. 1999.

[60] G. Hu, K. Dam-Johansen, S. Wedel, and J. Peter Hansen, "Review of the direct sulfation reaction of limestone," *Prog. Energy Combust. Sci.*, vol. 32, no. 4, pp. 386–407, Jan. 2006.

[61] W. Li, M. Xu, and S. Li, “Calcium sulfation characteristics at high oxygen concentration in a 1MWth pilot scale oxy-fuel circulating fluidized bed,” *Fuel Process. Technol.*, vol. 171, pp. 192–197, Mar. 2018.

[62] A. Konist *et al.*, “Calculation of the Amount of Estonian Oil Shale Products from Combustion in Regular and Oxy-Fuel Mode in a CFB Boiler,” *Oil Shale*, vol. 31, no. 3, pp. 211–224, Jul. 2014.

[63] S. Rahiala, K. Myöhänen, and T. Hyppänen, “Modeling the behavior of limestone particles in oxy-fuel CFB processes,” *Fuel*, vol. 127, pp. 141–150, Jul. 2014.

[64] T. Czakiert, Z. Bis, W. Muskala, and W. Nowak, “Fuel conversion from oxy-fuel combustion in a circulating fluidized bed,” *Fuel Process. Technol.*, vol. 87, no. 6, pp. 531–538, Jun. 2006.

[65] H. Li *et al.*, “Experimental Results for Oxy-fuel Combustion with High Oxygen Concentration in a 1MWth Pilot-scale Circulating Fluidized Bed,” *Energy Procedia*, vol. 63, pp. 362–371, Jan. 2014.

[66] F. Scala and P. Salatino, “Flue gas desulfurization under simulated oxyfiring fluidized bed combustion conditions: The influence of limestone attrition and fragmentation,” *Chem. Eng. Sci.*, vol. 65, no. 1, pp. 556–561, Jan. 2010.

[67] M. Gómez, A. Fernández, I. Llavona, and R. Kuivalainen, “Experiences in sulphur capture in a 30 MWth Circulating Fluidized Bed boiler under oxy-combustion conditions,” *Appl. Therm. Eng.*, vol. 65, no. 1–2, pp. 617–622, Apr. 2014.

[68] P. Basu, *Combustion and Gasification in Fluidized Beds*. 2006.

[69] J.-L. Fernandez-Turiel, A. Georgakopoulos, D. Gimeno, G. Papastergios, and N. Kolovos, “Ash Deposition in a Pulverized Coal-Fired Power Plant after High-Calcium Lignite Combustion,” *Energy Fuels*, vol. 18, no. 5, pp. 1512–1518, Sep. 2004.

[70] R. Yoshiie *et al.*, “Effects of coal types on ash fragmentation and coalescence behaviors in pulverized coal combustion,” *Proc. Combust. Inst.*, vol. 34, no. 2, pp. 2895–2902, Jan. 2013.

[71] S. Tian, Y. Zhuo, and C. Chen, “Characterization of the Products of the Clay Mineral Thermal Reactions during Pulverization Coal Combustion in Order to Study the Coal Slagging Propensity,” *Energy Fuels*, vol. 25, no. 11, pp. 4896–4905, Nov. 2011.

[72] Y. Wang, S. Lin, and Y. Suzuki, “Study of Limestone Calcination with CO2 Capture: Decomposition Behavior in a CO2 Atmosphere,” *Energy Fuels*, vol. 21, no. 6, pp. 3317–3321, Nov. 2007.

[73] Y. Khraisha and D. Dugwell, “Effect of Water-Vapor on the Calcination of Limestone and Raw Meal in a Suspension Reactor,” *Chem. Eng. Res. Des.*, vol. 69, no. 1, pp. 76–78, Jan. 1991.

[74] J. Yin, X. Kang, C. Qin, B. Feng, A. Veeraragavan, and D. Saulov, “Modeling of CaCO3 decomposition under CO2/H2O atmosphere in calcium looping processes,” *Fuel Process. Technol.*, vol. 125, pp. 125–138, Sep. 2014.

[75] H. Liu, S. Katagiri, U. Kaneko, and K. Okazaki, “Sulfation behavior of limestone under high CO2 concentration in O2/CO2 coal combustion,” *Fuel*, vol. 79, no. 8, pp. 945–953, Jun. 2000.

[76] C. Rodriguez-Navarro, K. Kudlacz, and E. Ruiz-Agudo, “The mechanism of thermal decomposition of dolomite: New insights from 2D-XRD and TEM analyses,” *Am. Mineral.*, vol. 97, no. 1, pp. 38–51, Jan. 2012.

[77] H. Wang, Z.-M. Zheng, L. Yang, X.-L. Liu, S. Guo, and S.-H. Wu, “Experimental investigation on ash deposition of a bituminous coal during oxy-fuel combustion in a bench-scale fluidized bed,” *Fuel Process. Technol.*, vol. 132, pp. 24–30, Apr. 2015.

[78] C. Sheng and Y. Li, “Experimental study of ash formation during pulverized coal combustion in O2/CO2 mixtures,” *Fuel*, vol. 87, no. 7, pp. 1297–1305, Jun. 2008.

[79] L. Fryda, C. Sobrino, M. Glazer, C. Bertrand, and M. Cieplik, “Study of ash deposition during coal combustion under oxyfuel conditions,” *Fuel*, vol. 92, no. 1, pp. 308–317, Feb. 2012.

[80] L. Fryda, C. Sobrino, M. Cieplik, and W. L. van de Kamp, “Study on ash deposition under oxyfuel combustion of coal/biomass blends,” *Fuel*, vol. 89, no. 8, pp. 1889–1902, Aug. 2010.

[81] R. S. Blissett and N. A. Rowson, “A review of the multi-component utilisation of coal fly ash,” *Fuel*, vol. 97, pp. 1–23, Jul. 2012.

[82] S. M. Carpenter and G. Koperna, “Development of the First Internationally Accepted Standard for Geologic Storage of Carbon Dioxide utilizing Enhanced Oil Recovery (EOR) under the International Standards Organization (ISO) Technical Committee TC-265,” *Energy Procedia*, vol. 63, pp. 6717–6729, Jan. 2014.

[83] C. Khan, R. Amin, and G. Madden, “Carbon dioxide injection for enhanced gas recovery and storage (reservoir simulation),” *Egypt. J. Pet.*, vol. 22, no. 2, pp. 225–240, Dec. 2013.

[84] S. Bachu, “Carbon dioxide storage capacity in uneconomic coal beds in Alberta, Canada: Methodology, potential and site identification,” *Int. J. Greenh. Gas Control*, vol. 1, no. 3, pp. 374–385, Jul. 2007.

[85] C. Xu, P. Dowd, and Q. Li, “Carbon sequestration potential of the Habanero reservoir when carbon dioxide is used as the heat exchange fluid,” *J. Rock Mech. Geotech. Eng.*, vol. 8, no. 1, pp. 50–59, Feb. 2016.

[86] N. Wei *et al.*, “Regional resource distribution of onshore carbon geological utilization in China,” *J. CO2 Util.*, vol. 11, pp. 20–30, Sep. 2015.

[87] M. zeinali Hasanvand, M. A. Ahmadi, S. R. Shadizadeh, R. Behbahani, and F. Feyzi, “Geological storage of carbon dioxide by injection of carbonated water in an Iranian oil reservoir: A case study,” *J. Pet. Sci. Eng.*, vol. 111, pp. 170–177, Nov. 2013.

[88] A. Said, H.-P. Mattila, M. Järvinen, and R. Zevenhoven, “Production of precipitated calcium carbonate (PCC) from steelmaking slag for fixation of CO2,” *Appl. Energy*, vol. 112, pp. 765–771, Dec. 2013.

[89] S. Eloneva, A. Said, C.-J. Fogelholm, and R. Zevenhoven, “Preliminary assessment of a method utilizing carbon dioxide and steelmaking slags to produce precipitated calcium carbonate,” *Appl. Energy*, vol. 90, no. 1, pp. 329–334, Feb. 2012.

[90] H.-P. Mattila, H. Hudd, and R. Zevenhoven, “Cradle-to-gate life cycle assessment of precipitated calcium carbonate production from steel converter slag,” *J. Clean. Prod.*, vol. 84, pp. 611–618, Dec. 2014.

[91] N. E. Altun, C. Hiçyilmaz, J.-Y. Hwang, A. Suat BaĞci, and M. V. Kök, “Oil Shales in the World and Turkey; Reserves, Current Situation and Future Prospects: A Review,” *Oil Shale*, vol. 23, no. 3, pp. 211–227, Jul. 2006.

[92] L. Jia, Y. Tan, C. Wang, and E. J. Anthony, “Experimental Study of Oxy-Fuel Combustion and Sulfur Capture in a Mini-CFBC,” *Energy Fuels*, vol. 21, no. 6, pp. 3160–3164, Nov. 2007.

[93] A. Ots, T. Pihu, A. Hlebnikov, and H. Arro, “Influence of sulfur dioxide on decomposition of oil shale mineral matter,” *Oil Shale*, vol. 18, no. 4, pp. 298–306, 2001.

[94] A. Konist, D. Neshumayev, O. Järvik, L. Loo, and M. Maasikmets, “Characterization of Emissions from Oil Shale Oxy-fuel CFB Firing,” presented at the International Conference on Fluidized bed Conversion, Seoul, Korea, 2018, p. 7.

[95] K. Plamus, A. Ots, T. Pihu, and D. Neshumayev, “Firing Estonian Oil Shale in CFB Boilers - Ash Balance and Behaviour of Carbonate Minerals,” *Oil Shale*, vol. 28, no. 1, pp. 58–67, 2011.

[96] K. Plamus, S. Soosaar, A. Ots, and D. Neshumayev, “Firing Estonian Oil Shale of Higher Quality in CFB Boilers - Environmental and Economic Impact,” *Oil Shale*, vol. 28, no. 1S, p. 113, 2011.

[97] C. Yörük, T. Meriste, A. Trikkel, and R. Kuusik, “Thermo-oxidation characteristics of oil shale and oil shale char under oxy-fuel combustion conditions,” *J. Therm. Anal. Calorim.*, vol. 121, no. 1, pp. 509–516, Jul. 2015.

[98] L. Loo, B. Maaten, A. Siirde, T. Pihu, and A. Konist, “Experimental analysis of the combustion characteristics of Estonian oil shale in air and oxy-fuel atmospheres,” *Fuel Process. Technol.*, vol. 134, pp. 317–324, Jun. 2015.

[99] T. F. Wall, “Combustion processes for carbon capture,” *Proc. Combust. Inst.*, vol. 31, no. 1, pp. 31–47, Jan. 2007.

[100] P. Kilpinen, S. Kallio, J. Konttinen, and V. Barišić, “Char-nitrogen oxidation under fluidised bed combustion conditions: single particle studies,” *Fuel*, vol. 81, no. 18, pp. 2349–2362, Dec. 2002.

[101] H. Arro, A. Prikk, and T. Pihu, “Calculation of CO2 Emission from CFB Boilers of Oil Shale Power Plants,” *Oil Shale*, vol. 23, no. 4, pp. 356–365, Oct. 2006.

[102] A. I. Escudero *et al.*, “Minimization of CO2 capture energy penalty in second generation oxy-fuel power plants,” *Appl. Therm. Eng.*, vol. 103, pp. 274–281, Jun. 2016.

List of other publications

- Alar Konist, Birgit Maaten, **Lauri Loo**, Dmitri Neshumayev, and Tõnu Pihu. “Mineral Sequestration of CO_2 by Carbonation of Ca-Rich Oil Shale Ash in Natural Conditions.” Oil Shale 33, no. 3 (juuli 2016): 248–259. https://doi.org/10.3176/oil.2016.3.04.
- Birgit Maaten, **Lauri Loo**, Alar Konist, Dmitri NešUmajev, Tõnu Pihu, and Indrek Külaots. “Decomposition Kinetics of American, Chinese and Estonian Oil Shales Kerogen.” Oil Shale 33, no. 2 (2016): 167–183. https://doi.org/10.3176/oil.2016.2.05.
- Birgit Maaten, **Lauri Loo**, Alar Konist, Tõnu Pihu, and Andres Siirde. “Investigation of the Evolution of Sulphur during the Thermal Degradation of Different Oil Shales.” Journal of Analytical and Applied Pyrolysis 128, no. Supplement C (November 1, 2017): 405–411. https://doi.org/10.1016/j.jaap.2017.09.007.
- Tõnu Pihu, Alar Konist, Dmitri Neshumayev, **Lauri Loo**, Artjom Molodtsov, and Aleksandr Valtsev. “Full-Scale Tests on Co-Firing Peat in a Oil Shale Fired Circulating Fluidized Bed Boiler.” Oil Shale 34, no. 3 (2017): 250–262.
- **Lauri Loo**, Birgit Maaten, Dmitri Neshumayev, and Alar Konist. “Oxygen Influence on Estonian Kukersite Oil Shale Devolatilization and Char Combustion.” Oil Shale 34, no. 3 (July 2017): 219–231. https://doi.org/10.3176/oil.2017.3.02.
- **Lauri Loo**, Alar Konist, and Ron Zevenhoven. “PCC Production from Calcium-Rich Oxy-Fuel CFBC Ash,” 30th International Conference on Efficiency, Cost, Optimization, Simulation and Environmental Impact of Energy Systems, ECOS 2017, 2–6 July 2017, San Diego, USA.
- Birgit Maaten, **Lauri Loo**, Alar Konist, and Andres Siirde. “Mineral Matter Effect on the Decomposition of Ca-Rich Oil Shale.” Journal of Thermal Analysis and Calorimetry 131, no. 3 (March 1, 2018): 2087–2091. https://doi.org/10.1007/s10973-017-6823-1.
- Alar Konist, Dmitri Neshumayev, Oliver Järvik, **Lauri Loo**, and Marek Maasikmets. ’’Characterization of Emissions from Oil Shale Oxy-fuel CFB Firing’’. 23rd International Conference on Fluidized Bed Conversion, 13–17 May 2018, Seoul, Korea.

Acknowledgements

I would like to express my gratitude to my advisors and colleagues at the Department of Energy Technology who contributed to the project.

This research was supported by the European Union through the European Regional Development Fund and by the Estonian Ministry of Education and Research Project AR12003 ‘Reduction of CO_2 emission of CFB boiler by enrichment of combustion air with oxygen’.

Abstract

Experimental Analysis of Combustion Characteristics of Estonian Oil Shale in Regular and Oxy-Fuel Atmospheres

Global energy consumption is increasing, but fossil fuels are still the main source of energy. Firing fossil fuels adds carbon dioxide (CO_2) to the atmosphere, which is believed to be the main cause of global warming. There are different ways of reducing CO_2 emissions from energy production, but this dissertation focuses on investigating oil shale CFB oxy-fuel combustion. The main difference of oxy-fuel combustion from conventional firing is the combustion of fuel in a mixture of oxygen (O_2) and recirculated flue gas instead of air. Combustion occurs in a CO_2-based mixture instead of an N_2 atmosphere. This affects the combustion of organic matter and chemical reactions of the minerals. Instead of the conventional N_2-based flue gas, oxy-fuel combustion generates a concentrated CO_2 stream, which facilitates the future use or storage of CO_2.

Oil shale is the main source of energy and CO_2 emissions in Estonia. It is used for the production of electricity and shale oil itself. Oil shale is a solid fuel containing an organic substance, kerogen, which contains a significant amount of hydrogen. The percentage of Estonian oil shale ash and volatile matter is high. Mineral matter in oil shale contains a significant amount of carbonates, which decompose depending on CO_2 partial pressures. Thus, the application of oxy-fuel technology can reduce the amount of CO_2 produced by the combustion of oil shale.

In this dissertation, the oxy-firing of Estonian oil shale was analysed in a CFB and a series of experiments were performed using a thermogravimetric analyser, a batch-reactor, and a 60 kW circulating fluidised bed combustion (CFBC) test rig. The effect of substitution of nitrogen (N_2) with CO_2 on the combustion of oil shale at various O_2 contents was investigated. During the tests, process progress, emissions, and ash were monitored. The carbon capture ability of ash was investigated and the amount of concentrated CO_2 produced during oxy-fuel combustion was predicted.

The oil shale oxy-fuel ash chemical composition was similar to that of conventional fluidised bed technology ash, with the exception of a significantly higher content of carbonate minerals. The results of the study indicate that because of the increased CO_2 content in the combustion chamber, calcite decomposes at elevated temperatures. Thermogravimetric analyses (TGA) and batch experiments showed that carbonaceous minerals were degraded in one stage during the combustion of oil shale in air, but by two separate reaction steps in the oxy-fuel mode: decomposition of dolomite ($CaMg(CO_3)_2$) and then decomposition of calcite ($CaCO_3$).

Tests in the batch reactor showed that higher CO_2 levels in the combustion chamber and only partial calcite degradation could affect sulfur binding and formation of anhydride. This may result in an increase in sulfur dioxide content of the flue gas, which may give rise to difficulties in the further treatment of CO_2.

The TGA of oil shale oxy-fuel combustion showed that the combustion of oil shale was slower. When the O_2 content in the oxidising mixture was increased, the differences between the normal and oxy-fuel combustion decreased. Experiments on a CFB combustor showed that when firing Estonian oil shale in a gas mixture where N_2 was replaced by CO_2, the temperature in the furnace decreased, as previous studies predicted. Increasing the O_2 content of the oxidant to 30% results in a furnace with a temperature field similar to that in the test using air as an oxidiser.

The concentration of pollutant measured in the combustion of oil shale in CFB in flue gas remained at the level as in ordinary oil shale combustion. Therefore, no additional sulfur or NO_x removal equipment is required before CO_2 utilisation. Rapid tests of ash wet landfilling have shown that oil shale oxy-fuel combustion ashes bind CO_2. Ash from oxy-fuel combustion sequestrated 5.5 t CO_2/TJ of fuel. This is a little more than the ash generated in PC, but less than the conventional CFB ash. The degradation of decomposition of carbonates should inhibit the ability of ash CO_2 binding, but previous studies have shown that the capability of carbon capture of ash depends strongly on the properties of the ash surface, which is determined by the combustion environment.

There are some additional costs for oxy-fuel combustion: O_2 production, flue gas recirculation, and formed CO_2 compression for transportation or other use. The calculations performed based on experiments showed that oxy-fuel firing the same amount of oil shale would produce less CO_2 than conventional fluidised bed combustion. However, because of the aforementioned additional costs, the same amount of electricity generated by oxy-fuel combustion generates a little more CO_2 than that in conventional CFBC.

The oxy-fuel combustion of Estonian oil shale was previously studied only by models and TGA. This dissertation is based on five high-level scientific articles describing and analysing the oil shale oxy-burning nuance. For the first time, real oxy-fuel combustion experiments were carried out in a CFB using Estonian oil shale and enough ashes were produced to assess the impact of the new technology. Future studies should investigate the effect of increasing the O_2 content in oxidiser. It can accelerate combustion whereas the circulating ash can maintain an optimum combustion environment and increase the capacity of the combustion plant of the same size. Another nuance that needs to be investigated is the effect of oil shale ash and oxy-fuel combustion on corrosion and formation of deposits on heat exchange surfaces. The formation of deposits and corrosion can greatly increase the operation cost of the combustion plant. Another interesting topic is oil shale and biomass co-firing in oxy-fuel CFB. This solution can lead to negative CO_2 net emissions, because CO_2 from biomass is considered neutral.

Lühikokkuvõte

Eesti põlevkivi põlemiskarakteristikute eksperimentaalne analüüs tavalises ja *oxy-fuel* keskkonnas

Globaalne energiatarbimine kasvab ja kogu maailmas on fossiilsed kütused olnud peamiseks energiaallikaks. Fossiilkütuste põletamise tõttu lisandub atmosfääri süsinikdioksiid, mis peetakse peamiseks globaalse soojenemise põhjustajaks. Energiatootmise CO_2 heitkoguste vähendamiseks on erinevaid võimalusi, ent käesolev väitekiri keskendub põlevkivi *oxy-fuel* põletamise uurimisele. Peamine *oxy*-põletamise erinevus konventsionaalsest põletamistehnoloogiast on kütuse põletamine õhu asemel hapniku ja retsirkuleeritud suitsugaasi segus, mis tähendab, et põlemine toimub lämmastiku keskkonna asemel süsihappegaasis. See mõjutab orgaanilise aine põlemist ja keemilisi reaktsioone mineraalses osas. Tavapärase lämmastikupõhise suitsugaasi asemel tekib *oxy*-põletamisel kontsentreeritud süsihappegaasi voog, mis hõlbustab CO_2 edaspidist kasutamist või ladestamist.

Põlevkivi on peamine energia- ja CO_2 heitmete allikas Eestis. Seda kasutatakse elektri ja põlevkiviõli tootmiseks. Põlevkivi on tahke kütus, mis sisaldab orgaanilist ainet, kerogeeni. Eesti põlevkivi lendosade ja tuha sisaldus on suur. Põlevkivi mineraalne osa sisaldab märkimisväärses koguses karbonaatseid mineraale, mille lagunemise temperatuur sõltub süsihappegaasi osarõhust. Kuna *oxy*-põletamisel on koldes oluliselt suurem süsihappegaasi kontsentratsioon, võib selle tehnoloogia rakendamine vähendada põlevkivi põletamisel moodustuva CO_2 kogust.

Käesoleva dissertatsiooni raames analüüsiti Eesti põlevkivi *oxy*-põletamist tsirkuleerivas keevkihis ja viidi läbi katseid, kasutades termogravimeetrilist analüsaatorit, portsjon-reaktorit ja 60 kW tsirkuleeriva keevkihiga põletusseadet. Uuriti lämmastiku süsinikdioksiidiga asendamise mõju põlevkivi põlemisele erinevate hapnikusisalduste juures. Katsete käigus jälgiti protsessi kulgu, tekkinud gaasilisi heitmeid ja tuhkasid. Uuriti tekkinud tuha süsihappegaasi sidumise võimet ja ennustati *oxy*-tehnoloogia rakendamisel tekkiva kontsentreeritud süsihappegaasi kogust.

Põlevkivi *oxy*-põletamisel tekkinud tuha keemiline koostis sarnanes tavalise keevkiht tehnoloogia tuhaga, välja arvatud oluliselt kõrgem karbonaatsete mineraalide sisaldus. Uuringu tulemused näitasid, et suurenenenud süsihappegaasi sisalduse tõttu põlemiskambris laguneb kaltsiit kõrgemal temperatuuril. Termogravimeetrilised analüüsid ja portsjon-eksperimendid näitasid, et põlevkivi põletamisel õhus lagunesid karbonaatsed mineraalid ühes etapis, kuid *oxy*-põletamisel toimus protsess kahe eraldiseisva reaktsioonina: kõigepealt dolomiidi ($CaMg(CO_3)_2$) lagunemine ja seejärel kaltsiidi ($CaCO_3$) lagunemine.

Põlevkivi *oxy*-põlemise termogravimeetriline analüüs näitas, et põlemise protsess aeglustus. Kui hapnikusisaldust oksüdeerivas segus tõsteti, siis erinevused tavalise ja *oxy*-põletuse vahel kahanesid. Katsed tsirkuleerivas keevkiht põletusseadmes näitasid, et Eesti põlevkivi *oxy*-põletamisel gaasisegus, kus lämmastik oli asendatud süsihappegaasiga, langes temperatuur koldes, nii nagu eelnevad uuringud termogravimeetrilise analüsaatoriga ennustasid. Oksüdandi hapnikusisalduse suurendamine 30% tekitas tsirkuleeriva keevkiht katseseadme koldes samasuguse temperatuurivälja nagu katsetel, kus kasutati oksüdeerijana õhku.

Katsed portsjon-reaktoril näitasid, et kõrgem süsinikdioksiidi sisaldus põlemiskambris ja vaid osaline kaltsiidi lagunemine võivad mõjutada väävli sidumist ja anhüdriidi moodustumist. Kuid põlevkivi tsirkuleerivas keevkihis põletamisel mõõdetud

saasteainete kontsentratsioon suitsugaasis jäi põlevkivi tavapärase põletamise tasemele. Seega ei ole enne CO_2 kasutamist või transportimist tarvis täiendavaid väävli või lämmastiku oksiidide eemaldamise seadmeid.

Tuha märgladustamise kiirkatsed näitasid, et põlevkivi *oxy*-põletamise tuhk seob süsihappegaasi. *Oxy*-põletamisel tekkinud tuhk sidus 5,5 t CO_2/TJ kütuse kohta. See on veidi rohkem kui põlevkivi tolmpõletusel tekkinud tuhad, kuid vähem kui tavalise tsirkuleeriva keevkiht põletamise tuhad. Vähenenud karbonaatide lagunemine peaks pärssima tuha süsihappegaasi sidumise võimet, kuid juba varasemad uuringud on näidanud, et see sõltub tugevalt tuha välispinna omadustest, mis on defineeritud põlemiskeskkonnaga.

Oxy-põletamisel on mõningad lisakulud: hapniku tootmine, suitsugaaside retsirkulatsioon ja moodustunud süsinikdioksiidi komprimeerimine transportimiseks või muuks kasutamiseks. Katsete põhjal teostatud arvutused näitasid, et sama koguse põlevkivi *oxy*-põletamisel moodustub vähem süsihappegaasi kui tavalisel keevkihtpõletamisel. Kuid eelnevalt loetletud lisakulude tõttu tekib *oxy*-põletamisel sama koguse elektri tootmisel veidi rohkem süsihappegaasi kui tavalist ringlevat keevkihtpõletamist ekspluateerides. Sellegi poolest tekib kontsentreeritud süsihappegaasi voog, mille edaspidine kasutamine on juba oluliselt lihtsam kui tavalise suitsugaasi käitlemine.

Eesti põlevkivi *oxy*-põletamist oli eelnevalt uuritud vaid mudelite ja termogravimeetrilise analüüsi abil. See dissertatsioon põhineb viiel kõrgetasemelisel teadusartiklil, mis kirjeldasid ja analüüsisid Eesti põlevkivi *oxy*-põletamise nüansse. Esmakordselt teostati reaalsed *oxy*-põletamise katsed tsirkuleerivas keevkihis kasutades Eesti põlevkivi, ja toodeti piisavalt tuhka, et hinnata uudse tehnoloogia mõju.

Edaspidistes uuringutes võiks uurida kuidas mõjub hapniku sisalduse suurendamine *oxy*-põlemisele. See võib kiirendada põlemist, kui samal ajal reguleerida ringleva tuha temperatuuri võib säilitada optimaalse temperatuuri ja suurendada samade mõõtmetega põletusseadme võimsust. Teine uurimist vajav nüanss on põlevkivituha ja *oxy*-põlemiskeskkonna mõju korrosioonile ja sadestiste moodustumisele soojusvahetuspindadele. Sadestiste teke ja korrosioon võivad oluliselt raskendada põletusseadme opereerimist. Maaimas tuntakse huvi biokütuste *oxy*-tehnoloogia abil koospõletamise vastu, selline lahendus võib viia negatiivse süsinikdioksiidi heitkoguseni, kuna biomassist pärinevat süsinikdioksiidi loetakse neutraalseks.

APPENDIX

Paper I

Alar Konist, **Lauri Loo**, Aleksandr Valtsev, Birgit Maaten, Andres Siirde, Dmitri Neshumayev, and Tõnu Pihu. “Calculation of the Amount of Estonian Oil Shale Products from Combustion in Regular and Oxy-Fuel Mode in a CFB Boiler.” Oil Shale 31, no. 3 (July 2014): 211–224. doi:10.3176/oil.2014.3.02.

Oil Shale, 2014, Vol. 31, No. 3, pp. 211–224
doi: 10.3176/oil.2014.3.02

ISSN 0208-189X

CALCULATION OF THE AMOUNT OF ESTONIAN OIL SHALE PRODUCTS FROM COMBUSTION IN REGULAR AND OXY-FUEL MODE IN A CFB BOILER

ALAR KONIST*, LAURI LOO, ALEKSANDR VALTSEV, BIRGIT MAATEN, ANDRES SIIRDE, DMITRI NESHUMAYEV, TÕNU PIHU

Department of Thermal Engineering, Tallinn University of Technology, Ehitajate tee 5, 19086 Tallinn, Estonia

Abstract. *Oxy-fuel combustion is considered as one of the promising carbon capture and storage (CCS) technologies for coal-fired boilers. In oxy-fuel combustion, the combustion gases are oxygen and the recirculating flue gas, and the main components of the combustion gas are* O_2, CO_2 *and* H_2O *[1].*

The paper presents the results of the calculation of the flue gas amount during combustion of oil shale using oxy-fuel technology in a circulated fluidized bed (CFB) mode. The calculations were performed for different oil shale heating values and different recycled flue gas (RFG) ratios. Oxy-fuel combustion with flue gas recycling was found to enable the decrease of the extent of carbonate minerals decomposition (ECD), thereby increasing the amount of heat released per 1 kg of fuel. To minimize ECD, the recycled flue gas ratio should be maintained at a level higher than 0.7. This condition allows an increase of the partial pressure of CO_2 *over the equilibrium state line of calcite decomposition reaction at the bed temperature. The decrease of ECD was observed up to* $k_{\mathrm{CO2\text{-}min}} = 0.28$. *The decrease of* k_{CO2} *leads to an additional increase in the amount of heat released during oil shale combustion per 1 kg and, depending on the mean lower heating value (LHV), the heat can be increased up to 0.34 MJ/kg.*

A comparison with the bituminous and anthracite coals revealed that the specific emission of CO_2 *per input fuel energy for oil shale is expected to be even smaller compared with those of the considered coals.*

Keywords: *oil shale, oxy-fuel combustion, extent of carbonate minerals decomposition, CFB,* CO_2 *emission.*

---

* Corresponding author: e-mail *alar.konist@ttu.ee*

1. Introduction

Currently, there seems to be no good alternative to coal power in the near future. Energy demand and CO_2 emissions continue to increase [2]. Coal-fired energy generation, which rose by an estimated 6% from 2010 to 2012, continues to grow faster than non-fossil energy sources on an absolute basis. Approximately half of the coal-fired power plants built in 2011 use inefficient technologies [3].

Improving the performance of coal-fired power plants can significantly reduce the CO_2 emissions [4, 5]. A unit operating at the global average efficiency would emit over 1000 g CO_2/kWh, whereas the best units working with ultra-supercritical steam conditions reduce this to closer to 740 g CO_2/kWh [2].

The next step beyond improving the efficiency is the implementation of carbon dioxide carbon capture and storage (CCS), that is, a set of technologies that can significantly reduce the CO_2 emissions from new and existing coal- and gas-fired power plants [2, 6]. Current available CCS technologies are: post-combustion CO_2 capture, pre-combustion CO_2 capture, chemical looping combustion and oxy-fuel combustion [5, 7, 8]. The captured carbon dioxide can be used for enhanced oil recovery or stored in depleted oil and gas reservoirs, coal beds, deep saline aquifers, etc. [9, 10].

Oxy-fuel combustion is seen as one of the major options for CO_2 capture for future clean coal technologies [6, 11]. Oxy-fuel combustion technology is considered to be the most energy- and cost-efficient of the carbon capture technologies [12–18]. The concept of oxy-fuel technology is the removal of nitrogen from oxidizer to perform the combustion process in an oxygen and recycled flue gas environment to decrease the combustion temperature [19]. As a result, the flue gas formed primarily consists of carbon dioxide and water [9].

Oxy-fuel combustion in a CFB for CO_2 capture has been rarely studied so far [20–28]. Most of those studies considered bituminous coals and lignites, and some of the studies considered biomass fuels. There is only one study dealing with oil shale [29]. The main part of these experimental and theoretical investigations covers the pulverized firing technology.

Estonia has no coal reserves; however, it has an unconventional fuel – oil shale. Oil shale is a sedimentary rock that contains organic matter called kerogen. The organic matter of oil shale contains relatively large amounts of carbon (up to $30\%_{dry}$), hydrogen (up to $3.8\%_{dry}$), and oxygen (up to $3.9\%_{dry}$). Oil shale has high contents of mineral matter, which consists of carbonaceous, sandy-clay-carbonaceous and sandy-clay parts. Oil shale is characterized as a fuel with a high content of sulfur (up to $2\%_{dry}$ including organic and pyritic sulfur), alkali metals and chlorine.

Oil shale is Estonia's primary energy resource, with approximately 90% of the electricity consumed is produced from oil shale. Today, the country's oil shale usage is the largest in the world. Most of the oil shale, approximately 12 million tons yearly, is used for power generation through the use of CFBC and pulverized combustion (PC) technologies [30]. Oil shale burned in power plants has the following proximate characteristics: W_i^r = 11–13% (moisture, as received fuel), A^r = 45–57% (ash content, as received fuel), CO_2 = 16–19% (carbonate CO_2 content, as received fuel), and Q_i^r = 8.3–8.7 MJ/kg (heating value, as received fuel). The molar ratio of Ca/S of 8–10 in oil shale exceeds by over 2–3 times the ratio of Ca/S sufficient to capture SO_2 completely [5]. Oil shale contains many carbonate minerals. Due to decomposition of carbonate minerals, the CO_2 footprint is larger than that of a typical coal firing power plant. The decomposition rate of carbonates in a PC boiler is 0.97, and the rate in a CFB boiler 0.68, depending on the fuel LHV and properties. The specific emission of CO_2 for PC and CFB is 974 g CO_2/kWh and 872 g CO_2/kWh, respectively. The specific emission of SO_2 for PC and CFB is 11.89 g SO_2/kWh and zero, respectively [31, 32].

CFB combustion is considered to be one of the best solutions for the use of low grade high ash fuels, such as oil shale. In the CFB boiler, the temperature is controlled using the circulating bed material, which is cooled in an external heat exchanger. The CFB units firing oil shale do not require a sophisticated burner design and management, and they do not require $DeNO_x$ and $DeSO_x$ facilities; therefore, it is considerably easier to retrofit an existing CFB boiler with the oxy-fuel combustion technology.

This study provides the first theoretical preliminary results of oil shale combustion in a CFB boiler applying oxy-fuel technology. The goal of this research was to determine the gas volumes in different parts of the CFB boiler at different recycled flue gas ratios. The comparisons with the bituminous and anthracite coals are also presented.

2. Initial data and the calculation methodology

The combustion calculations were performed for oil shale with varying LHV from 7 to 11.5 MJ/kg. To obtain the corresponding results of the proximate and ultimate analysis data for the oil shale, the method described in [33, 34] was used. The quantitative theoretical analysis method is based on the research experience that has proven to have a statistically significant relationship between the heating value (HV) and the proximate/ultimate analysis data for the Estonian oil shale. Therefore, knowing the oil shale HV, it is possible to calculate the average fuel characteristics, such as the ash and CO_2 contents, the organic part distribution and the average mineralogical composition. The results of the calculation are listed in Table 1. The detailed description of the theoretical methods can be found in [33, 34].

To determine the stoichiometric amount of oxygen required to oxidize inorganic FeS_2, the following reaction was taken into account:

$$4FeS_2 + 11O_2 \rightarrow 2Fe_2O_3 + 8SO_2 \quad (1)$$

During oil shale firing, the amount of heat released and the amount of ash formed in combustion per mass unit of fuel is significantly affected by the endothermic and exothermic processes occurring in the mineral matter. The main thermal effects are related to the decomposition of oil shale calcite and dolomite, FeS_2 oxidation, and sulfation of CaO. The extent of these reactions affects the amount of heat released, the amount of ash and combustion products produced and ultimately the flue gas composition. In PC boilers, almost complete decomposition of the oil shale carbonate minerals occurs. The extent of carbonate minerals decomposition (ECD) can be as high as 0.97, $k_{CO2} \approx 0.97$ [33], which is mainly due to the high combustion temperature (1400–1500 °C) and certainly due to the low partial pressure of CO_2 and small particle size of the fuel. However, under CFB combustion conditions, incomplete decomposition of carbonates is observed ($k_{CO2} \approx 0.6–0.8$), which is mainly due to the relatively low temperature compared to PC systems, due to the slow kinetics of decomposition in the furnace and due to the coarse particle size of the parent fuel resulting in the decrease of the carbonate originated CO_2 content in the flue gas [34].

An additional decrease of ECD would be expected when applying oxy-fuel combustion technology in CFB boilers. This effect is primarily attributed to the significant increase of the CO_2 partial pressure in the flue gas, which exceeds the equilibrium state line of the calcite $CaCO_3$ decomposition.

Under these conditions, the thermal decomposition of dolomite would be observed by the following reaction because it is not correlated with the CO_2 partial pressure:

$$CaMg(CO_3)_2 \rightarrow CaCO_3 + MgO + CO_2 \qquad (2)$$

In addition, in oxy-fuel mode, the CO_2 content in the flue gas increases. The sulfur is bound with CaO or most likely directly bound with $CaCO_3$.

Accounting for all the above, and assuming that the CO_2 formation from dolomite is approximately 16% of the total mineral CO_2 in the fuel [35], the minimum amount of carbonate CO_2 released during thermal decomposition and sulfur capture was calculated as follows:

$$V_{CO_2\text{-carb}} = 0.00509 k_{CO_2\text{-min}} (CO_2)^{r}_{M}, \qquad (3)$$

$$k_{CO_2\text{-min}} = 1.375 S^{d}_{p} k_{s} / (CO_2)^{d}_{M} + 0.16, \qquad (4)$$

where

$V_{CO_2\text{-carb}}$ – minimum amount of carbonate CO_2 formed by decomposition of carbonates, nm^3/kg;

$k_{CO_2\text{-min}}$ – minimum extent of carbonate decomposition;

$(CO_2)^{r}_{M}$ – carbonate CO_2 content of as received fuel, %;

S^{d}_{p} – content of pyrite (marcasite) sulfur in dry fuel, %;

k_{s} – extent of sulfur binding in the boiler;

$(CO_2)^{d}_{M}$ – carbonate CO_2 content of dry fuel, %.

During the calculation of the specific parameters related to LHV, the sulfur capture was corrected as follows. In the case of oil shale the LHV is a conditional value representing the amount of heat released during the combustion of 1 kg fuel under conditions when carbonate minerals decompose completely ($k_{CO2} = 1$), the formation of calcium sulfate does not occur ($k_s = 0$) and new minerals are not formed. However, in practice, the conditional heating value is widely used, where the extent of the sulfation is not directly determined by detailed analysis of the ash contained in a calorimetric bomb. In this case, it is assumed that during combustion of oil shale in a calorimetric bomb, $k_s = 0.4$. In the present study, the thermal effects due to both the incomplete decomposition of carbonaceous minerals and the calcium sulfate formation were taken into account.

Table 1. Calculated proximate and ultimate oil shale fuel characteristics

LHV (ar) Q^r_i, MJ/kg	7.0	7.5	8.0	8.5	9.0	9.5	10.0	10.5	11.0	11.5
Ash A^d, $\%_{dry}$	53.64	52.78	51.96	51.16	50.40	49.67	48.98	48.32	47.70	47.11
Water W^r_t, $\%_{ar}$	10.60	10.94	11.27	11.60	11.94	12.27	12.61	12.94	13.28	13.61
Content of the organic part R^d, $\%_{dry}$										
C^d	19.69	21.00	22.31	23.63	24.94	26.25	27.56	28.87	30.18	31.49
H^d	2.47	2.63	2.79	2.96	3.12	3.29	3.45	3.62	3.78	3.94
S^d_o	0.45	0.48	0.51	0.54	0.57	0.60	0.63	0.66	0.69	0.72
N^d	0.08	0.09	0.10	0.10	0.11	0.11	0.12	0.12	0.13	0.13
Cl^d	0.19	0.20	0.22	0.23	0.24	0.25	0.27	0.28	0.29	0.30
O^d	2.54	2.71	2.88	3.05	3.22	3.39	3.56	3.73	3.90	4.07
Total, R^d	25.42	27.11	28.81	30.50	32.20	33.89	35.59	37.28	38.97	40.66
Content of the carbonate part K^d, $\%_{dry}$										
CaO^d	23.09	22.56	21.95	21.24	20.44	19.54	18.55	17.44	16.24	14.93
MgO^d	3.17	3.10	3.01	2.92	2.81	2.68	2.54	2.39	2.23	2.05
FeO^d	0.10	0.09	0.09	0.09	0.09	0.08	0.08	0.07	0.07	0.06
Carbonate $CO_2{}^d$	21.65	21.16	20.58	19.92	19.17	18.33	17.39	16.36	15.23	14.00
Total, K^d	47.99	46.91	45.64	44.17	42.50	40.63	38.56	36.27	33.76	31.04
Content of the sandy-clay part L^d, $\%_{dry}$										
$SiO_2{}^d$	15.90	15.53	15.28	15.15	15.13	15.23	15.46	15.82	16.30	16.92
CaO^d	0.19	0.18	0.18	0.18	0.18	0.18	0.18	0.19	0.19	0.20
$Al_2O_3{}^d$	4.28	4.18	4.11	4.08	4.07	4.10	4.16	4.26	4.39	4.56
$Fe_2O_3{}^d$	0.74	0.73	0.72	0.71	0.71	0.71	0.72	0.74	0.76	0.79
$TiO_2{}^d$	0.19	0.18	0.18	0.18	0.18	0.18	0.18	0.19	0.19	0.20
MgO^d	0.11	0.10	0.10	0.10	0.10	0.10	0.10	0.11	0.11	0.11
Na_2O^d	0.21	0.21	0.20	0.20	0.20	0.20	0.21	0.21	0.22	0.23
K_2O^d	1.68	1.64	1.61	1.60	1.59	1.60	1.63	1.67	1.72	1.78
$FeS_2{}^d$	2.47	2.42	2.38	2.36	2.35	2.37	2.40	2.46	2.54	2.63
Sulfate sulfur, $SO_3{}^d$	0.13	0.13	0.13	0.13	0.13	0.13	0.13	0.13	0.14	0.14
Crystal water, H_2O^d	0.69	0.68	0.66	0.66	0.66	0.66	0.67	0.69	0.71	0.74
Total, L^d	26.59	25.98	25.55	25.33	25.30	25.47	25.86	26.45	27.26	28.30
Total, $R^d + K^d + L^d$	100	100	100	100	100	100	100	100	100	100

The calculations of the flue gas volumes in the oxy-fuel combustion of oil shale were performed for a steady state regime, implementing the process for which the schematic diagram is shown in Figure 1. The recycled flue gas

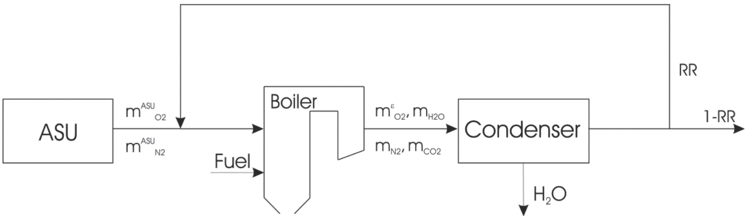

Fig. 1. Schematic of the proposed oxy-fuel combustion process.

(RFG) stream was assumed to be taken after the water vapor condenser. To simplify the calculations, the water content in the gases after the condenser was assumed to be 0.05 kg_{H_2O} per kg of fuel burned.

The flue gas recycle ratio was defined as the ratio of the mass of the recycled flue gas stream m_{RFG} to the total mass of flue gas at the boiler outlet:

$$\text{RFG ratio} \equiv \text{RR} = \frac{m_{\text{RFG}}}{m_{\text{RFG}} + m_{\text{PFG}}}, \tag{5}$$

where m_{PFG} is the mass of the product flue gas stream.

In addition, based on an overview article [9], the oxygen content in flue gas after the air separation unit was assumed to be $95\%_{\text{vol}}$, with $5\%_{\text{vol}}$ of nitrogen and argon. The oil shale calculations were performed for an excess O_2 constant value of $5\%_{\text{vol}}$ at the boiler outlet. In the steady state regime, the mass CO_2 content per kg fuel m_{CO_2} at the boiler outlet for different RFG ratios was calculated as follows:

$$m_{\text{CO}_2} = \frac{m_{\text{CO}_2}^{\text{F}}}{1 - RR}, \tag{6}$$

where $m_{\text{CO}_2}^{\text{F}}$ is the total mass of CO_2 occurring during combustion of 1 kg oil shale, including CO_2 from organic carbon combustion and calculated according to Equation (3) CO_2 from carbonate minerals decomposition.

The nitrogen content at the boiler outlet can be determined from:

$$m_{\text{N}_2} = \frac{m_{\text{N}_2}^{\text{ASU}} + m_{\text{N}_2}^{\text{F}}}{1 - RR}, \tag{7}$$

where m_{N_2} is the specific amount of N_2 from fuel nitrogen, and $m_{\text{N}_2}^{\text{ASU}}$ is the N_2 coming from the air separation unit (ASU), calculated as:

$$m_{\text{N}_2}^{\text{ASU}} = \left(m_{\text{O}_2}^{\text{St}} + m_{\text{O}_2}^{\varepsilon}(1 - RR)\right)\frac{k_{\text{N}_2}^{\text{ASU}}}{k_{\text{O}_2}^{\text{ASU}}}, \tag{8}$$

where $m_{\mathrm{O}_2}^{\mathrm{St}}$ is the stoichiometric amount of O_2, $m_{\mathrm{O}_2}^{\varepsilon}$ is the excess amount of O_2 at the boiler outlet, $m_{\mathrm{N}_2}^{\mathrm{ASU}}$ is the mass fraction of N_2 at the ASU outlet, and $k_{\mathrm{O}_2}^{\mathrm{ASU}}$ is the mass fraction of O_2 at the ASU outlet.

The calculated gas characteristics at the boiler outlet and inlet for different LHV values are presented in Tables 2, 3 and 4. In the tables to each RFG ratio there corresponds a different amount of circulating ash, used to

Table 2. Gas characteristics at the boiler outlet and inlet for LHV = 8.4 MJ/kg

RFG ratio	kg/kg	0.1	0.2	0.3	0.4	0.5	0.6	0.7	0.8	0.9
At the boiler outlet										
Excess O_2 content	Nm^3/kg	0.03	0.03	0.03	0.04	0.05	0.06	0.08	0.12	0.23
CO_2 content	Nm^3/kg	0.45	0.51	0.58	0.68	0.82	1.02	1.36	2.04	4.08
Nitrogen content	Nm^3/kg	0.03	0.04	0.04	0.05	0.06	0.08	0.10	0.15	0.31
H_2O content	Nm^3/kg	0.45	0.45	0.46	0.46	0.47	0.47	0.48	0.48	0.49
Flue gas amount, dry	Nm^3/kg	0.51	0.58	0.66	0.77	0.92	1.16	1.54	2.31	4.62
Excess O_2 content	%	5.00	5.00	5.00	5.00	5.00	5.00	5.00	5.00	5.00
CO_2 content	%	47.13	49.47	52.11	55.13	58.61	62.65	67.39	73.05	79.90
Flue gas amount, wet	Nm^3/kg	0.96	1.03	1.12	1.23	1.39	1.63	2.02	2.80	5.11
CO_2 amount	t/MWh	0.027	0.031	0.035	0.041	0.049	0.062	0.082	0.124	0.247
At the boiler inlet										
CO_2 content	Nm^3/kg	0.05	0.10	0.18	0.27	0.41	0.61	0.95	1.63	3.68
N_2 content	Nm^3/kg	0.03	0.04	0.04	0.05	0.06	0.08	0.10	0.15	0.31
H_2O content	Nm^3/kg	0.01	0.01	0.02	0.02	0.03	0.03	0.04	0.04	0.05
O_2 content	Nm^3/kg	0.56	0.56	0.56	0.57	0.58	0.59	0.61	0.65	0.76
Total gas amount	Nm^3/kg	0.64	0.71	0.80	0.91	1.07	1.31	1.70	2.47	4.79
CO_2 content	%	7.08	14.38	21.94	29.83	38.11	46.84	56.12	66.05	76.74
O_2 content	%	86.92	78.90	70.76	62.44	53.89	45.05	35.83	26.16	15.92

Table 3. Gas characteristics at the boiler outlet and inlet for LHV = 7.0 MJ/kg

RFG ratio	kg/kg	0.1	0.2	0.3	0.4	0.5	0.6	0.7	0.8	0.9
At the boiler outlet										
Excess O_2 content	Nm^3/kg	0.02	0.02	0.03	0.03	0.04	0.05	0.07	0.10	0.20
CO_2 content	Nm^3/kg	0.39	0.44	0.50	0.59	0.71	0.88	1.18	1.76	3.53
Nitrogen content	Nm^3/kg	0.03	0.03	0.04	0.04	0.05	0.07	0.09	0.13	0.26
H_2O content	Nm^3/kg	0.39	0.40	0.40	0.41	0.41	0.42	0.42	0.43	0.43
Flue gas amount, dry	Nm^3/kg	0.44	0.50	0.57	0.67	0.80	1.00	1.33	2.00	3.99
Excess O_2 content	%	5.00	5.00	5.00	5.00	5.00	5.00	5.00	5.00	5.00
CO_2 content	%	46.87	49.18	51.80	54.80	58.26	62.31	67.08	72.79	79.75
Flue gas amount, wet	Nm^3/kg	0.84	0.90	0.97	1.07	1.21	1.42	1.75	2.42	4.42
CO_2 amount	t/MWh	0.028	0.031	0.036	0.042	0.050	0.063	0.084	0.125	0.251
At the boiler inlet										
CO_2 content	Nm^3/kg	0.04	0.09	0.15	0.24	0.35	0.53	0.82	1.41	3.17
N_2 content	Nm^3/kg	0.03	0.03	0.04	0.04	0.05	0.07	0.09	0.13	0.26
H_2O content	Nm^3/kg	0.01	0.01	0.02	0.02	0.03	0.03	0.04	0.04	0.05
O_2 content	Nm^3/kg	0.48	0.48	0.48	0.49	0.50	0.51	0.52	0.56	0.65
Total gas amount	Nm^3/kg	0.55	0.61	0.69	0.79	0.93	1.13	1.47	2.14	4.14
CO_2 content	%	7.12	14.44	22.01	29.88	38.14	46.85	56.11	66.03	76.74
O_2 content	%	86.76	78.63	70.42	62.08	53.53	44.72	35.57	25.97	15.83

Table 4. Gas characteristics at the boiler outlet and inlet for LHV = 10.5 MJ/kg

RFG ratio	kg/kg	0.1	0.2	0.3	0.4	0.5	0.6	0.7	0.8	0.9
At the boiler outlet										
Excess O_2 content	Nm^3/kg	0.03	0.03	0.04	0.05	0.06	0.07	0.09	0.14	0.28
CO_2 content	Nm^3/kg	0.54	0.61	0.70	0.82	0.98	1.22	1.63	2.45	4.89
Nitrogen content	Nm^3/kg	0.04	0.05	0.05	0.06	0.07	0.09	0.12	0.19	0.37
H_2O content	Nm^3/kg	0.53	0.54	0.54	0.55	0.55	0.56	0.56	0.57	0.57
Flue gas amount, dry	Nm^3/kg	0.62	0.69	0.79	0.92	1.11	1.39	1.85	2.77	5.54
Excess O_2 content	%	5.00	5.00	5.00	5.00	5.00	5.00	5.00	5.00	5.00
CO_2 content	%	47.38	49.74	52.42	55.46	58.94	62.98	67.70	73.30	80.03
Flue gas amount, wet	Nm^3/kg	1.15	1.23	1.33	1.47	1.66	1.94	2.41	3.34	6.11
CO_2 amount	t/MWh	0.027	0.030	0.035	0.041	0.049	0.061	0.081	0.122	0.243
At the boiler inlet										
CO_2 content	Nm^3/kg	0.05	0.12	0.21	0.33	0.49	0.73	1.14	1.96	4.40
N_2 content	Nm^3/kg	0.04	0.05	0.05	0.06	0.07	0.09	0.12	0.19	0.37
H_2O content	Nm^3/kg	0.01	0.01	0.02	0.02	0.03	0.03	0.04	0.04	0.05
O_2 content	Nm^3/kg	0.67	0.68	0.68	0.69	0.70	0.71	0.74	0.78	0.92
Total gas amount	Nm^3/kg	0.77	0.86	0.96	1.10	1.29	1.57	2.04	2.96	5.74
CO_2 content	%	7.02	14.28	21.84	29.73	38.02	46.78	56.08	66.02	76.71
O_2 content	%	87.11	79.22	71.16	62.88	54.32	45.44	36.15	26.39	16.04

control the furnace temperature, as the adiabatic combustion temperature depends on both the heating value of the fuel and the concentration of O_2 and CO_2. In the current study, the amount of circulating ash was not calculated.

3. Results and discussion

The temperature in the CFB boiler furnace is maintained at 750–850 °C. Between those temperature limits, the sulfur binding process is at its maximum intensity. The bed temperature in a CFB boiler is mainly controlled by adjusting the cyclone ash recirculating ratio. The external solid heat exchanger(s) is(are) used to extract heat from the combustion process/ recirculating ash. This extraction allows a significant reduction of the amount of recycled flue gas required for combustion temperature control in the case of oxy-fuel combustion. This feature can be used to reduce the RFG ratio in the CFB during the retrofitting to oxy-mode combustion [24].

Applying the assumed initial conditions, the calculated contents of CO_2 and O_2 in the gas at the inlet of the boiler at different RFG ratios are shown in Figure 2. The oil shale was found to contain a large fraction of carbonate minerals, mainly calcite $CaCO_3$. The reduction of the carbonate mineral decomposition increases the conditional heating value of oil shale and reduces the CO_2 emission. The calcite decomposition is suppressed when the CO_2 partial pressure exceeds the equilibrium state line of the calcite decomposition reaction at a given temperature [36]. For a bed temperature of 850 °C, the equilibrium pressure of CO_2 is ca. 60 kPa. According to Figure 2 the RFG ratio should be maintained at a level higher than 0.7 to achieve the partial pressure of CO_2 over equilibrium. Under these conditions, ECD decreases, and it is defined by Equation (4) $k_{CO_2\text{-min}}$ minimum. According to Equation (4) $k_{CO_2\text{-min}}$ minimum, the decrease of ECD would be observed from k_{CO_2} = 0.7 (the mean value in CFB in air mode) down to $k_{CO_2\text{-min}}$ = 0.28, depending on LHV. The decrease of k_{CO_2} leads to an additional increase in the amount of heat released during oil shale combustion per 1 kg and, depending on the mean LHV, it can amount up to 0.34 MJ/kg. The calculations and estimations are based on the calculation method by Arro et al. [33, 34].

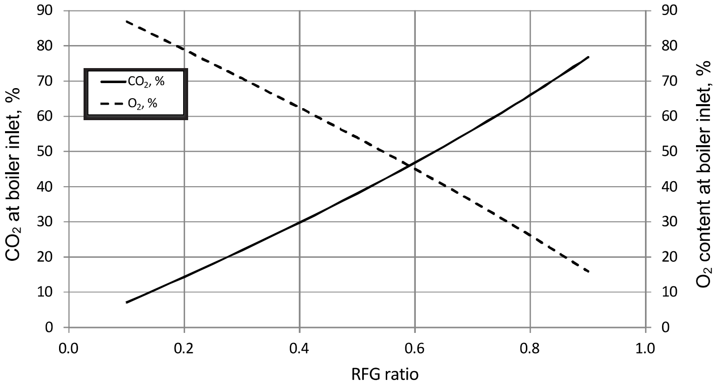

Fig. 2. CO_2 and O_2 content at the boiler inlet at different RFG ratios.

The specific flue gas volume per 1 kg oil shale for different values of LHV and different RFG ratios is shown in Figure 3. On the same plot, the specific gas volumes occurring during air mode combustion are depicted. From Figure 3 it is clear that to obtain in oxy mode the same gas volume as in the conventional mode, the RFG ratio should be maintained at 83.

Figures 4 and 5 depict the specific content of CO_2 per 1 kg oil shale and per fuel energy of oil shale at the boiler outlet for different LHV values and RFG ratios, respectively. For comparison, on the same plot, the calculations of the specific content of CO_2 per fuel energy for bituminous coal and anthracite are shown. These calculations were performed using the proximate and ultimate fuel analysis found in [37, 38]. From Figure 5 it can be seen that the specific CO_2 for selected coals is slightly higher than that for oil shale. This behavior could be explained by the high hydrogen-to-carbon ratio in oil shale and the additional reduction of carbonate minerals decomposition in oil shale due to the increased partial pressure of CO_2. The difference of the specific CO_2 could be additionally increased due to the addition of lime to the coal in the direct desulfurization process.

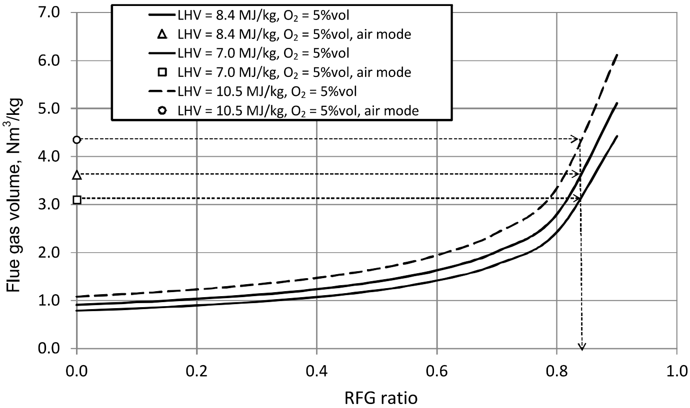

Fig. 3. Flue gas volume per 1 kg oil shale at different RFG ratios in oxy mode.

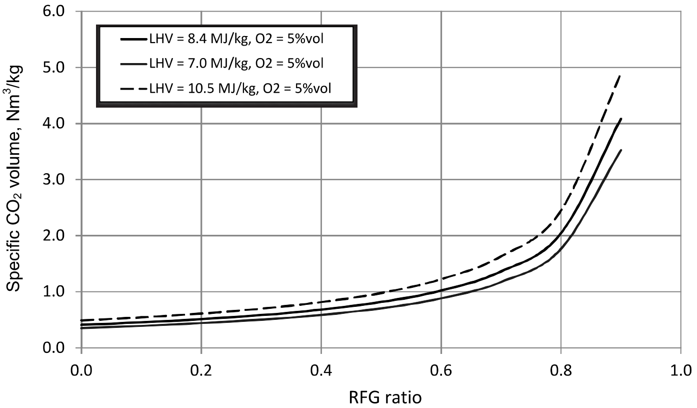

Fig. 4. Specific CO_2 volume at the boiler outlet for different oil shale LHV values and RFG ratios in oxy mode.

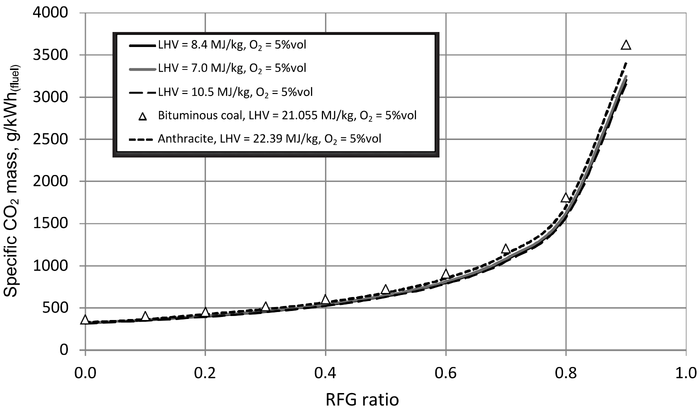

Fig. 5. Specific CO_2 emission per fuel energy at the boiler outlet for different oil shale LHV values and RFG ratios in oxy mode.

4. Conclusions

The gas volume calculations for oil shale combustion applying oxy-fuel technology in a circulated fluidized bed environment for different oil shale LHV values and different recycled flue gas ratios were performed. It was found that to minimize ECD, the recycled flue gas ratio should be maintained at a level higher than 0.7. This condition allows for an increase of the partial pressure of CO_2 over the equilibrium state line of the calcite decomposition reaction at the bed temperature. The decrease of ECD would be observed down to $k_{CO_2\text{-min}} = 0.28$. The decrease of k_{CO_2} leads to an additional increase in the amount of heat released during oil shale combustion per 1 kg and, depending on the mean LHV value, it could be as high as 0.34 MJ/kg.

The calculations indicated that to obtain in oxy mode the same gas volume as in the conventional mode, the RFG ratio should be maintained at 83.

The comparison with the bituminous and anthracite coals indicates that the specific emission of CO_2 per input fuel energy for oil shale could be expected to be even smaller than that of the considered coals.

Acknowledgements

This research was supported by the European Union through the European Regional Development Fund.

REFERENCES

1. Fujimori, T., Yamada, T. Realization of oxyfuel combustion for near zero emission power generation. *P. Combust. Inst.*, 2013, **34**(2), 2111–2130.
2. IEA. *World Energy Outlook 2012*. International Energy Agency, Paris, France, 2012.
3. IEA. *Tracking Clean Energy Progress 2013*. International Energy Agency, 2013.
4. Wall, T. Fundamentals of oxy-fuel combustion. In: *Proceedings of the Inaugural Workshop of the Oxy-fuel Combustion Network,* November 29–30, 2005 Cottbus, Germany.
5. Wall, T., Liu, Y., Spero, C., Elliott, L., Khare, S., Rathnam, R., Zeenathal, F., Moghtaderi, B., Buhre, B., Sheng, C., Gupta, R., Yamada, T., Makino, K., Yu, J. An overview on oxyfuel coal combustion – State of the art research and technology development. *Chem. Eng. Res. Des.*, 2009, **87**(8), 1003–1016.
6. Suraniti, S. L., Nsakala, N. Y., Darling, S. L. Alstom oxyfuel CFB boilers: A promising option for CO_2 capture. *Energy Procedia*, 2009, **1**(1), 543–548.
7. Figueroa, J. D., Fout, T., Plasynski, S., McIlvried, H., Srivastava, R. D. Advances in CO_2 capture technology – The U.S. Department of Energy's Carbon Sequestration Program. *Int. J. Greenh. Gas Con.*, 2008, **2**(1), 9–20.
8. Kanniche, M., Gros-Bonnivard, R., Jaud, P., Valle-Marcos, J., Amann, J.-M., Bouallou, C. Pre-combustion, post-combustion and oxy-combustion in thermal power plant for CO_2 capture. *Appl. Therm. Eng.*, 2010, **30**(1), 53–62.
9. Toftegaard, M. B., Brix, J., Jensen, P. A., Glarborg, P., Jensen, A. D. Oxy-fuel combustion of solid fuels. *Prog. Energ. Combust.*, 2010, **36**(5), 581–625.
10. Scheffknecht, G., Al-Makhadmeh, L., Schnell, U., Maier, J. Oxy-fuel coal combustion – A review of the current state-of-the-art. *Int. J. Greenh. Gas Con.*, 2011, **5(**Supplement 1), S16–S35.
11. Buhre, B. J. P., Elliott, L. K., Sheng, C. D., Gupta, R. P., Wall, T. F. Oxy-fuel combustion technology for coal-fired power generation. *Prog. Energ. Combust.*, 2005, **31**(4), 283–307.
12. Okawa, M., Kimura, N., Kiga, T., Takano, S., Arai, K., Kato, M. Trial design for a CO_2 recovery power plant by burning pulverized coal in O_2/CO_2. *Energ. Convers. Manage.*, 1997, **38**(S), S123–S127.
13. Horn, F. L., Steinberg, M. Control of carbon dioxide emissions from a power plant (and use in enhanced oil recovery). *Fuel*, 1982, **61**(5), 415–422.
14. Herzog, H., Golomb, D., Zemba, S. Feasibility, modeling and economics of sequestering power plant CO_2 emissions in the deep ocean. *Environ. Prog.*, 1991, **10**(1), 64–74.
15. Abraham, B. M., Asbury, J. G., Lynch, E. P., Teotia, A. P. S. Coal-oxygen process provides CO_2 for enhanced recovery. *Oil Gas J.*, 1982, **80**(11), 68–70.
16. Nakayama, S., Noguchi, Y. Pulverized coal combustion in O_2/CO_2 mixtures on a power plant for CO_2 recovery. *Energ. Convers. Manage.*, 1992, **33**(5–8), 379–386.
17. Simmons, M., Miracca, I., Gerdes, K. Oxyfuel technologies for CO_2 capture: a techno-economic overview. In: *Proceedings of the 7th International Conference on Greenhouse Gas Control Technologies,* 5–9 September 2004, Vancouver, Canada.
18. Châtel-Pélage, F., Varagani, R., Pranda, P., Perrin, N., Farzan, H., Vecci, S. J., Lu, Y., Chen, S., Rostam-Abadi, M., Bose, A. C. Applications of oxygen for

NO_x control and CO_2 capture in coal-fired power plants. *Therm. Sci.*, 2006, **10**(3), 119–142.

19. Tan, Y., Croiset, E., Douglas, M. A., Thambimuthu, K. V. Combustion characteristics of coal in a mixture of oxygen and recycled flue gas. *Fuel*, 2006, **85**(4), 507–512.
20. Romeo, L. M., Diez, L. I., Guedea, I., Bolea, I., Lupiáñez, C., González, A., Pallarés, J., Teruel, E. Design and operation assessment of an oxyfuel fluidized bed combustor. *Exp. Therm. Fluid Sci.*, 2011, **35**(3), 477–484.
21. Czakiert, T., Bis, Z., Muskala, W., Nowak, W. Fuel conversion from oxy-fuel combustion in a circulating fluidized bed. *Fuel Process. Technol.*, 2006, **87**(6), 531–538.
22. Scala, F., Salatino, P. Flue gas desulfurization under simulated oxyfiring fluidized bed combustion conditions: The influence of limestone attrition and fragmentation. *Chem. Eng. Sci.*, 2010, **65**(1), 556–561.
23. Jia, L., Tan, Y., Wang, C., Anthony, E. J. Experimental study of oxy-fuel combustion and sulfur capture in a mini-CFBC. *Energ. Fuel.*, 2007, **21**(6), 3160–3164.
24. Jia, L., Tan, Y., Anthony, E. J. Emissions of SO_2 and NO_x during oxy-fuel CFB combustion tests in a mini-circulating fluidized bed combustion reactor. *Energ. Fuel.*, 2010, **24**(2), 910–915.
25. Stewart, M. C., Symonds, R. T., Manovic, V., Macchi, A., Anthony, E. J. Effects of steam on the sulfation of limestone and NO_x formation in an air- and oxy-fired pilot-scale circulating fluidized bed combustor. *Fuel*, 2012, **92**(1), 107–115.
26. Rahiala, S., Myöhänen, K., Hyppänen, T. Modeling the behavior of limestone particles in oxy-fuel CFB processes. *Fuel*, 2014, **127**, 141–150.
27. Duan, L., Sun, H., Zhao, C., Zhou, W., Chen, X. Coal combustion characteristics on an oxy-fuel circulating fluidized bed combustor with warm flue gas recycle. *Fuel*, 2014, **127**, 47–51.
28. Varol, M., Atimtay, A. T., Olgun, H., Atakül, H. Emission characteristics of co-combustion of a low calorie and high sulfur–lignite coal and woodchips in a circulating fluidized bed combustor: Part 1. Effect of excess air ratio. *Fuel*, 2014, **117**, Part A, 792–800.
29. Al-Makhadmeh, L., Maier, J., Al-Harahsheh, M., Scheffknecht, G. Oxy-fuel technology: An experimental investigation into oil shale combustion under oxy-fuel conditions. *Fuel*, 2013, **103,** 421–429.
30. Konist, A., Pihu, T., Neshumayev, D., Külaots, I. Low grade fuel - oil shale and biomass co-combustion in CFB boiler. *Oil Shale*, 2013, **30**(2S), 294–304.
31. Konist, A., Pihu, T., Neshumayev, D., Siirde, A. Oil shale pulverized firing: boiler efficiency, ash balance and flue gas composition. *Oil Shale*, 2013, **30**(1), 6–18.
32. Plamus, K., Ots, A., Pihu, T., Neshumayev, D. Firing Estonian oil shale in CFB boilers – ash balance and behaviour of carbonate minerals. *Oil Shale*, 2011, **28**(1), 58–67.
33. Arro, H., Prikk, A., Pihu, T. Calculation of qualitative and quantitative composition of Estonian oil shale and its combustion products. Part 1. Calculation on the basis of heating value. *Fuel*, 2003, **82**(18), 2179–2195.
34. Arro, H., Prikk, A., Pihu, T. Calculation of qualitative and quantitative composition of Estonian oil shale and its combustion products. Part 2. Calculation on the basis of technical analysis data. *Fuel*, 2003, **82**(18), 2197–2204.

35. Ots, A. *Oil Shale Fuel Combustion*. Tallinn University of Technology, Tallinn, 2006.
36. Külaots, I., Ots, A., Yrjas, P., Hupa, M., Backman, P. Sulphation of Estonian and Israeli oil shale ashes under atmospheric and pressurized combustion conditions. *Oil Shale*, 1997, **14**(3S), 265–283.
37. Czakiert, T., Sztekler, K., Karski, S., Markiewicz, D., Nowak, W. Oxy-fuel circulating fluidized bed combustion in a small pilot-scale test rig. *Fuel Process. Technol.*, 2010, **91**(11), 1617–1623.
38. Duan, L., Zhao, C., Zhou, W., Qu, C., Chen, X. O_2/CO_2 coal combustion characteristics in a 50 kW_{th} circulating fluidized bed. *Int. J. Greenh. Gas Con.*, 2011, **5**(4), 770–776.

Received November 26, 2013

Paper II

Lauri Loo, Birgit Maaten, Andres Siirde, Tõnu Pihu, and Alar Konist. “Experimental Analysis of the Combustion Characteristics of Estonian Oil Shale in Air and Oxy-Fuel Atmospheres.” Fuel Processing Technology 134 (June 2015): 317–324. doi:10.1016/j.fuproc.2014.12.051.

Fuel Processing Technology 134 (2015) 317–324

Contents lists available at ScienceDirect

Fuel Processing Technology

journal homepage: www.elsevier.com/locate/fuproc

Experimental analysis of the combustion characteristics of Estonian oil shale in air and oxy-fuel atmospheres

Lauri Loo [a,*], Birgit Maaten [a], Andres Siirde [a], Tõnu Pihu [a], Alar Konist [a,b]

[a] Department of Thermal Engineering, Tallinn University of Technology, Ehitajate tee 5, Tallinn 19086, Estonia
[b] School of Engineering, Brown University, 182 Hope St., Providence, RI 02912, USA

ARTICLE INFO

Article history:
Received 19 August 2014
Received in revised form 10 December 2014
Accepted 11 December 2014
Available online 27 February 2015

Keywords:
Oil shale
Oxy-fuel combustion
Carbonate mineral decomposition
DSC
TGA
O_2/CO_2 combustion

ABSTRACT

A non-isothermal experimental study using thermogravimetric analysis and differential scanning calorimetry coupled with a quadrupole mass spectrometer was conducted to investigate Estonian oil shale combustion characteristics. The analyses were performed in air (N_2/O_2) and oxy-fuel (CO_2/O_2) atmospheres with various oxygen ratios (10, 20 and 30 vol.%). Our experimental results in TGA show that combustion in the CO_2/O_2 atmosphere is delayed compared to that in the N_2/O_2 atmosphere. Carbonate minerals in oil shale decompose in air in one step and in the oxy-fuel atmosphere in two separate steps: the decomposition of dolomite ($CaMg(CO_3)_2$) and the subsequent decomposition of calcite ($CaCO_3$). An increased oxygen ratio in combustion in the oxy-fuel atmosphere increases the overall combustion rate, whereas the CO_2 emission volumes decrease because of the lower decomposition extent of carbonates. The quadrupole mass spectrometer measurements indicate several combustion products. A higher CO reading is registered in the CO_2/O_2 atmosphere, but there is no other significant difference. Based on the measurement results, a combustion model for Estonian oil shale is proposed. Combustion in the oxy-fuel atmosphere is similar to combustion in air, which eases the design of oxy-fuel combustors.

1. Introduction

The world's growing demand for energy enforces the usage of low-grade fuels. In Estonia, oil shale (OS) power and oil production sectors are the largest CO_2 emitters. Estonia depends on OS because over 90% of its electricity is produced from OS [1,2]. Therefore, improving the OS combustion process has large environmental and economic benefits.

OS is a low-grade fossil fuel that consists of kerogen (organic) and mineral components. The organic matter contains a relatively large amount of hydrogen, and the H/C atomic ratio is 1:4–1:5 [3]. Estonian OS has a high content of mineral matter, which consists of carbonaceous, sandy-clay-carbonaceous and sandy-clay parts [4]. A higher CO_2 concentration can alter the decomposition of carbonates and decrease CO_2 emission [5]. Therefore, implementation of oxy-fuel technology offers many benefits.

The most energy- and cost-effective CCS technology is considered to be the oxy-fuel technology [6]. Implementing the carbon capture and storage (CCS) systems on oxy-fuel combustion technology significantly reduces CO_2 emission. The concept of the oxy-fuel technology is the removal of nitrogen from the combustion process, that is, combustion occurs in an oxygen and carbon dioxide atmosphere. As a result, the formed flue gas mainly consists of carbon dioxide and water vapor, and the volume of flue gas considerably decreases [7,8].

Previous studies [5,9–14] concluded that a higher carbon dioxide concentration in the combustion atmosphere decreases the decomposition of carbonate minerals in the OS, but to our best knowledge, there is no data about higher CO_2 atmosphere effects on the combustion of OS kerogen. Thermogravimetric analysis (TGA) of coal oxy-fuel combustion has proven that the oxy-fuel atmosphere considerably changes the combustion process [15–18]. Nevertheless, Niu and co-workers considered that the investigation of the reaction mechanism and kinetic parameters of the oxy-fuel combustion of coal are not sufficiently reviewed [15]. The same applies to OS oxy-fuel combustion.

Simultaneous use of TGA, DSC and QMS allow one to obtain more data with higher precision from different processes that occur in the OS during the thermal treatment. TGA is a common technique to rapidly investigate and compare thermal events and kinetics during the combustion and pyrolysis of a material [19]. TGA measures the mass loss of the sample as a function of time and temperature. A quadrupole mass spectrometer (QMS) improves the analyses of the processes by adding information about the evolving gases. The temperatures at which the mass changes occur can be viewed using TGA, and quantitative methods can be applied to the data to obtain the kinetic parameters. DSC adds thermal information about the processes that occur during the measurement, and QMS detects the evaporating ions.

---

[*] Corresponding author.

http://dx.doi.org/10.1016/j.fuproc.2014.12.051
0378-3820/

This paper provides detailed information about all of the steps of OS combustion in air and oxy-fuel atmospheres and compares the obtained results with the existing model.

2. Experiment

2.1. Materials

All experiments were conducted with an OS sample that was obtained from an underground mine in Estonia and was provided by the Eesti Power Plant. The OS sample was dried and crushed to pass through a sieve with 1 mm openings. The mineral composition of the OS sample is shown in Table 1, and the chemical composition and laboratory ash analysis are shown in Table 2.

2.2. Equipment and procedures

The thermal analyses were performed on a Netzsch STA 449 F3 Jupiter Simultaneous Thermal Analyzer (TG–DSC/DTA Apparatus), which was coupled with a Netzsch QMS 403D Aeolos (mass 1–300 amu). The samples were analyzed in Pt/Rh crucibles with a lid and a removable liner composed of thin-walled Al_2O_3 in the gas flows, as shown in Fig. 1. In the combustion experiments, approximately 20 mg of the oil shale sample was used. The total gas flow during all measurements was 60 ml/min. In the TGA, the oil shale samples were heated to 1240 °C, with a heating rate of 10 K/min. The instrument temperature and heat sensitivity were calibrated with In, Sn, Zn, Al and Au standards. The produced gases were analyzed using QMS during the entire heating process. The mass/charge (m/z) values of 8–150 were collected with a sampling rate of 0.2 s/m/z. All measurements were performed at least twice for sufficient reproducibility. The used material was non-homogeneous. Nevertheless, notably good reproducibility was achieved.

2.3. Visual inspection of the product oil shale ash

No visual differences among different ash samples from various experiments were noticed after removing the samples from the TG/DSC apparatus. As expected, all of the samples were slightly sintered at this high temperature (1240 °C) but remained easily removable with a small brush.

2.4. Characteristic parameters of the combustion and decomposition of carbonates

The following characteristic parameters that were previously used by researchers [15,16,20] were measured using the TGA: ignition temperature T_i; temperatures of the maximum mass loss rate T_{max1} and T_{max2}; burn-out temperature T_b. These parameters describe the thermal behavior of the OS's organic part.

The following parameters for the carbonate decomposition were obtained: beginning temperature T_{d1} of the reaction; temperature of the maximum mass loss rate T_{max3}; and ending temperature T_{e1} of the carbonate decomposition. In the CO_2/O_2 atmosphere, the decomposition of carbonate minerals occurs in two steps. The beginning temperature T_{d2} of the second decomposition step, temperature of the maximum mass loss rate T_{max4} and ending temperature T_{e2} of the second step were measured. The identical parameters were obtained using DSC, and some differences were noticed.

Table 1
Mineral composition of the Estonian oil shale sample, wt%.

Dolomite	Calcite	Quartz	K-feldspar	Illite	Chlorite	Kaolinite	Pyrite	Sum
18.6	41.8	12.1	5.87	16.4	1.77	tr.	3.27	99.9

Table 2
Elemental composition of the OS and the laboratory ash.

Oil shale	%	Oil shale ash	%
$CO_2{}^d{}_{carb}$	20.12	SiO_2^d	30.74
H^d	2.90	FeO_3^d	4.84
C^d	27.90	$Al_2O_3^d$	6.08
N^d	0.02	CaO^d	39.00
$S^d{}_0$	1.20	MgO^d	8.68
$S^d{}_{sulphate}$	0.08	K_2O^d	1.81
$S^d{}_{sulphide}$	1.12	Na_2O^d	0.13
		$Ash_{815°C}$	47.0
Q_b^d	10.038 MJ/kg		

2.5. Oil shale combustion model

It has been suggested that a six-step mechanism can describe the OS combustion mechanism [21,22]. Potentially, the following reaction steps occur:

1. water removal,
2. decomposition of kerogen,
3. dissociation of volatile matter into bitumen and gases,
4. oxidation of volatile matter,
5. oxidation of fixed carbon, and
6. decomposition of carbonate minerals.

The scope of the reaction steps depends on the specific OS, but all of the reaction steps should be noticeable during the measurement. TG–DSC–QMS analysis is used to further investigate the reaction steps.

3. Results and discussion

The plots of the TG, DTG and DSC measurements in different N_2/O_2 and CO_2/O_2 mixtures (Fig. 1) are shown in Fig. 2.

The measurements are shown in Table 3 and Fig. 3 and will be analyzed.

3.1. Overall combustion analysis

According to the earlier presented theory [21,22], the first combustion step is the separation of water vapor. Many researchers [21, 23–26] suggest that even with an air-dry material, a small mass loss is observed in the temperature range of 60 to 200 °C, which is connected to the evaporation of water. In addition to moisture, the OS contains crystal water (clay minerals, such as illite, chlorite, and kaolinite,

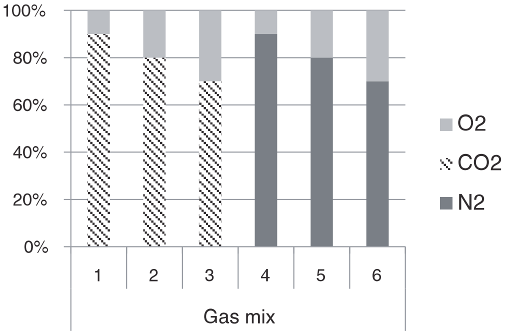

Fig. 1. Gas mixtures in the experiments.

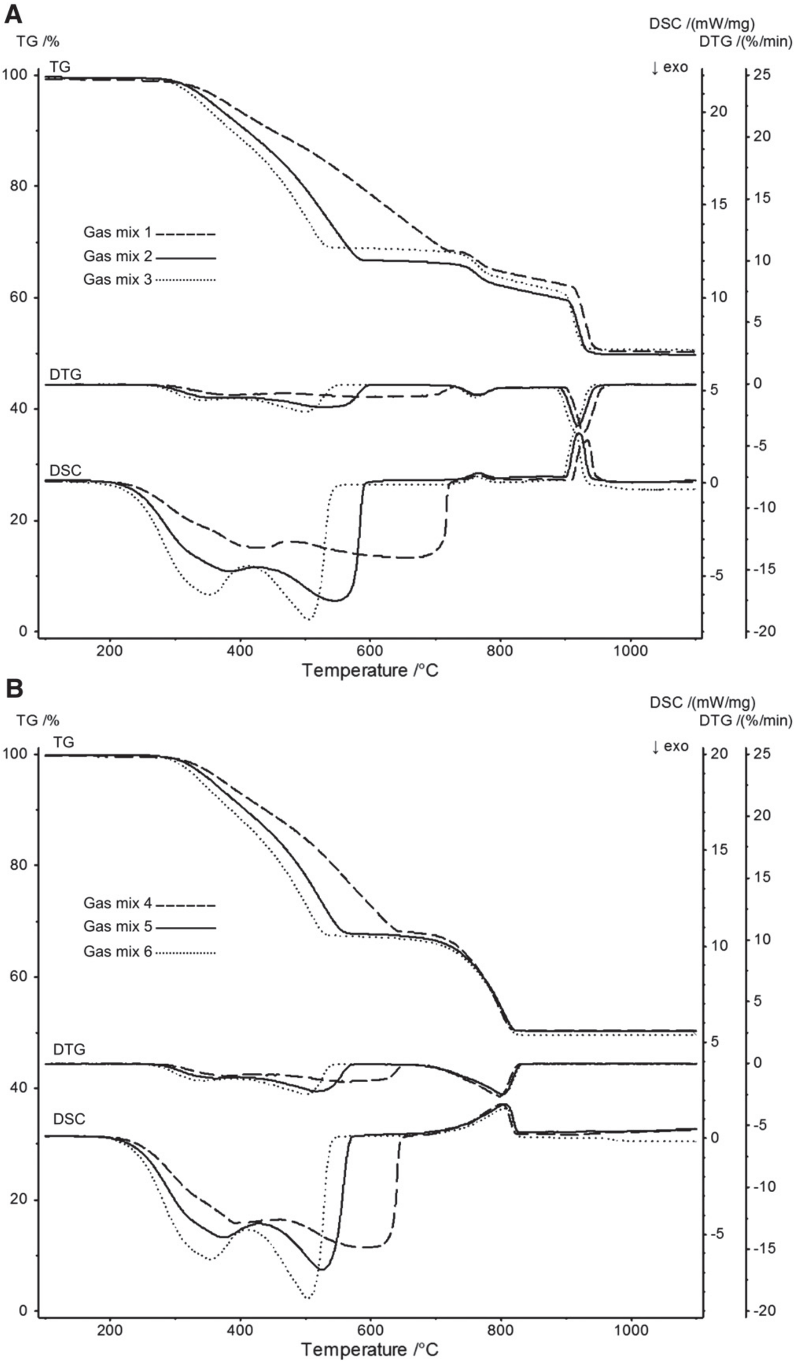

Fig. 2. Oil shale combustion measurements in (A) oxy-fuel and (B) air atmospheres.

which separate in the temperature range of 120–140 °C [4]). In the conducted measurements, only a minimal mass loss was observed in the water evaporation zone.

The next combustion steps occur relatively simultaneously. The most interesting observation was the difference in the ignition temperature that was measured using TG and DSC. The DSC curve indicates that

Table 3
The characteristic parameters of oil shale combustion measured with TGA and DSC in regular and oxy-fuel atmospheres.

	Gas composition				Combustion				Decarbonisation					
	Gas mix	O_2, %	N_2, %	CO_2, %	T_i, °C	T_{max1}, °C	T_{max2}, °C	T_b, °C	T_{d1}, °C	T_{max3}, °C	T_{e1}, °C	T_{d2}, °C	T_{max4}, °C	T_{e2}, °C
TG	1	10	–	90	330	385	607	714	737	770	775	915	931	942
	2	20	–	80	318	357	525	578	749	767	776	908	919	931
	3	30	–	70	301	344	499	528	750	763	780	900	912	925
	4	10	90	–	326	382	571	645	667	786	822	–	–	–
	5	20	80	–	310	383	515	562	695	792	822	–	–	–
	6	30	70	–	300	342	500	530	680	802	822	–	–	–
DSC	1	10	–	90	245	441	659	728	728	767	788	911	933	960
	2	20	–	80	223	385	545	589	739	766	787	903	920	935
	3	30	–	70	210	353	505	538	738	764	789	897	914	929
	4	10	90	–	246	394	590	649	694	800	820	–	–	–
	5	20	80	–	226	374	525	572	700	806	824	–	–	–
	6	30	70	–	220	354	504	545	695	805	826	–	–	–

the exothermal peak occures 80 °C before the TGA records any mass loss. All of the following characteristic temperatures have a minimal difference between the DSC- and TGA-measured results. The lower ignition temperatures measured using the DSC indicate the decomposition of kerogen. Because the decomposition of the organic part began, but no volatiles were separated, no mass loss was recorded.

The major mass loss (31–33%) occurred in the temperature range of 300 to 715 °C. As visible on all curves, two strong activity peaks were recognized: the first one in the range of 340 to 440 °C and the second one between 500 and 660 °C. The QMS measurements indicate the separation of H_2O (m/z 18 and 17, see Fig. 4), CO (m/z 28) and HCl (m/z 36 and 37) at the first peak of combustion. These gases are the combustion products of the organic part of the OS. The second peak of combustion matches the CO_2 (m/z 46, 44, 16 and 12) and SO_2 (m/z 64, 48 and 32) peaks (see Fig. 5). In this case, the H_2O reading was lower than that during the first phase of combustion, which indicated that hydrocarbons had already burned, and the combustion of aliphatic and aromatic compounds and char occurred during the second phase. The low readings of SO_2 during combustion were caused by organic sulfur. At 500 °C, marcasite (FeS_2) decomposes; thus, sulfur dioxide was formed, which causes the strong reading of SO_2 during the second combustion phase.

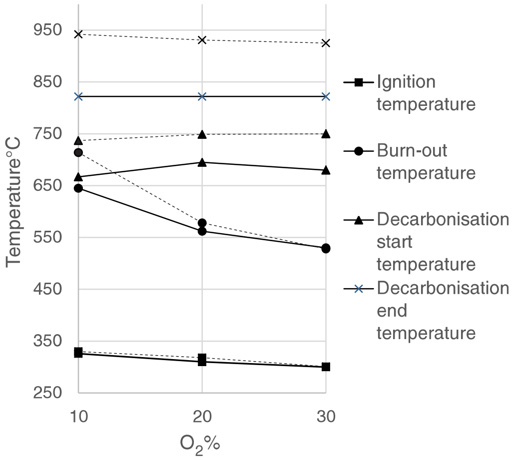

Fig. 3. OS combustion parameters that were measured using the TGA. The solid lines represent measurements in air atmospheres, and the dashed lines represent measurements in the oxy-fuel atmospheres.

Based on a previously suggested OS combustion model, it can be claimed that this phase consists of the conversion of organic matter into volatiles and fixed carbon, oxidation of the formed volatiles and finally the combustion of carbon.

Above 650 °C, all of the following reactions are endothermic, which suggests that the organic compounds have been oxidized. The mass loss step(s) between 670 and 940 °C indicate the decomposition of carbonate minerals. In the air atmosphere, only one step occurs, whereas in the oxy-fuel atmosphere, two reaction steps can be distinguished. The QMS indicates a clear peak of CO_2 in the N_2-based gas mixtures, whereas in the CO_2 atmosphere, the readings are covered by the background. For the endothermic reaction steps, the DSC and TGA measurements indicate a similar reaction start point, end point and maximum mass loss rate temperatures.

As previously mentioned, the Estonian OS is a heterogeneous material. In the completed experiments, a notably good repeatability was obtained, as shown in Table 4. There are some minor differences in the burn-out percentage. The mass loss at the end of the combustion was 32% in all gas mixtures, and the total mass loss was 50%.

3.2. Effect of different oxygen ratios

A higher O_2 ratio in the gas mix with CO_2 leads to faster combustion: the temperatures of the maximum mass loss rate during the combustion phase and burn-out temperature decrease (Fig. 2) for lower O_2 ratios. The effect was stronger in CO_2 atmosphere than in N_2. The burn-out temperature decreases by 185 °C for CO_2/O_2 and 115 °C for N_2/O_2. Simultaneously, the ignition temperature decreases by only 30 °C in both atmospheres. The QMS measurements indicate a lower CO level in the gas mixes with higher O_2 contents. A faster combustion also increases the maximum mass loss rates in the combustion phase.

The oxygen ratio in the gas mix does not affect the decomposition of carbonates in the N_2/O_2 mixture. In CO_2/O_2, a higher oxygen ratio decreases the characteristic temperatures of the second step of carbonate decomposition but has a minimal effect on the first step. This phenomenon should be attributed to a lower partial pressure of CO_2, which increases the calcite decomposition [5,10,12]. The mass loss rates for carbonate decomposition remain similar.

3.3. Differences in the combustion parameters in air and oxy-fuel atmospheres

The measurements were performed with three different O_2 ratios (10, 20 and 30%) in CO_2 and N_2 atmospheres (Figs. 3, 6 and 7). A change in the main gas from N_2 to CO_2 with an identical oxygen level leads to a

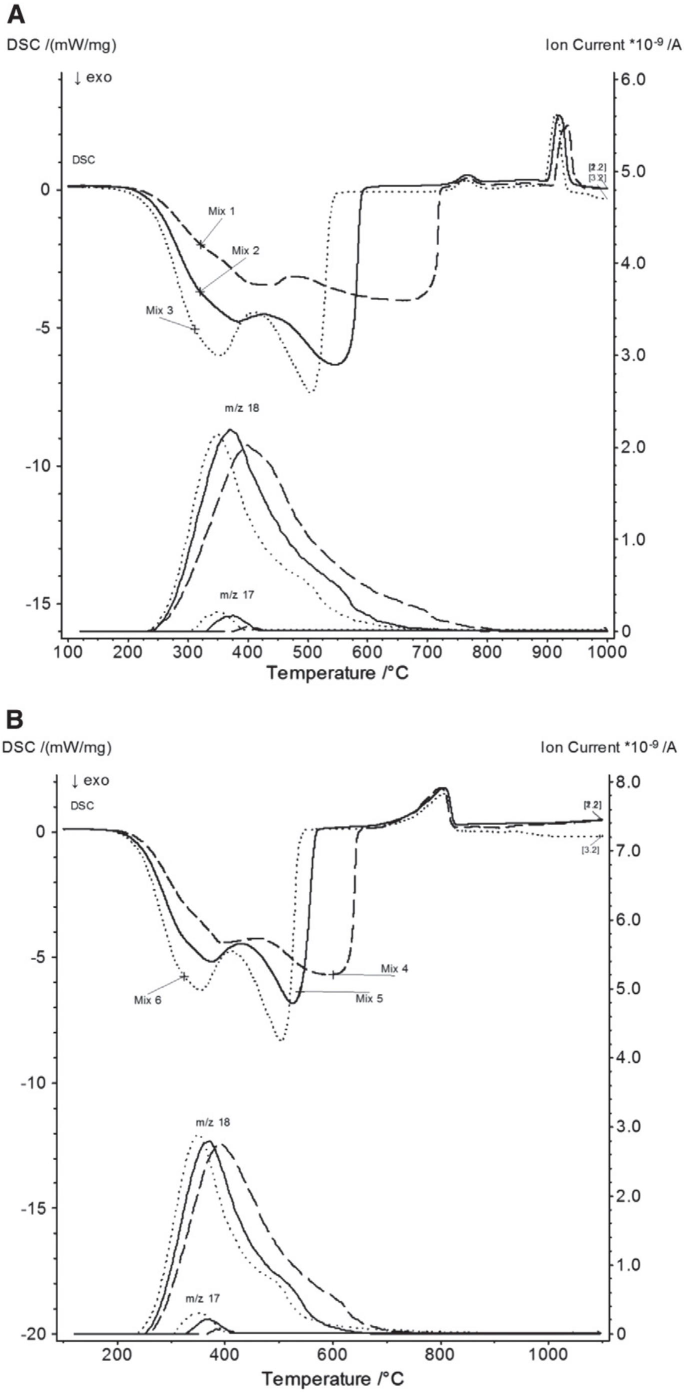

Fig. 4. Water separation (m/z 17 and 18) during the OS combustion measurements in (A) oxy-fuel and (B) air atmospheres.

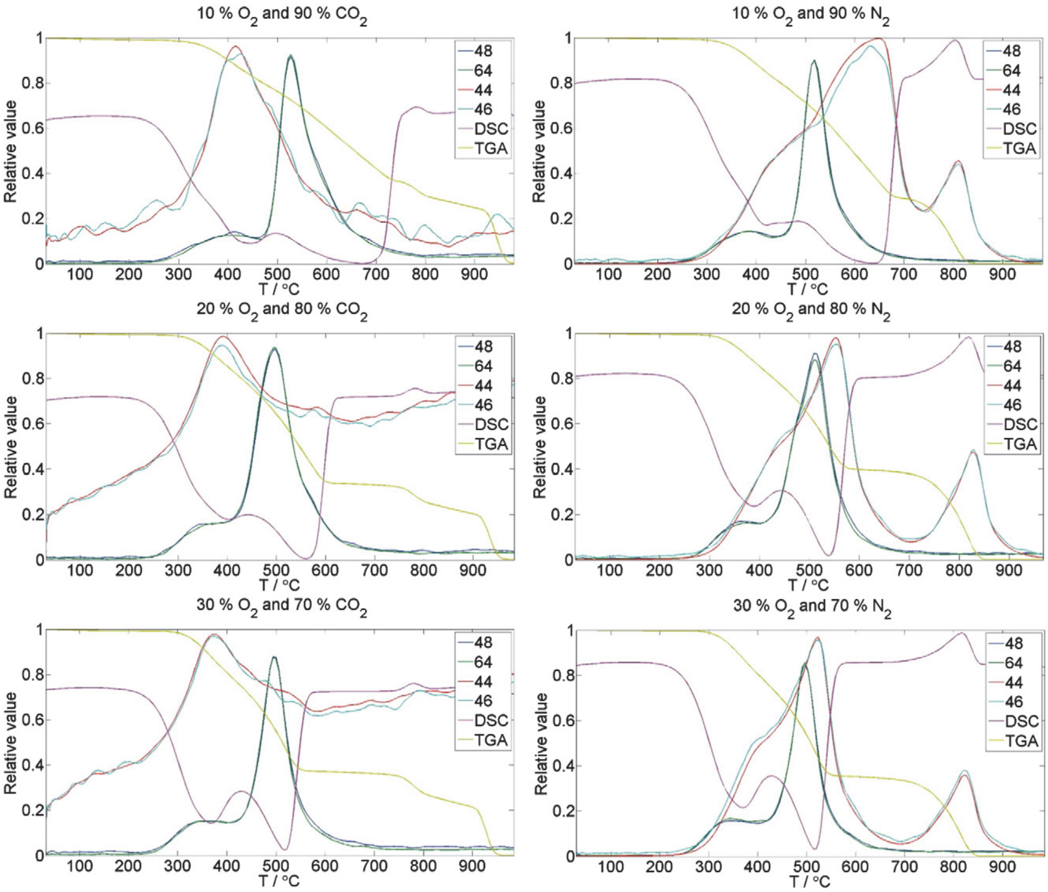

Fig. 5. QMS measurements of SO_2 (m/z 48 and 64) and CO_2 (m/z 44 and 46).

slower combustion process and changes the carbonate decomposition process. The ignition temperature is almost identical for both main gases. Other characteristic temperatures of combustion are slightly higher in the oxy-fuel atmosphere. The differences decrease with the increase of the oxygen ratio in the gas mix. For example, the burn-out temperature in the gas mix 1 is 70 °C higher than that in gas mix 4 (10 vol.% O_2). If the oxygen ratio in the gas mixes is 20 vol.%, the burn-out temperature in CO_2 atmosphere is 15 °C higher than that in N_2. If the oxygen ratio in the gas mixes is 30 vol.%, no differences of burn-out temperatures are noticed. Simultaneously, the QMS measurements

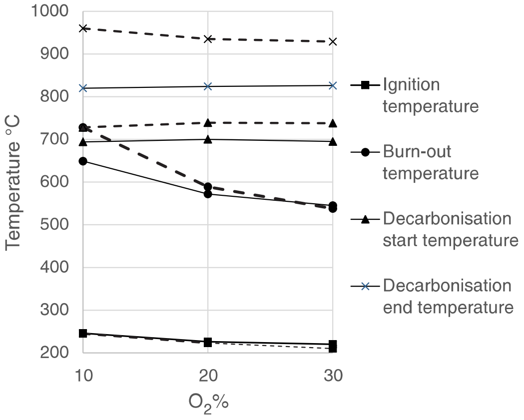

Fig. 6. OS combustion parameters that were measured using the DSC. The solid lines and dashed lines represent measurements in air atmospheres and oxy-fuel atmospheres, respectively.

Table 4
Mass loss percentages in different combustion environments.

Gas mix	Gas composition			Mass loss	
	O_2, %	N_2, %	CO_2, %	Burn-out, %	Total, %
1	10	–	90	32	50
2	20	–	80	33	50
3	30	–	70	31	49
4	10	90	–	32	50
5	20	80	–	32	50
6	30	70	–	33	50

show a considerably higher CO level on the evaporating gases (nearly 10 times stronger ion current of m/z 28). The combustion process begins at the identical temperature in air and oxy-fuel atmospheres but lasts longer in the oxy-fuel atmosphere and increases the CO concentration in the evaporating gases, particularly when the gas mix has a low oxygen content.

The decomposition of carbonate minerals occurs in air in one mass loss step between 670 and 825 °C. The TGA measurements indicate a small variation of the temperatures of the start and maximum mass loss, but the DSC measurements indicate stricter reaction boundaries.

The decomposition of carbonate minerals in the oxy-fuel atmosphere occurs in two reaction steps: the decomposition of dolomite ($CaMg(CO_3)_2$) and then the decomposition of calcite ($CaCO_3$) [5,10]. The DSC measurements show two separated reaction steps. The first endothermic heat flow is recorded between 730 and 790 °C. The second endothermic reaction step occurs between 910 and 960 °C, when the oxygen content is low (10%), and between 900 and 930 °C, when the oxygen content is relatively high (30%). The TG curve hinders the analysis, that is, there are two mass loss rate peaks in the TGA curve and a small mass loss (4%) between the peaks, but the DSC shows no readings in the gap. This result indicates that the heat flow is too small to be registered.

The carbonate breakdown reactions occur in the identical temperature range in the air atmospheres, whereas the calcite is stabilized to a higher temperature in the CO_2 atmospheres. The dolomite breakdown is merged with the larger calcite breakdown peak in the air atmosphere. Compared to the N_2/O_2 mixture, the CO_2/O_2 atmosphere increases the burn-out temperature and divides the decomposition process of carbonate minerals into two steps. The separation of these two peaks likely occurs at intermediate CO_2 contents of the atmosphere.

3.4. QMS analysis

The separation of major combustion products was previously discussed. The analysis of weaker m/z readings and some hypotheses set by other researchers [14,27–30] are discussed below.

Because the nitrogen content in OS is notably low (Table 2), the m/z peaks that are connected to nitrogen (14, 26, 27, 28, 30, 44 and 46) are attributed to organic or other combustion products.

The separation of methane was attempted for confirmation, but the methane peaks overlap with water (m/z 16) and carbon monoxide (m/z 14). The m/z 15 peak indicates CH_3^+ ions and m/z 13 CH^+ ions. m/z 13 is not recognized in the N_2/O_2 atmosphere, but in the CO_2/O_2 atmosphere, it has approximately 30% of the intensity of the m/z 15 peak. These peaks are attributed to organic molecules in general and may indicate something more complex than methane. This result requires further investigation with preferably other analytical techniques.

One possible organic component was identified: 1-butene, which has a more complex spectrum than the previously shown compounds. The NIST MS Search tool provides a match of 796, and it suggests 2-butene, with a match of 763. Therefore, both compounds can be considered to be possible evaporating gases.

Earlier industrial and laboratory measurements indicate the formation of VOCs [28,29,31], but the conducted QMS measurements could not confirm them. It is possible that the ambient noise covers the m/z peaks. Applying advanced data treatment methods may resolve the problem. The obtained results indicate that the QMS analysis of evolved gases does not provide full information about the composition of the gas phase. Meriste et al. [14] made similar conclusions after applying FTIR. Combining different analytic equipment can provide more information about the gaseous compounds.

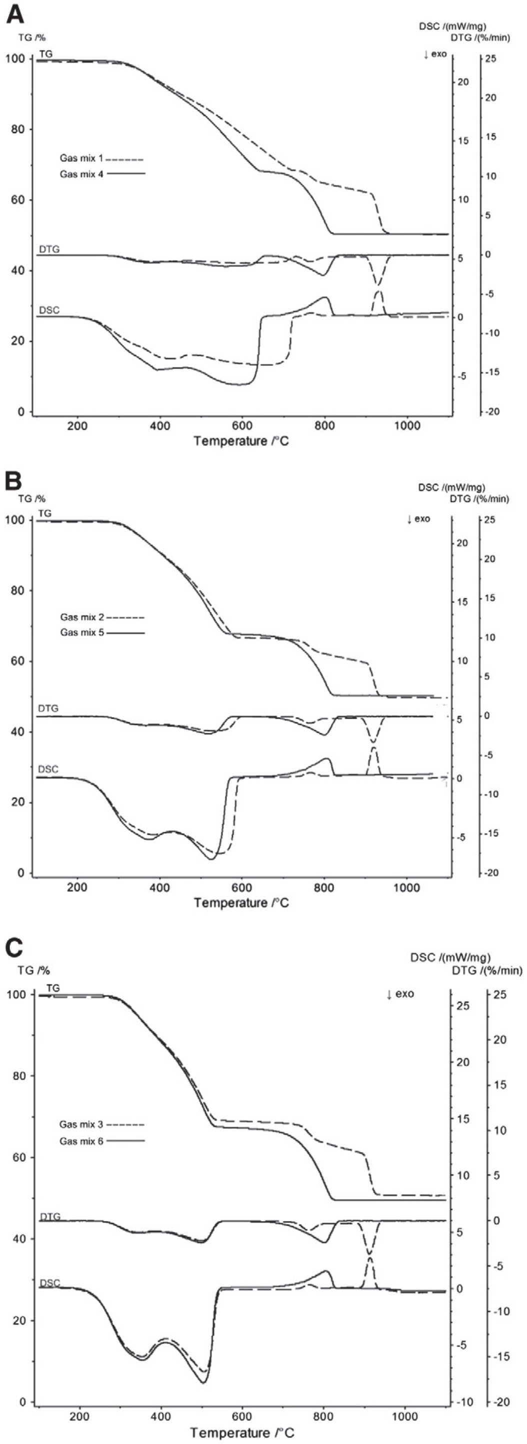

Fig. 7. Oil shale combustion measurement in different gas mixes: A — gas mix 1 (10% O_2 and 90% CO_2) and gas mix 4 (10% O_2 and 90% N_2); B — gas mix 2 (20% O_2 and 80% CO_2) and gas mix 5 (20% O_2 and 80% N_2); and C — gas mix 6 (30% O_2 and 70% CO_2) and gas mix 3 (30% O_2 and 70% N_2).

3.5. Combustion model of Estonian OS

Based on the experiments for Estonian OS, the combustion model is as follows:

1. Separation of moisture and crystal water (120–200 °C);
2. Decomposition of organic matter (220–300 °C);
3. Combustion (300–730 °C):
   a. Combustion of volatiles (300–500 °C);
   b. Combustion of fixed carbon (350–730 °C);
   c. Decomposition of pyrite (400–500 °C);

4. Decomposition of carbonate minerals (670–960 °C):
   a. Decomposition of dolomite (in air: 670–820 °C; in oxy-fuel atmosphere: 730–790 °C);
   b. Decomposition of calcite (in air: 670–820 °C, in oxy-fuel atmosphere: 890–960 °C).

All of the mentioned steps occur but may roughly simultaneously occur depending on the conditions.

3.6. Conclusions

In conclusion, this paper provides a TGA–MS measurement data analysis of Estonian oil shale combustion in air and an oxy-fuel environment using various oxygen ratios. The released gases were analyzed and identified using a mass-spectrometer. This study shows that the characteristic temperatures of the process differ in air and oxy-fuel environments: combustion is delayed in the oxy-fuel environment. A major difference is that the decomposition of carbonaceous minerals occurs in one step in air and in two steps in the oxy-fuel atmosphere. In addition, varying the oxygen ratios helps to improve combustion and decrease CO_2 emissions. When the atmosphere is changed from N_2 to CO_2 with the identical oxygen content, combustion is delayed. A higher oxygen content decreases the differences of the air and oxy-fuel combustion parameters. It is important to study combustion and its products in the oxy-fuel environment to simplify the design of oxy-fuel combustors and decrease CO_2 emission.

Acknowledgments

This study was supported by the European Union through the European Regional Development Fund.

References

[1] T. Pihu, A. Konist, D. Neshumayev, J. Loosaar, A. Siirde, T. Parve, A. Molodtsov, Short-term tests on firing oil shale fuel applying low-temperature vortex technology, Oil Shale 29 (1) (2012).
[2] A. Siirde, Oil shale—global solution or part of the problem? Oil Shale 25 (2) (2008) 201–202.
[3] N. Altun, C. Hicyilmaz, J.-Y. Hwang, A.S. Bagci, M. Kök, Oil shales in the world and Turkey; reserves, current situation and future prospects: a review, Oil Shale 23 (3) (2006) 211–227.
[4] A. Ots, Oil Shale Fuel Combustion, Tallinna Raamatutrükikoda, 2006.
[5] C. Rodriguez-Navarro, K. Kudlacz, E. Ruiz-Agudo, The mechanism of thermal decomposition of dolomite: new insights from 2D-XRD and TEM analyses, Am. Mineral. 97 (1) (2012) 38–51.
[6] F. Châtel-Pélage, R. Varagani, P. Pranda, N. Perrin, H. Farzan, S.J. Vecci, L. Yongqi, S. Chen, M. Rostam-Abadi, A.C. Bose, Applications of oxygen for NOx control and CO2 capture in coal-fired power plants, Therm. Sci. 10 (3) (2006) 119–142.
[7] Y. Tan, E. Croiset, M.A. Douglas, K.V. Thambimuthu, Combustion characteristics of coal in a mixture of oxygen and recycled flue gas, Fuel 85 (4) (2006) 507–512.
[8] M.B. Toftegaard, J. Brix, P.A. Jensen, P. Glarborg, A.D. Jensen, Oxy-fuel combustion of solid fuels, Prog. Energy Combust. Sci. 36 (5) (2010) 581–625.
[9] A. Aboulkas, K. El Harfi, Study of the kinetics and mechanisms of thermal decomposition of Moroccan Tarfaya oil shale and its kerogen, Oil Shale 25 (4) (2008).
[10] P. Engler, M.W. Santana, M.L. Mittleman, D. Balazs, Non-isothermal, in situ XRD analysis of dolomite decomposition, Thermochim. Acta 140 (1989) 67–76.
[11] J.L. Goldfarb, A. D'Amico, C. Culin, E.M. Suuberg, I. Külaots, Oxidation kinetics of oil shale semicokes: reactivity as a function of pyrolysis temperature and shale origin, Energy Fuel 27 (2) (2013) 666–672.
[12] A. Konist, L. Loo, A. Valtsev, B. Maaten, A. Siirde, D. Neshumayev, T. Pihu, Calculation of Estonian oil shale combustion products in regular and oxy-fuel mode in a CFB boiler, Oil Shale 31 (2014) 211–224.
[13] A. Konist, A. Valtsev, L. Loo, T. Pihu, M. Liira, K. Kirsimäe, Influence of oxy-fuel combustion of Ca-rich oil shale fuel on carbonate stability and ash composition, Fuel 139 (2014) 671–677.
[14] T. Meriste, C. Yörük, A. Trikkel, T. Kaljuvee, R. Kuusik, TG–FTIR analysis of oxidation kinetics of some solid fuels under oxy-fuel conditions, J. Therm. Anal. Calorim. 114 (2) (2013) 483–489.
[15] S. Niu, C. Lu, K. Han, J. Zhao, Thermogravimetric analysis of combustion characteristics and kinetic parameters of pulverized coals in oxy-fuel atmosphere, J. Therm. Anal. Calorim. 98 (1) (2009) 267–274.
[16] S. Niu, K. Han, C. Lu, Characteristic of coal combustion in oxygen/carbon dioxide atmosphere and nitric oxide release during this process, Energy Convers. Manag. 52 (1) (2011) 532–537.
[17] A.A. Raeva, N. Dongari, A.A. Artemyeva, E.I. Kozliak, D.T. Pierce, W.S. Seames, Experimental simulation of trace element evolution from the excluded mineral fraction during coal combustion using GFAAS and TGA–DSC, Fuel 124 (2014) 28–40.
[18] O. Senneca, L. Cortese, Kinetics of coal oxy-combustion by means of different experimental techniques, Fuel 102 (2012) 751–759.
[19] M. Gil, D. Casal, C. Pevida, J. Pis, F. Rubiera, Thermal behaviour and kinetics of coal/biomass blends during co-combustion, Bioresour. Technol. 101 (14) (2010) 5601–5608.
[20] Q. Li, C. Zhao, X. Chen, W. Wu, Y. Li, Comparison of pulverized coal combustion in air and in O2/CO2 mixtures by thermo-gravimetric analysis, J. Anal. Appl. Pyrolysis 85 (1) (2009) 521–528.
[21] M.A. Bazelatto Zanoni, H. Massard, M. Ferreira Martins, Formulating and optimizing a combustion pathways for oil shale and its semi-coke, Combust. Flame 159 (10) (2012) 3224–3234.
[22] M. Martins, S. Salvador, J.-F. Thovert, G. Debenest, Co-current combustion of oil shale — part 2: structure of the combustion front, Fuel 89 (1) (2010) 133–143.
[23] A. Aboulkas, et al., Pyrolysis behaviour and kinetics of Moroccan oil shale with polystyrene, Int. J. Mech. Syst. Eng. 1 (1) (2011).
[24] A.J. Berkovich, J.H. Levy, S.J. Schmidt, B.R. Young, Heat capacities and enthalpies for some Australian oil shales from non-isothermal modulated DSC, Thermochim. Acta 357 (2000) 41–45.
[25] J. Jaber, S. Probert, Non-isothermal thermogravimetry and decomposition kinetics of two Jordanian oil shales under different processing conditions, Fuel Process. Technol. 63 (1) (2000) 57–70.
[26] Z. Wang, S. Deng, Q. Gu, Y. Zhang, X. Cui, H. Wang, Pyrolysis kinetic study of Huadian oil shale, spent oil shale and their mixtures by thermogravimetric analysis, Fuel Process. Technol. 110 (2013) 103–108.
[27] E.L. Capel, J.M. de la Rosa Arranz, F.J. González-Vila, J.A. González-Perez, D.A. Manning, Elucidation of different forms of organic carbon in marine sediments from the Atlantic coast of Spain using thermal analysis coupled to isotope ratio and quadrupole mass spectrometry, Org. Geochem. 37 (12) (2006) 1983–1994.
[28] A. Konist, T. Pihu, D. Neshumayev, I. Külaots, Low grade fuel-oil shale and biomass co-combustion in CFB boiler, Oil Shale 30 (2013).
[29] A. Konist, T. Pihu, D. Neshumayev, A. Siirde, Oil shale pulverized firing: boiler efficiency, ash balance and flue gas composition, Oil Shale 30 (1) (2013).
[30] V. Mislej, B. Novosel, T. Vuk, V. Grilc, E. Mlakar, Combustion behaviour and products of dried sewage sludge—prediction by thermogravimetric analysis and monitoring the co-incineration process in a cement factory, Chem. Eng. 29 (2012).
[31] T. Parve, J. Loosaar, M. Mahhov, A. Konist, Emission of fine particulates from oil shale fired large boilers, Oil Shale 28 (2011).

Paper III

Alar Konist, Aleksandr Valtsev, **Lauri Loo**, Tõnu Pihu, Martin Liira, and Kalle Kirsimäe. "Influence of Oxy-Fuel Combustion of Ca-Rich Oil Shale Fuel on Carbonate Stability and Ash Composition." Fuel 139 (January 1, 2015): 671–677. doi:10.1016/j.fuel.2014.09.050.

Fuel 139 (2015) 671–677

Contents lists available at ScienceDirect

Fuel

journal homepage: www.elsevier.com/locate/fuel

Influence of oxy-fuel combustion of Ca-rich oil shale fuel on carbonate stability and ash composition

A. Konist [a,*], A. Valtsev [a], L. Loo [a], T. Pihu [a], M. Liira [b], K. Kirsimäe [b]

[a] Department of Thermal Engineering, Tallinn University of Technology, Kopli 116, 11712 Tallinn, Estonia
[b] Department of Geology, University of Tartu, Ravila 14a, 50411 Tartu, Estonia

HIGHLIGHTS

- This study provides results of oil shale combustion in a batch reactor applying oxy-fuel conditions.
- Elevated CO_2 levels and inhibited carbonate decomposition rate have effect on SO_2 binding and stable anhydrite formation.
- Content of calcite in remaining ash increases with increasing CO_2 levels and decreased firing temperatures.
- Carbonate decomposition is delayed and composition of ash is changed in oil-shale firing at elevated CO_2 levels.
- Formation of secondary Ca–Mg silicate phases is directly proportional to firing temperature.

ARTICLE INFO

Article history:
Received 28 April 2014
Received in revised form 1 July 2014
Accepted 11 September 2014
Available online 27 September 2014

Keywords:
Oil shale
Oxy-fuel combustion
Carbonate stability
Ash composition
Kukersite

ABSTRACT

Oil shale is an unconventional low-calorific-value fossil fuel, the usage of which is increasing due to increasing energy demand. Today, Estonia's oil shale usage is the largest in the world. Approximately 90% of the electricity consumed is produced from Ca-rich oil shale. Most of the oil shale, approximately 12 million tons yearly, is used for power generation utilizing pulverized combustion (PC) and circulating fluidized bed combustion (CFBC) technologies. As a result, Estonia has one of the world's highest CO_2 emission rates per capita. This study provides results of oil shale combustion in a batch reactor applying oxy-fuel conditions. The combustion experiments were performed at temperatures of 800, 850 and 900 °C while varying the N_2, O_2 and CO_2 ratios. In addition to different temperatures and air-composition variation, water vapor was injected into the gas flow entering the furnace to study the water vapor influence on the solid combustion products. Our results indicated that elevated CO_2 levels have a significant influence on the carbonate-decomposition extent and therefore on the SO_2-binding properties.

1. Introduction

Global concern regarding climate warming and stringent limitations on greenhouse-gas emissions have made the oxy-fuel combustion of solid fuels an attractive potential firing technology. Oxy-fuel combustion is considered the most energy- and cost-efficient of the carbon-capture technologies, and it therefore may reduce the level of environmental harm that results from energy production [1–7]. Oxy-fuel technology applies fuel combustion in an O_2–CO_2 environment resulting in flue gas with a CO_2 concentration high enough for efficient CO_2 sequestration and subsequent storage [8,9].

Previous studies have suggested that the chemical and mineralogical composition of the ash forming during the combustion of various coals and lignite do not differ significantly between air and oxy-fuel combustion conditions [10–12]; however, the ash deposition rate, particulate formation (grain-size) and proportions of minerals are reported to vary under oxy-fuel conditions [12–14].

The possible influence of oxy-fuel combustion on ash formation and composition would result from the high CO_2 partial pressures in the high-temperature mineral transformation processes [15–17]. In coal and/or biomass solid fuels, the inorganic (mineral) part of the fuel is low (<20 wt%) and dominated by (alumo)silicate phases (including quartz) that are typically thermally resistant/unreactive.

In contrast, oil shales that are low-quality, organic-rich sedimentary rocks [18] and contain a considerable amount of mineral matter (usually 30–90 wt%, e.g., [19]) can be more sensitive to the conditions present in oxy-fuel-combustion environments.

Oil shales are generally rich in bituminous organic matter [20] and are processed worldwide as an energy resource in a number

---

* Corresponding author.

http://dx.doi.org/10.1016/j.fuel.2014.09.050
0016-2361/

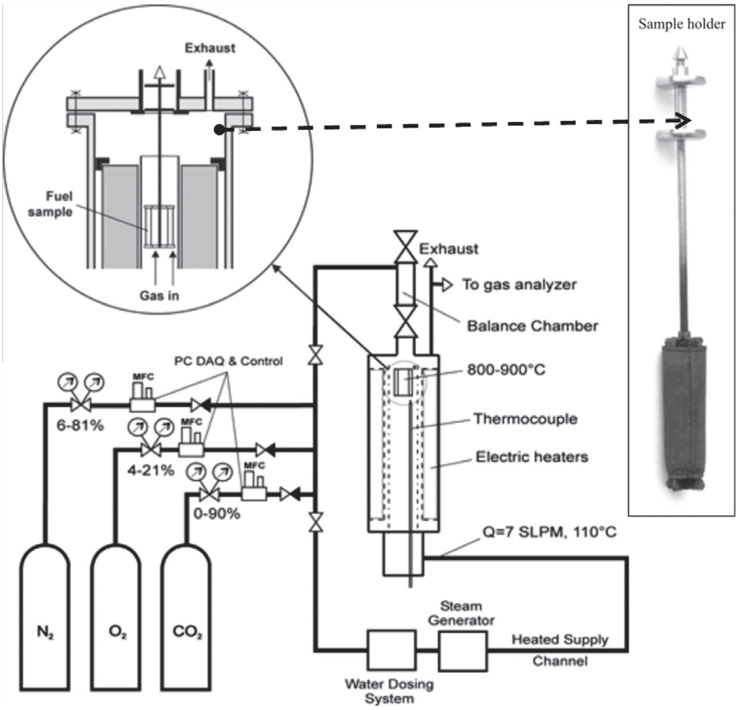

Fig. 1. Simplified schematic of the batch reactor and a sample holder.

Table 1
Firing temperatures and environmental conditions for the oil-shale combustion experiments, vol%.

Gas/temperature	800 °C	800 °C	800 °C	850 °C	850 °C	850 °C	900 °C	900 °C	900 °C
N_2	79	81	6	79	81	6	79	81	0
O_2	21	4	4	21	4	4	21	4	4
CO_2	0	15	90	0	15	90	0	15	96
H_2O	0/8/15	0/8/15	0/8/15	0/8/15	0/8/15	0/8/15	0/8/15	0/8/15	0/8/15

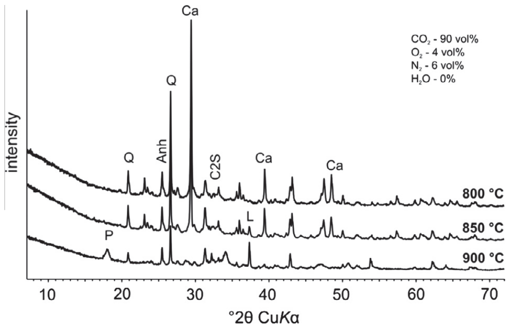

Fig. 2. Representative X-ray diffraction patterns of the collected ash. Experimental conditions are indicated in the figure. Anh – anhydrite, Ca – calcite, C2S – dicalcium silicate (belite), L – lime (CaO_{free}), and P – portlandite.

of countries, including China, Brazil, Jordan and Estonia, although large known reserves also exist in the U.S.A., Australia, Russia and elsewhere [21]. However, the increasing needs for energy (esp. in developing countries), the depletion of easily accessible oil reserves and the concurrently increasing oil prices have significantly raised the interest in oil-shale mining and processing in the last few decades.

A significant drawback of oil-shale usage is its large CO_2 footprint, which is due to the low calorific value of the fuel as well as the composition of the mineral matter. A considerable portion of the oil-shale deposits worldwide are found in shallow marine or lacustrine sediments dominated by carbonate-mineral assemblages. The thermal dissociation of Na-, Ca- and/or Ca–Mg-carbonate phases liberates large amounts of CO_2 and oxidizes organic carbon. As a result, oxy-fuel combustion technology and consequent CO_2 sequestration would be specifically demanded for oil-shale processing. On the other hand, the thermal decomposition of carbonate minerals is sensitive to the CO_2 partial pressure [22], and in contrast to the case of coal-type fuels, combustion air enriched with CO_2 can influence the mineral-transformation pathways and rates in oil-shale combustion. Moreover, the CO_2 levels can influence the melting of silicate phases and the formation of secondary Ca-silicate minerals that have a significant influence on the physical and chemical properties of the ash, such as the pozzolanic properties of the fine fractions of ash, and therefore the potential usability of the ash waste as a binder/cement additive.

Table 2
Mineral composition of ash (wt%).

Sample ID	1	2	3	4	5	6	7	8	9	10	11	12	13	14	15	16	17	18	19	20	21	22	23	24	25	26	27
Environment																											
Temp. (°C)	800	800	800	850	850	850	900	900	900	800	800	800	850	850	850	900	900	900	800	800	800	850	850	850	900	900	900
N_2, vol%	79	81	6	79	81	6	79	81	0	79	81	6	79	81	6	81	79.5	6	79	81	6	79	81	6	79	81	7.5
O_2, vol%	21	4	4	21	4	4	21	4	4	21	4	4	21	4	4	20.9	5	4	21	4	4	21	4	4	21	4	4.5
CO_2, vol%	0	15	90	0	15	90	0	15	96	0	15	90	0	15	90	0	15.5	90	0	15	90	0	15	90	0	15	88
H_2O vol%	0	0	0	0	0	0	0	0	0	8	8	8	8	8	8	8	8.1	7	15	15	15	15	15	15	15	14.7	15
Phases (wt%)																											
Calcite		3.1	36.8		1.2	30.6			0.2		1.8	42.1		0.9	30.4			0.6	0	1	37.5	0	2.4	14.3			2.9
Lime	27.4	25.1	0.1	23.6	27.2	0.8	23.1	22.5	22.4	25.2	25.9	0.1	26	26.9	2.3	23.9	23.7	24.3	27.4	30.4	0.1	25.2	29.1	13.5	23.6	22.9	23.9
Periclase	7.4	7.5	6.3	6.8	7.2	7.1	6.5	7.1	7.3	7.2	8	5.3	7.4	7.6	6.6	7.6	7	7	7.5	8.2	6.6	7.1	7.6	6.2	7.5	7	7.3
Anhydrite	7.2	6.9	5.2	6.8	6.5	5	6.9	6.7	5.4	6.2	6.9	4.3	7.6	6.6	4.6	7.3	6.8	5.3	5.9	6.8	4.2	6.3	5.6	4.5	6.3	6.1	4.9
C2S/belite	7.1	5.2	4.2	5.4	5.7	7.2	8.2	9.6	10.6	7.2	4.4	4.4	6.2	4.9	7.1	9.3	9.6	9.1	6.9	4.1	5.2	7.2	5.4	7.6	9.6	9.9	9.1
Merwinite	3	3.8	3.2	3.6	2.7	3.7	2.8	3.6	4	3.8	4.1	3.2	2.9	2.7	4	3.2	3.6	3.8	3.5	3.6	3.7	3.4	3	4.3	3	3.4	3.7
Wollastonite	1.7	1.9	2.2	1.8	2.7	2.3	2.2	2.2	2.4	1.7	2.3	2	2.6	2.6	2.4	2.1	2.4	2.5	1.5	1.9	2.2	1.9	2.3	2.7	2.8	2.5	2.4
Melilite	9.7	6.2	8.6	13.6	10.5	12.2	14.6	13.9	14.5	7.1	7.9	8	11.3	10.8	10.8	13.1	12.5	14	7.6	7.9	8.1	10.5	9.7	11.9	15.4	13.7	13.5
C3S	1.2	1.8	1.2	1.3	1.1	1.1	1.2	1.6	1.5	1.7	1.7	1.2	1.2	1.3	1.2	1.5	1.5	2	1.7	1.5	1.3	1.4	1.4	1.9	1.1	1.4	1.5
$(MgCa)_2SiO_6$			1.2	1	1.5	1.3	1.3		0.1			1.1	0.8	0.9	1.3	1.2	1.5	1.8			1.1	1.2	0.9	1.3	1.8	1.4	1.9
Quartz	12.1	12.9	11.4	10.5	10.8	9.5	10.2	9.7	8.2	11.1	11.2	10	10.7	11	10.3	9.7	8.7	8.9	11.3	12.1	11.4	10.5	11.2	10.5	8.9	10.2	8.8
K-feldspar	11.8	13.7	11.9	15.3	14.1	10.6	14.5	14.2	12.9	16.9	13.3	11.3	13.6	13	12.2	14.6	15.5	14.8	14.7	12.1	11.4	16.4	12.8	12.7	14.6	14.8	14.3
K-mica	2.7	3.4	1.5	2.5	1.3	0.8	0.8	0.9	1.5	2.6	3.8	1.1	1.8	2.5	tr.		0.8		2.8	2.5	1.3	1.1	1.2	1.2			
Hematite	8.8	8.5	6.1	7.7	7.4	7.7	7.5	8	8.1	9.3	8.7	5.8	7.9	8.1	6.8	6.7	6.5	5.9	9.1	7.8	5.8	7.5	7.1	7.3	5.3	6.6	5.6
Sylvite						tr.			0.8							tr.								tr.			

Table 3
Mineral composition of raw oil shale, wt%.

Sample	OS1	OS2	OS3
Phase	Mineral composition (wt%)		
Dolomite	18.6	18.2	19.1
Calcite	41.7	42.7	41
Quartz	12.1	12.4	11.9
K-feldspar	5.8	5.7	6.1
Illite	16.6	16.4	16.2
Chlorite	1.8	1.5	2
Kaolinite	tr.		tr.
Pyrite	3.2	3.1	3.5

Kukersite oil shale is a highly calcareous, fine-grained, organic-rich sediment [23]. The organic matter of kukersite (20–60%) is composed mostly of kerogen with a few percent bitumen [24]. The mineral matrix of the oil shale is mainly composed of calcite and, to a lesser extent, dolomite (altogether 20–70%) and terrigenous phases (quartz, feldspar and clay minerals) that compose approximately 15–60% of the oil shale [25]. Oil shale burned in power plants shows the following properties: moisture content (as-received fuel W_i^r = 11–13%), ash content (as-received fuel A^r = 45–57%), carbonate CO_2 (16–19%), and heating value (Q_i^r = 8.3–8.7 MJ/kg). In addition, the molar ratio of Ca/S = 8–10 in oil shale exceeds by more than 2–3 times the ratio of Ca/S sufficient to capture SO_2 completely [26–28]. The calorific value of the oil shale fired in power plants is at least two times lower than that of the average bituminous brown coal – 22.5 MJ/kg [23,29].

Various combustion technologies presently used in Estonia – pulverized combustion (PC) and circulating fluidized bed combustion (CFBC) [30] – cause significant differences in the composition of the ash, mainly due to different carbonate decomposition and reaction extents at various combustion temperatures [25,28,31–33]. Therefore, the goal of this study is to investigate influence of elevated CO_2 levels in various temperature regimes on carbonate-decomposition extents and secondary-phase formation using Estonian kukersite oil shale.

2. Material and methods

A laboratory batch reactor was used to provide a combustion environment at a specified temperature. The laboratory experimental facility (Fig. 1) is designed to burn a portion of the solid fuel. The experimental facility consists of a reactor-heater, a temperature-control system, a gas mixing-control system, a steam generator-insertion system, a flue gas analyzer and a data-acquisition and control system. The gas mixing-control system comprises mass-flow controllers (MFC), calibrated according to the gas to be used, and check valves. Water vapor, up to 25%, was added to the gas mixture with an integrated steam generator. To prevent water vapor condensation in the path from the steam generator to the reactor, a heated supply channel was used. The inlet of the reactor is also heated for the same reason. The batch reactor is designed to reach a working temperature up to 950 °C.

The kukersite oil shale in oxy-fuel experiments was sampled from crushed oil shale mined in Estonia underground mine. The oil shale was dried and crushed by passing through a 2-mm sieve opening. The median size of the oil shale used for the experiments was D_{mean} = 0.25 mm.

The combustion experiments were performed at temperatures of 800, 850 and 900 °C while varying the N_2, O_2 and CO_2 ratios (see Table 1 for the experimental conditions). In addition to the different temperatures and air-composition variation, water vapor was injected into the gas flow entering the furnace to study the water vapor influence on the solid-combustion products.

For each experiment a stainless steel bound net sample holder (Fig. 1) was used where approximately 5 g of oil shale were loaded into. In each run, the sample holder with the sample was loaded into the balance chamber (vertical chamber on the top of the reactor with ball valves at both ends). The balance chamber was filled with the gas mixture used in the experiment, and the pressures in the reactor and in the balance chamber were equilibrated. From the balance chamber, the sample holder was dropped into the reactor. Because combustion and the reactions with the oil shale minerals and coke require time, a period of 1.5 h that was sufficient for complete combustion was selected. The holding time was selected according to earlier studies on the behavior of oil-shale carbonates [34]. FTIR gas analyzer was used to monitor the combustion process. After 1.5 h the sample holder with residual ash was removed from batch reactor at preset test temperature and cooled down within minutes in exicator at room temperature.

Ash derived from the combustion reactor operated under various conditions was analyzed for the mineral composition and micromorphology of the ash particles. The mineral composition

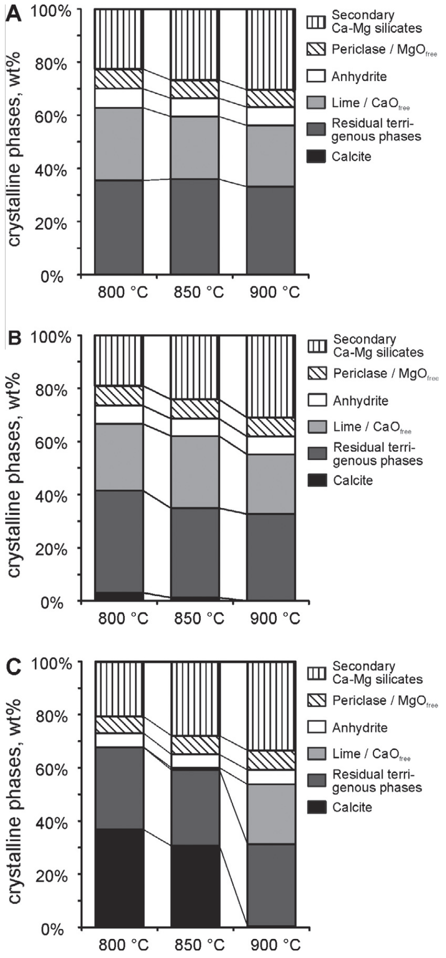

Fig. 3. Changes in the mineral composition of the crystalline phases under various experimental conditions. A – CO_2 = 0 vol%, H_2O = 0%, B – CO_2 = 15 vol%, H_2O = 0%, C – CO_2 = 90 vol%, and H_2O = 0%. Residual terrigenous phases – sum of quartz, K-mica, K-feldspar and hematite; Secondary Ca–Mg silicates – sum of C2S, C3S, merwinite, wollastonite, melilite and the $(MgCa)_2SiO_6$ phase.

of the crystalline phases in the ash and the raw oil shale was studied using powder X-ray diffraction (XRD) with a Bruker D8 diffractometer using Cu Kα radiation in the 2θ range of 3–72°, with a step size of 0.02° 2θ and a counting time of 0.1 s per step using a LynxEye linear detector. The X-ray tube was operated at 40 kV and 40 mA. The samples were powdered by hand using agate mortar, and unoriented preparations were made for the mineral analysis. The mineral composition of the samples was interpreted and modeled using the Rietveld algorithm-based code Siroquant 3.0 [35]. Most of the samples show the presence of secondary portlandite, which indicates the partial hydration of the original lime during the storage of the samples prior to XRD analysis (Fig. 2). The measured portlandite content was recalculated to the respective original amount of lime (CaO_{free}).

The micromorphology of the ash was investigated using a scanning electron microscope (SEM). Scanning electron microscopy (SEM) imaging and analysis of the samples was performed on a variable-pressure Zeiss EVO MA15 SEM equipped with an Oxford X-MAX energy dispersive detector system and AZTEC software for elemental analysis.

3. Results and discussion

The mineral composition of the raw oil shale and the ash derived from various experiments is reported in Tables 2 and 3, and representative X-ray patterns are shown in Fig. 2.

The mineral composition of the raw oil shale used in the experiments (Table 3) corresponds to a typical oil-shale feed used for power generation at thermal power plants and for shale-oil extraction [35] and is characterized by high calcite and dolomite contents of ~42 wt% and 19 wt%, respectively, and a terrigenous mineral assemblage of quartz (~12 wt%), K-feldspar (~6 wt%), clay minerals (~19 wt%) and pyrite (~3 wt%). The ash composition (Table 2) is dominated by lime (CaO_{free}), residual terrigenous mineral phases (quartz, K-feldspar and K-mica resulting from the dehydroxylation of illitic clay minerals), secondary Ca–Mg silicate phases (belite-C2S, merwinite and melilite), anhydrite, periclase (MgO_{free}) and undecomposed calcite. The lime content varies from trace amounts (<0.5 wt%) in experiments fired in an atmosphere containing 90 vol% CO_2 to a maximum of 25–30 wt% in a normal-air (79 vol% N_2 and 21 vol% O_2) environment at a 900 °C combustion temperature (Fig. 3). In contrast to the lime content, the content of calcite in the remaining ash increases with increasing CO_2 levels and decreased firing temperatures (Fig. 3). At 800 °C in 90 vol% CO_2 atmosphere, calcite composes more than 35% of the crystalline phases in the ash, and the injected H_2O vapor amount varies from 0 to 15 wt% (Table 2). The calcite-decomposition extent increased with temperature in CO_2 atmosphere, but a minor amount of calcite is still found in the ashes even at 900 °C. Unlike for calcite, however, the combustion temperatures were sufficiently high for the complete decomposition of Ca–Mg carbonate – dolomite, independent of the firing atmosphere composition. The dolomite content in the raw oil shale used in the experiment was 19 wt% of the crystalline phase, but this phase was not detected in any of the ashes that remained in the experiments. Instead, its decomposition products – periclase (MgO_{free}), lime (CaO_{free}) – and reaction products, such as secondary Ca–Mg silicate phases (e.g., merwinite), were present. In contrast, the decomposition of calcite, which begins to decompose at 620 °C and exhibits its maximal decomposition extent at 895–900 °C [22], was not completed if oil shale was fired at elevated CO_2 levels.

The thermal dissociation/decomposition of calcite and dolomite is strongly dependent on the CO_2 partial pressures [22]. Dolomite decomposes at low CO_2 (typically < 0.27 bar) pressures in a single step to CaO and MgO, and CO_2:

$$CaMg(CO_3)_2 = CaO + MgO + 2CO_2. \tag{1}$$

At higher CO_2 partial pressures, the decomposition occurs by a two-stage mechanism [36]:

$$\text{(a)}\ CaMg(CO_3)_2 = CaCO_3 + MgO + CO_2 \tag{2}$$

$$\text{(b)}\ CaCO_3 = CaO + CO_2. \tag{3}$$

It is important that the second reaction of the dolomite decomposition (and the decomposition of calcite) occurs at progressively higher temperatures if the CO_2 partial pressure is increased; the behavior of the first reaction is anomalous because it is initially shifted to lower temperatures as the CO_2 partial pressure increases and then becomes displaced to higher temperatures when the

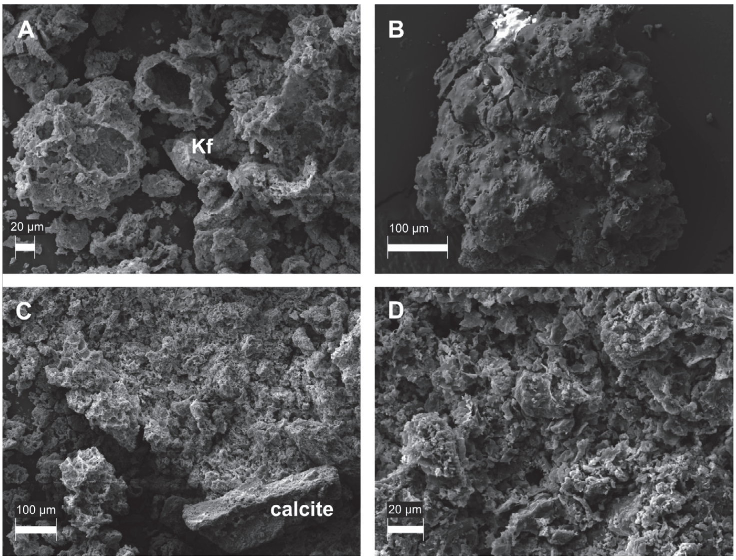

Fig. 4. Scanning electron micrographs of the ash fractions. A and B – 850 °C air conditions, $H_2O = 0\%$; C and D – 850 °C, $CO_2 = 90$ vol%, and $H_2O = 0\%$.

partial pressure of the carbon dioxide continues to increase [37,38]. However, equilibrium modeling of the mineral reactions under oxy-fuel combustion conditions [39] suggest that the high CO_2 levels do not delay the carbonate-mineral decomposition and that oxy-fuel firing would have little effect on the composition of the ash.

Nevertheless, our data suggest that the carbonate decomposition is delayed and that the composition of the ash is changed in oil-shale firing at elevated CO_2 levels. It is evident that, in our experiments under normal-air (79 vol% N_2 and 21 vol% O_2) conditions, the temperatures in the reactor were high enough for the complete decomposition of both dolomite and calcite, and the composition of the ash remaining is the same as under normal fluidized-bed combustion conditions [25]. However, at a CO_2 concentration of 15 vol%, the $CaCO_3$ (calcite) is already partly preserved at firing temperatures of 800 and 850 °C and is also present in trace amounts at 900 °C in a 90 vol% CO_2 atmosphere (Table 2, Fig. 3). Because the MgO content in the ash does not vary under the various combustion conditions, it can be suggested that reaction (2) is completed in all cases, whereas reaction (3) is delayed at elevated CO_2 levels.

The effect of the CO_2 concentration on oil-shale combustion is well illustrated by the scanning electron microscopy observation of the respective ashes (Fig. 4). No residual calcite- and/or dolomite-derived $CaCO_3$ particles were observed for normal-air (79 vol% N_2 and 21 vol% O_2) combustion, and the material is composed of highly porous ash particle aggregates, whereas the aggregates have a fused crust or have fused together into clumps of up to a few hundred micrometers in places (Fig. 4B). However, the residual and partly calcined calcite particles are abundant at the temperatures 800 and 850 °C in a 90 vol% CO_2 atmosphere (Fig. 4C), and the ash is composed of irregular 2–10 μm particle aggregates (Fig. 4D).

This conclusion is further supported by the calcite and secondary Ca–Mg phase ratios at various temperatures and CO_2 levels (Fig. 5) that show a ratio >1 (that is, showing “excess” calcite) in the ashes formed during the oil shale combustion in a 90 vol% CO_2 atmosphere at 800 °C, whereas the same ratio is approximately 0.75 at low H_2O vapor concentrations in the experiment at 850 °C. The calcite and secondary Ca–Mg phase ratio is well below 0.1 in the combustion experiments at 900 °C, indicating the nearly complete decomposition of calcite. This observation concurs with *in situ* XRD studies [40] suggesting that, in an air environment, reactions (2) and (3) occur simultaneously and are already complete by 750–780 °C. In a CO_2 atmosphere, however, the discrete $CaCO_3$ formed in reaction (2) and the primary calcite are stable up to 900–910 °C, at which temperature reaction (3) begins, which is completed at approximately 950–960 °C [40].

The formation of the secondary Ca–Mg silicate phases is directly proportional to the firing temperature (and the decomposition extent of the carbonate minerals), but it does not to appear to depend on the CO_2 level or the injected-H_2O vapor amounts (Table 2). The sum of the secondary Ca–Mg silicates as a percentage of the total crystalline phases varies, with averages of 20–21% at 800 °C, approximately 25% at 850 °C, and approximately 31% at 900 °C. H_2O vapor injection in low-temperature combustion (800 °C) and low CO_2 levels do not produce a significant influence on the carbonate decomposition and secondary-phase formation (Fig. 5). However, the ratio of the residual calcite and secondary Ca–Mg phases is influenced by the amounts of injected H_2O vapor at higher temperatures in 90 vol% CO_2 atmosphere (Fig. 5). At 850 °C, the injection of 15% water vapor facilitated the calcite decomposition compared to the results of the experiments with 8% or no water vapor. In contrast, although the scale is different, the effect at 900 °C is opposite, and the decomposition of calcite is nearly complete in the dry environment, whereas while some calcite is still preserved if 8% and 15% water vapor were added. The latter observation is interesting because the decomposition rate is typically enhanced in the presence of water (vapor) due to either catalytic function of H_2O on the Ca-carbonate surface reactions [38,41] or effects on gas physical properties influencing heat transfer from gas to solid [42]. However, Khraisha and Dugwell [43] reported a positive effect on calcination rate when 2.22% H_2O was added, while the rate decreased when 6.09% H_2O was added, which they explained as due to the reduced CO_2 diffusion rate at higher water vapor levels. Moreover, numerical modeling

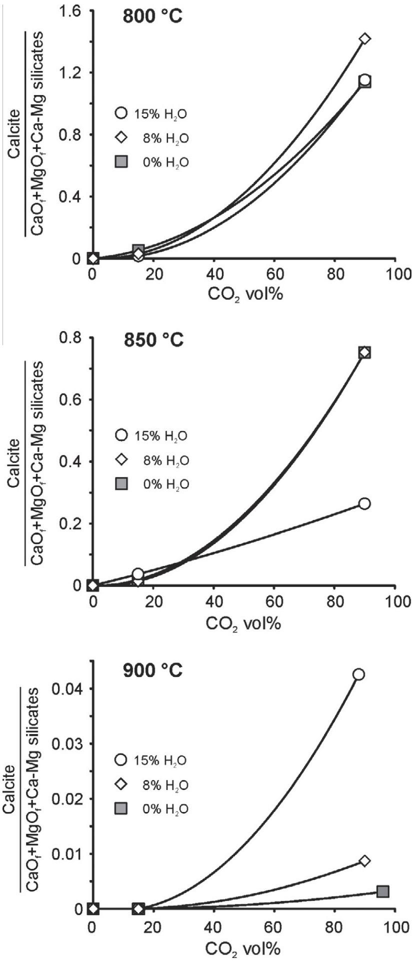

Fig. 5. Ratio of the calcite and secondary Ca–Mg phases at various combustion temperatures, CO_2 levels and H_2O injections.

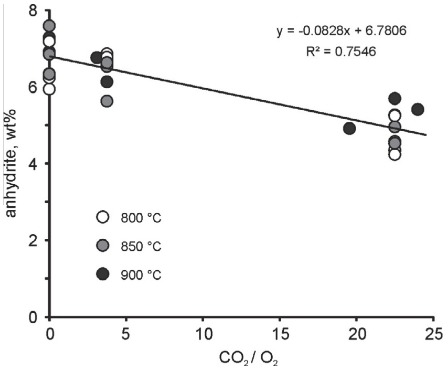

Fig. 6. Variation in the anhydrite content in the ash at various CO_2/O_2 ratios.

of $CaCO_3$ decomposition under oxy-fuel conditions [44], indicates that as the increase of CO_2 concentration from 70% to 80%, the decomposition rate of $CaCO_3$ decreases significantly, but the enhancement in the calcination rate diminishes when increasing the H_2O concentration from 5% to 20% at a fixed CO_2 concentration.

Our experiments suggest that the elevated CO_2 levels and the inhibited carbonate decomposition rate have a noticeable effect on the SO_2 binding and the stable anhydrite formation in oil-shale ash (Fig. 6). The anhydrite content decreases from approximately 7 wt% of the crystalline phases in the remaining ash under air conditions, independent of the firing temperature, to approximately 6.5 wt% in the experiment with 15 vol% of CO_2 and an average of 5 wt% in the 90 vol% atmosphere. This is a somewhat unexpected finding because, for a study of competitive carbonation and sulfonation under high-CO_2-concentration coal combustion, direct and effective sulfation of the carbonate occurred in a fixed-bed reactor experiment [45]. Similarly, Zheng and Furinsky [39] suggested, using equilibrium calculations, that sulfation, rather than carbonation, would be the preferred reaction under oxy-fuel conditions. On the other hand, it must be considered that high degree of sulfation in [45] experiments were attained only after prolonged (~1.4 h) reaction times under continuous fed of external SO_2 gas. Though the reaction times in our experiments were comparable (1.5 h), then in oil shale burning the sulfur is deliberated *in situ* from the oil shale itself – initial stages of the burning organics and the decomposition of sulfide minerals (mainly pyrite) that occurs at temperatures well below 700 °C when calcination was still not completed. This would suggest that SO_2 was in the very contact with lime particles during a shorter time in our experiment. Also, at higher CO_2/O_2 ratios the O_2 is more or less absent in the very vicinity of the fuel particles and the conditions were not favoring the stability of $CaSO_4$. Alternatively, this phenomenon could be related to the competition between the formation of Ca(Mg)silicate and Ca-sulfate secondary phases. Thus, further investigation is required.

4. Conclusion

Laboratory batch-reactor experiments of highly calcareous oil-shale combustion under oxy-fuel conditions were performed at temperatures of 800, 850 and 900 °C while varying the N_2, O_2 and CO_2 ratios. In addition to different temperatures and air-composition variation, water vapor was injected into the gas flow entering the furnace to study the water vapor influence on the solid-combustion products. Our experiments show that decomposition of the Ca–Mg carbonate phase dolomite is completed in all temperature regimes in the various combustion atmospheres. However, the decomposition of the $CaCO_3$ phase (calcite) is significantly delayed at elevated CO_2 levels. Our results suggest that the elevated CO_2 levels and the inhibited carbonate (calcite) decomposition extent have a noticeable effect on the SO_2 binding and, consequently, on the stable anhydrite formation in oil-shale ash.

Acknowledgments

This research was supported by the European Union through the European Regional Development Fund and by the Estonian Ministry of Education and Research Project AR12003 “Reduction of CO_2 emission of CFB boiler by enrichment of combustion air with oxygen.”

References

[1] Okawa M, Kimura N, Kiga T, Takano S, Arai K, Kato M. Trial design for a CO_2 recovery power plant by burning pulverized coal in O_2/CO_2. Energy Convers Manage 1997;38:S123–7.

[2] Horn FL. Steinberg M control of carbon dioxide emissions from a power plant (and use in enhanced oil recovery). Fuel 1982;61:415–22.

[3] Herzog H, Golomb D, Zemba S. Feasibility, modeling and economics of sequestering power-plant CO_2 emissions in the deep ocean. Environ Prog 1991;10:64–74. http://dx.doi.org/10.1002/ep.670100118.

[4] Abraham BM, Asbury JG, Lynch EP. Teotia APS coal-oxygen process provides CO_2 for enhanced recovery. Oil Gas J 1982;80:68.

[5] Nakayama S, Noguchi Y, Kiga T, et al. Pulverized coal combustion in $O2/CO_2$ mixtures on a power plant for CO_2 recovery. Energy Convers Manage 1992;33:379–86.

[6] Simmonds M, Miracca I. Gerdes K oxyfuel technologies for CO_2 capture: a techno-economic overview. Greenhouse Gas Control Technol 2005:1125–30.

[7] Châtel-Pélage Fabienne, Rajani V, Pavol P, et al. Applications of oxygen for NOx control and CO_2 capture in coal-fired power plants 2006;10:119–42.

[8] Fujimori T, Yamada T. Realization of oxyfuel combustion for near zero emission power generation. Proc Combust Inst 2013;34:2111–30.

[9] Wall TF, Liu Y, Spero C, Elliot LK, Khare S, Rathnam R, et al. An overview on oxyfuel coal combustion – state of the art research and technology development. Chem Eng Res Des 2009;87:1003–16.

[10] Sheng C, Li Y. Experimental study of ash formation during pulverized coal combustion in O_2/CO_2 mixtures. Fuel 2008;87:1297–305.

[11] Fryda L, Sobrino C, Cieplik M, Van de Kamp WL. Study on ash deposition under oxyfuel combustion of coal/biomass blends. Fuel 2010;89:1889–902.

[12] Fryda L, Sobrino C, Bertrand C, Cieplik M. Study of ash deposition during coal combustion under oxyfuel conditions. Fuel 2012;92:1–10.

[13] Sheng C, Lu Y, Gao X, Yao H. Fine ash formation during pulverized coal combustion – a comparison of O_2/CO_2 combustion versus air combustion. Energy Fuels 2007;21:435–40.

[14] Li G, Li S, Dong M, Yao Q, Guo CY, Axelbaum RL. Comparison of particulate formation and ash deposition under oxy-fuel and conventional pulverized coal combustions. Fuel 2013;106:544–51. http://dx.doi.org/10.1016/j.fuel.2012.10.035.

[15] Hurst HJ, Levy JH, Patterson JH. Siderite decomposition in retorting atmospheres. Fuel 1993;72:885–90.

[16] West AR. Solid state chemistry and its applications. New York: Wiley; 1984. p. 734.

[17] Cohn A. Formation of magnetite nanoparticles by thermal decomposition of iron bearing carbonates: implications for the evidence of fossil life on Mars. In: National nanotechnology infrastructure network, research experience for undergraduates, accomplishments program. NY, USA: Cornell; 2006. p. 58–9.

[18] Qian J. Oil shale-petroleum alternative. Beijing: China Petrochemical Press; 2010.

[19] Bauert H, Kattai V. Kukersite oil shale. In: Raukas A, Teedumäe A, editors. Geology and mineral resources of Estonia. Tallinn: Estonian Academy Publishers; 1997. p. 313–27.

[20] Craig JR, Vaughan DJ, Skinner BJ. Resources of the earth: origin, use, and environmental impact. 4th ed. Upper Saddle River, NJ: Prentice-Hall; 2001.

[21] World Energy Council. Oil Shale. In: Clarke AW, Trinnaman JA, Clarke AW, Trinnaman JA, editors. Survey of energy resources. London: World Energy Council; 2010. p. 93–123.

[22] L'vov BV. Mechanism and kinetics of thermal decomposition of carbonates. Thermochim Acta 2002;386:1–16.

[23] Ots A. Oil shale fuel combustion. Tallinn: Tallinna Raamatutrükikoda; 2006.

[24] Koel M. Estonian oil shale, Oil Shale extra; 1999 (<http://www.kirj.ee/oilshale/Est-OS.htm>) 08.10.10.

[25] Kuusik R, Uibu M, Kirsimäe K, Mõtlep R, Meriste T. Open-air deposition of Estonian oil shale ash: formation, state of art, problems and prospects for the abatement of environmental impact. Oil shale 2012;29:376–403.

[26] Konist A, Pihu T, Neshumayev D, Külaots I. Low grade fuel-oil shale and biomass co-combustion in CFB boiler. Oil shale 2013;30:294–304.

[27] Konist A, Pihu T, Neshumayev D, Siirde A. Oil shale pulverized firing: boiler efficiency, ash balance and flue gas composition. Oil shale 2013;30:6–18.

[28] Bityukova L, Mõtlep R, Kirsimäe K. Composition of pulverized firing and circulating fluidized-bed boiler oil shale ashes in Narva thermal power plants, Estonia. Oil Shale 2010;27:339–53.

[29] Dyni JR. Geology and resources of some world oil-shale deposits. Oil Shale 2003;20:193–252.

[30] Plamus K, Ots A, Pihu T, Neshumayev D. Firing Estonian oil shale in CFB boilers – ASH balance and behaviour of carbonate minerals. Oil shale 2011;28:58–67.

[31] Kuusik R, Uibu M, Kirsimäe K. Characterization of oil shale ashes formed at industrial-scale CFBC boilers. Oil shale 2005;22:407–19.

[32] Pihu T, Arro H, Prikk A, et al. Oil shale CFBC ash cementation properties in ash fields. Fuel 2012;93:172–80.

[33] Liira M, Kirsimäe K, Kuusik R, Mõtlep R. Transformation of calcareous oil-shale circulating fluidized-bed combustion boiler ashes under wet conditions. Fuel 2009;88:712–8.

[34] Ots A, Pihu T, Hlebnikov A, Arro H. Influence of sulfur dioxide on decomposition of oil shale mineral matter. Oil shale 2001;18:298–305.

[35] Taylor JC. Computer programs for standardless quantitative analysis of minerals using the full powder diffraction profile. Powder Diffr 1991;6:2–9.

[36] Mõtlep R, Kirsimäe K, Talviste P, Puura E, Jürgenson J. Mineral composition of Estonian oil shale semi-coke sediments. Oil shale 2007;24(3):405–22.

[37] Samtani M, Dollimore D, Alexander KS. Thermal decomposition of dolomite in an atmosphere of carbon dioxide. J Therm Anal Calorim 2001;63:93–101.

[38] McIntosh RM, Sharp JH, Wilburn FW. The thermal decomposition of dolomite. Thermochim Acta 1990;165:281–96.

[39] Zheng L, Furimsky E. Assessment of coal combustion in O_2 + CO_2 by equilibrium calculations. Fuel Process Technol 2003;81:23–34.

[40] Engler P, Santana MW, Mittleman ML, Balazs D. Non-isothermal, in situ XRD analysis of dolomite decomposition. Thermochim Acta 1989;140(C):67–76.

[41] MacIntire WH, Stansel TB. Steam catalysis in calcinations of dolomite and limestone fines. Ind Eng Chem 1953;45:1548–55.

[42] Wang Y, Lin S, Suzuki Y. Limestone calcination with CO_2 capture (II): decomposition in CO_2/steam and CO_2/N_2 atmospheres. Energy Fuels 2008;22:2326–31.

[43] Khraisha YH, Dugwell DR. Effect of water-vapor on the calcination of limestone and raw meal in a suspension reactor. Chem Eng Res Des 1991;69:76–8.

[44] Yin J, Kang X, Qin C, Feng B, Veeraragavan A, Saulov D. Modeling of $CaCO_3$ decomposition under CO_2/H_2O atmosphere in calcium looping processes. Fuel Process Technol 2014;125:125–38.

[45] Liu H, Katagiri S, Kaneko U, Okazaki K. Sulfation behavior of limestone under high CO_2 concentration in O_2/CO_2 coal combustion. Fuel 2000;79(8):945–53.

Paper IV

Lauri Loo, Alar Konist, Dmitri Neshumayev, Tõnu Pihu, Birgit Maaten, Andres Siirde. "Ash and Flue Gas from Oil Shale Oxy-Fuel Circulating Fluidized Bed Combustion" Energies 11, no. 5 (May 10, 2018): 1218. https://doi.org/10.3390/en11051218.

energies

Article

Ash and Flue Gas from Oil Shale Oxy-Fuel Circulating Fluidized Bed Combustion

Lauri Loo *, **Alar Konist**, **Dmitri Neshumayev**, **Tõnu Pihu**, **Birgit Maaten** and **Andres Siirde**

Department of Energy Technology, Tallinn University of Technology, 19086 Tallinn, Estonia;
alar.konist@ttu.ee (A.K.); dmitri.nesumajev@ttu.ee (D.N.); tonu.pihu@ttu.ee (T.P.); birgit.maaten@ttu.ee (B.M.);
andres.siirde@ttu.ee (A.S.)
* Correspondence: lauri.loo@ttu.ee; Tel.: +372-620-3907

Received: 13 April 2018; Accepted: 9 May 2018; Published: 10 May 2018

Abstract: Carbon dioxide emissions are considered a major environmental threat. To enable power production from carbon-containing fuels, carbon capture is required. Oxy-fuel combustion technology facilitates carbon capture by increasing the carbon dioxide concentration in flue gas. This study reports the results of calcium rich oil shale combustion in a 60 kW_{th} circulating fluidized bed (CFB) combustor. The focus was on the composition of the formed flue gas and ash during air and oxy-fuel combustion. The fuel was typical Estonian oil shale characterized by high volatile and ash contents. No additional bed material was used in the CFB; the formed ash was enough for the purpose. Two modes of oxy-fuel combustion were investigated and compared with combustion in air. When N_2 in the oxidizer was replaced with CO_2, the CFB temperatures decreased by up to 100 °C. When oil shale was fired in the CFB with increased O_2 content in CO_2, the temperatures in the furnace were similar to combustion in air. In air mode, the emissions of SO_2 and NO_x were low (<14 and 141 mg/Nm^3 @ 6% O_2, respectively). Pollutant concentrations in the flue gas during oxy-fuel operations remained low (for OXY30 SO_2 < 14 and NO_x 130 mg/Nm^3 @ 6% O_2 and for OXY21 SO_2 23 and NO_x 156 mg/Nm^3 @ 6% O_2). Analyses of the collected ash samples showed a decreased extent of carbonate minerals decomposition during both oxy-fuel experiments. This results in decreased carbon dioxide emissions. The outcomes show that oxy-fuel CFB combustion of the oil shale ensures sulfur binding and decreases CO_2 production.

Keywords: circulating fluidized bed combustion; carbon capture; storage and utilization; sulfur binding; nitrogen oxides; emissions; ash behavior; carbonate minerals

1. Introduction

Carbon dioxide emissions continue to be a major environmental concern of solid fuel combustion. Carbon capture and storage is required in order to meet future targets for greenhouse gas emissions. The typical technologies related to CO_2 capture are pre-combustion, post-combustion and oxy-fuel combustion [1]. Oxy-fuel combustion is considered as one of the most promising carbon dioxide capture approaches [2–4]. It involves combustion of fuel in a mixture of nearly pure oxygen and recycled flue gas to control the combustion temperature. There is a number of ongoing oxy-fuel combustion commercialization and demonstration projects, most of them are utilizing pulverized combustion (PC) technology [5,6]. Circulating fluidized bed (CFB) combustion technology is proven and has advantages such as fuel flexibility and environmental performance. When applying oxy-fuel combustion with a CFB, the circulating solid matter offers another temperature control method. Due to this, less circulated flue gas is required for temperature control. Regardless of the exact solution, the main purpose of applying an oxy-fuel approach is to enable power production without carbon dioxide emissions by producing an enriched carbon dioxide flow at the combustion unit's outlet to simplify its utilization or sequestration.

The fuel used in this study was typical Estonian oil shale. Oil shale is a low-grade fossil fuel that has extremely high ash and volatile contents. The worldwide oil shale reserves have enormous energy potential, but it is industrially used only in Estonia, Brazil and China [7]. Oil shale can be utilized for energy production via gasification, pyrolysis or combustion. Estonian oil shale based power production relies on PC and CFB combustion technologies [8,9]. Industrial experience has shown that, due to a high process efficiency, low emissions, and no requirements for SO_x or NO_x emission control systems, CFB combustion of oil shale is the best available technology [10–13]. Industrial trials [12,14] have shown that CFB combustion technology is suitable for oil shale co-firing with biomass, pyrolysis gas and peat, thereby enabling fuel flexibility.

Substituting N_2 with CO_2 has an influence on combustion, pollutant formation, mineral matter behavior and temperature in the combustor. Previous research has shown that, when the oxidizer contains a similar amount of O_2, then, in CO_2, the combustion is delayed [15–17]. Delayed combustion and increased specific heat of the gas mix leads to up to a 100 °C temperature decrease in the furnace [3,18]. To overcome this obstacle, O_2 concentration is increased. Generally, a mixture containing 30% O_2 and 70% CO_2 allows obtaining similar temperatures in furnace as in a regular air-fired CFB.

Sulfur oxides are one of the main pollutants from combustion, causing acid rains and disturbing CO_2 compression when applying oxy-fuel combustion. The SO_2 concentration in flue gas can be reduced by injecting sorbents, such as limestone or dolomite, into a CFB. Estonian oil shale has a high content of carbonate minerals (mostly calcite and dolomite). Due to this, no additional bed material is needed. The sulfur capture process depends on calcination, which depends on CO_2 partial pressure and temperature. If the CO_2 partial pressure is lower than the equilibrium pressure [19], limestone decomposes and forms CaO and CO_2,

$$\mathrm{CaCO_3(s) \leftrightarrow CaO(s) + CO_2(g).} \tag{1}$$

The CaO then reacts with SO_2,

$$\mathrm{CaO(s) + SO_2(g) + 0.5O_2 \leftrightarrow CaSO_4(s).} \tag{2}$$

This process is called indirect sulfation. If the calcination process does not take place, then SO_2 may react directly with $CaCO_3$,

$$\mathrm{CaCO_3(s) + SO_2(g) + 0.5O_2 \leftrightarrow CaSO_4(s) + CO_2(g).} \tag{3}$$

In air-fired atmospheric units, sulfur capture occurs via relatively rapid calcination (Equation (1)) and much slower sulfation reactions (Equation (2)). In oxy-fuel CFB combustors, sulfation can occur directly without the calcination step (Equation (3)). Theoretical calculations [20–22] and a previous study in a lab-scale fluidized bed batch reactor [23] revealed that carbonate minerals do not fully decompose under oxy-fuel combustion environment and the sulfur binding rate decreases, similar to the experiments of Li et al. [24]. On the contrary, some other experiments [18,25,26] showed a decrease in sulfur emissions or increased sulfur capture efficiency when applying oxy-combustion. This means that, it is still unclear if sulfur binding rate is sufficient.

Other important pollutants from combustion are nitrogen oxides (NO_x) [27,28]. Nitrogen content in the Estonian oil shale is low, below 0.1% in dry fuel. Due to this and the low temperatures in CFB combustors, no problems with excess nitrogen oxide formation were recorded from the utility boilers [10]. One advantage of oxy-fuel technology is its potentially lower NO_x production. Results from different experimental facilities are rather diverse [18,29–33]. Overall, the results indicate that nitrogen behavior in the oxy-fuel mode is similar to combustion in air and no drastic changes are expected in fuel nitrogen conversion to oxides.

Changes in the gas composition in a combustor may alter the transformation of minerals and cause fouling or particles agglomeration in the bed. Estonian oil shale has a high ash and carbonates content. When PC was applied to Estonian oil shale combustion, major difficulties due to sediments formation on heating surfaces occurred [34]. Applying CFB technology resolved such problems, because it was possible to decrease temperatures in furnace below 850 °C [10]. From previous experience, we know that decreased decomposition of carbonate minerals results in up to 13% smaller carbon dioxide production [20]; at the same time, it increases total ash production from combustion.

Mapping waste is important for finding solutions to turn ash, or at least a part of it, into products [35,36]. Wang et al. [37] found no major differences in oxy-fuel residues when compared to regular ash. Our previous experiments at laboratory scale fluidized bed reactor showed a considerable decrease of carbonaceous minerals decomposition in oxy-fuel environment [23]. This means that CO_2 emissions decrease, but the production of ash increases. [36]. More than 90% of oil shale ash is currently landfilled [38]. In landfills, it cements and binds approximately 8% of the total emitted carbon dioxide [39]. Experiments with oxy-fuel CFB ash showed that the ash can still fix a similar amount of CO_2 [40]. The natural CO_2 sequestration uses only a part of the ash's total potential, because only the surface of the particles is available for the reaction. The calcium rich ash could be employed for improved CO_2 sequestration [41]. For example, Zevenhoven et al. [42] proposed precipitated calcium carbonate production from calcium-containing industrial wastes. The concept could be applied with oil shale ash; as a result, a large amount of CO_2 would be fixed, and waste ash would be used and a valuable product would be produced.

Higher CO_2 concentration in flue gas eases utilization or gas transportation to geological storage sites. The nearest option for CO_2 storing from a possible oxy-fuel power plant in Estonia would be in the South Kandava sandstone in Latvia (500 km from the oil shale mines). The formation has been evaluated to be suitable for CO_2 geological storage [43,44].

The experience shows that substituting nitrogen with carbon dioxide as diluent is not trivial and generates important differences. To investigate possible changes in the flue gas and produced ash when applying oxy-fuel combustion on Estonian oil shale, combustion experiments in a 60 kW_{th} CFB combustor were performed using air and mixed gases to simulate possible oxy-fuel combustion environments. Flue gas and produced ash samples were collected and analyzed.

2. Experimental Section

2.1. The Oil Shale

The experiments were carried out with typical Estonian oil shale from the Ojamaa underground mine. The fuel was dried, crushed and sieved to under 3 mm. The ultimate and proximate analysis of the oil shale is listed in Table 1. The oil shale contained a considerable amount of sulfur, but had a low nitrogen content. The laboratory ash composition is shown in Table 2. The Ca/S molar ratio in the oil shale was 8.0. The values were typical for oil shale used in the Estonian oil shale industry. The only major difference was the fuel moisture content. The oil shale used in the experiments was room dry. Normally, the oil shale used in the industry has a moisture content slightly over 10% [11,45].

Table 1. Proximate and ultimate analysis of the oil shale.

Net Heating Value, MJ/kg	Proximate Analysis, $wt._{as\ received}$ %				Ultimate Analysis, $wt._{dry}$ %					
	Moisture	Volatile Matter *	Fixed Carbon	Ash	C	N	S	H	TOC **	$(CO_2)_{mineral}$
8.56	0.50	47.5	1.3	50.7	27.4	0.07	1.6	2.7	21.8	20.6

* Volatile matter includes mineral CO_2 from decomposition of carbonate minerals; ** TOC—total organic carbon.

Table 2. Chemical composition of the oil shale laboratory ash.

Constituent	CaO	SiO_2	Al_2O_3	SO_3	MgO	Fe_2O_3	K_2O	Cl	Na_2O	Other
Content, wt %	43.9	27.5	8.6	5.5	4.9	4.8	3.3	0.4	0.1	1.0

2.2. The Circulating Fluidized Bed Combustion Test Facility

The experiments were conducted using a 60 kW_{th} CFB combustor, which was designed and constructed for fuels with high, up to 60 wt %, ash content. The main components of the test facility are shown in Figure 1. The height of the furnace was 4.90 m and its inner diameter was 0.12 m. The combustion chamber was isolated with ceramics and high temperature thermal isolation material. To minimize leaks, the combustor was enclosed in a stainless steel shell. The fuel was fed with a screw conveyer at the height of 0.49 m, and the recirculated solids were fed back at a height of 0.86 m with secondary air.

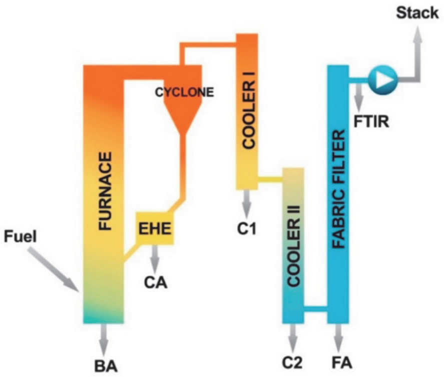

Figure 1. The 60 kW_{th} circulating fluidized bed combustion test facility.

The solid particles were separated from flue gas in a cyclone (cut-point 10 µm) and returned to the bottom bed through a return leg and an external heat exchanger (EHE) where solids were cooled in order to control the temperature of the bed. After the cyclone, the flue gas was cooled with a two-stage cooling system, consisting of two shell-and-tube heat exchangers in series. The heat transfer surfaces of these heat exchangers were composed of longitudinally-streamlined tubes. The fly ash was removed from flue gas with a fabric filter. The cleaned flue gas was led out of the system by means of an induced high pressure fan through the stack.

The combustion air was supplied with a compressor. The simulation of recycle flue gas was performed using bottled CO_2 and O_2. All gas lines, for O_2, CO_2 and compressed air, were equipped with mass flow controllers for exact control of the mass flow rates and the ratio of O_2/CO_2. The combustion air tubes were equipped with electrical heaters to maintain the necessary gas temperature. Extra bed material was not needed since oil shale contains more than enough ash.

The test facility was equipped with two independent fuel/bed material feed silos and a gas burner. The control and data acquisition of the test facility was fully automated and operated by a LabVIEW system. The flue gas composition was simultaneously analyzed with a FTIR spectrometer and was presented as dry gases at 6% O_2. Ash samples were collected from five points: bottom ash (BA), cyclone ash (CA), cooler 1 ash (C1), cooler 2 ash (C2) and fabric filter ash (FA). The collected samples were pulverized. The chemical composition of the produced ashes and the fuel were measured with Rigaku ZSX Primus II wavelength dispersive X-ray fluorescence spectrometer and elemental analyzer Vario

Macro CHNS Cube. Mineral CO_2 amount was measured in the samples with the elemental analyzer using the total inorganic carbon module applying diluted HCl to decompose the carbonate minerals.

The combustor can operate both in a conventional air mode regime as well as in oxy-fuel regime. During the experiments the test facility was started in air-fired mode. After achieving the steady state regime, the gradual switch to oxy-fuel mode was started. The results presented in this paper were obtained at steady-state CFB combustion mode. The experiments were conducted using three different gas mixtures: air, OXY21 (21% oxygen and 79% carbon dioxide) and OXY30 (30% oxygen and 70% carbon dioxide). The air was used to create a base case scenario. In OXY21 mixture, nitrogen was replaced with CO_2, thus showing the effect of replacing the carrier gas. Since previous experiments have shown temperature drops when using similar oxygen concertation in the oxy-fuel mode, OXY30 was chosen to try to obtain a similar temperature field in the furnace as in conventional CFB.

2.3. Description of the Experiments

For the startup, a small amount (3 kg) of oil shale ash was inserted into the return leg. The typical startup began with preheating the riser, with electrically-heated air, up to 300 °C. Then the first small amount of oil shale was fed into the riser. The fuel ignited and the furnace was gradually warmed up to a working temperature.

CFB combustor main working parameters are shown in Table 3. During the experiments, the thermal load of the combustor was 24 ± 3 kW. The OXY30 experiment was conducted at a lower thermal load due to fuel feeder problems. The primary and secondary air ratio was 4/6, because the fuel had a high volatile content. Although the thermal load varied due to fuel feeding problems, the data in Table 3 show that temperatures during all the experiments in the CFB combustor were similar.

Table 3. Average working parameters of the circulating fluidized bed (CFB) during different experiments.

	Air	OXY21	OXY30
Bed temperature, °C	749	676	773
Riser temperature, °C	752	692	743
Combustion air temperature, °C	284	250	242
Primary oxidizer flow, SLPM	394	279	198
Total oxidizer flow, SLPM	857	710	438
Thermal load, kW	25.3	23.8	14.1
Pressure drop in bed, kPa	2.4	3.6	1.4
Gas velocity in the bed, m/s	2.17	1.43	1.12

Temperature profiles in the riser during stable operation in air and oxy-fuel modes are shown in Figure 2. The temperatures in the riser during air operation were similar to the values used in oil shale industrial CFB boilers (800 °C) [10]. During OXY21 operation, the temperature in the riser dropped by up to 100 °C. Similar temperature drops in the furnace, when substituting N_2 with CO_2, have been noticed before when oxy-firing coals [3,18]. At the same time, the temperature in the cyclone exit remained similar. Slight drop of primary air temperature from 284 to 250 °C was noticed. This might be the reason for decreased temperatures in the riser, together with decreased fuel reactivity and increased heat capacity of the CO_2 atmosphere [15]. During the experiment with an increased O_2 concentration (OXY30), the temperature distribution was similar to air mode. Specific heat and oxygen diffusivity were similar to air and most retrofit experiments suggest such a mixture for oxy-fuel operations [46].

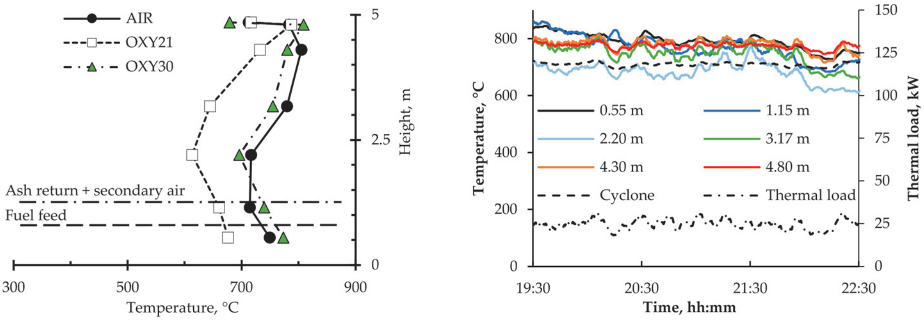

(**a**) (**b**)

Figure 2. (**a**) Temperature distribution along the circulating fluidized bed (CFB) combustor riser and in the cyclone; (**b**) temperatures in the CFB cyclone exit and furnace at different heights. The temperatures deviance, due to fuel feeder, was up to 5%.

3. Results and Discussion

3.1. Sulfur Oxides Emissions

The average emission values during stable operation are shown in Table 4 and Figure 3. In spite of decreased temperatures in the riser during oxy-fuel operations (Figure 2), the SO_2 concentration in the flue gas remained similar. Higher CO_2 partial pressure and lower temperature in the system inhibited decomposition of $CaCO_3$, but the Ca/S molar ratio in the oil shale was as high as 8.0. It means that there was a lot of excess calcium in the system and even if the sulfur binding rate was inhibited as noted in reference [23], it was still enough to bind more than 99% of the sulfur. The oxy-fuel ashes contained a considerable amount of carbonates ($(CO_2)_{mineral}$) (see Figure 4) indicating decreased decomposition of carbonate minerals. During oxy-fuel combustion, sulfation was likely direct (see Equation (3)); the calcite reacted directly with sulfur oxide. When the oil shale was fired in air, the sulfation likely occurred via indirect reaction, because low carbonate concentration in ash indicated free lime availability for indirect sulfation (Equation (2)). Our results suggest that the elevated CO_2 levels and the inhibited carbonate decomposition extent do not have a noticeable effect on the SO_2 binding (see Table 5).

Table 4. Average emissions of oil shale firing in the CFB combustor.

Item	Unit	Air	OXY21	OXY30
O_2	$\%_{dry}$	10.0 ± 1.9	8.5 ± 2.1	12.9 ± 2.9
NO_x	mg/Nm^3 @ 6%O_2	141 ± 29	156 ± 20	130 ± 65
SO_2	mg/Nm^3 @ 6%O_2	<14 ± 9	23 ± 14	<14 ± 4
CO	mg/Nm^3 @ 6%O_2	943 ± 99	2361 ± 953	337 ± 466
Desulfurization efficiency	%	99	99	99
SO_2 emission	mg/MJ	<8	9	<8
NO_x emission	mg/MJ	34	40	33
Fuel nitrogen conversion ratio	%	20	24	20

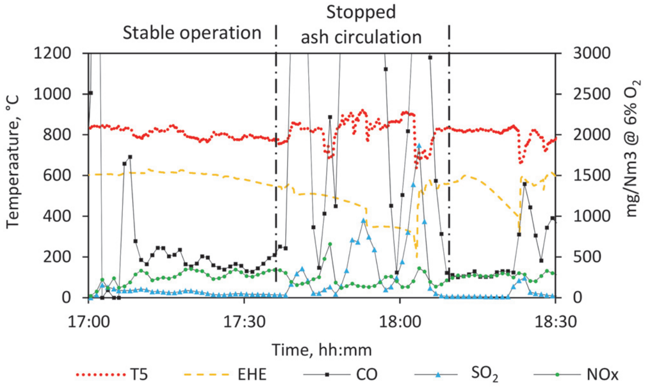

Figure 3. Pollutant emissions during oil shale CFB and fluidized bed combustion.

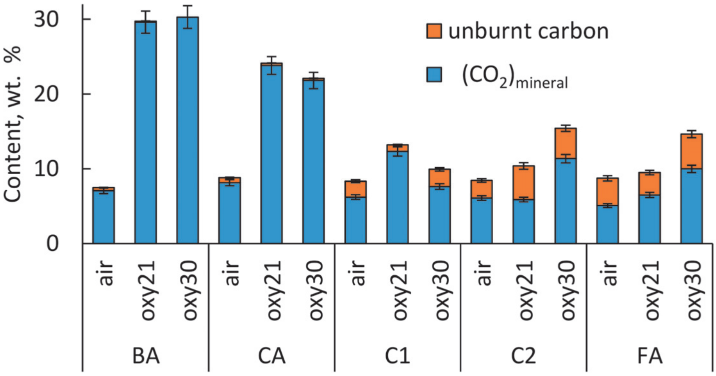

Figure 4. Mineral CO_2 ($(CO_2)_{mineral}$) and unburnt carbon content in the CFB combustion ashes.

Table 5. Chemical composition of oil shale air and oxy-fuel firing carbon free ashes, wt %. Other denotes minor components with concentrations below 0.1% as F, P_2O_5, TiO_2, MnO, SrO, ZrO_2.

Ash Flow	Combustion Mode	CaO	SiO_2	MgO	Al_2O_3	SO_3	Fe_2O_3	K_2O	Na_2O	Cl	Other
BA	Air	60.1	10.2	13.4	3.2	8.0	3.2	1.0	0.1	0.2	0.5
	OXY21	65.2	8.9	9.5	2.8	8.2	3.5	0.8	0.4	0.3	0.5
	OXY30	63.9	10.6	8.5	3.5	7.2	3.6	1.0	0.1	0.1	0.5
EHE	Air	48.7	18.9	11.4	5.8	8.0	4.1	2.1	0.1	0.2	0.6
	OXY21	51.8	18.3	9.1	5.6	8.4	3.8	1.7	0.2	0.2	0.8
	OXY30	50.3	20.2	8.7	6.2	7.2	4.3	2.2	0.1	0.1	0.8
CI	Air	30.9	35.8	5.6	10.7	5.8	4.9	4.6	0.2	0.4	1.0
	OXY21	33.9	32.7	6.7	10.1	6.5	4.7	3.9	0.3	0.3	0.9
	OXY30	28.3	38.0	5.5	11.1	5.8	5.0	4.7	0.2	0.3	1.0
CII	Air	31.1	35.7	5.6	10.6	5.8	4.9	4.6	0.2	0.5	1.0
	OXY21	28.6	36.2	5.7	11.6	6.4	4.9	4.8	0.2	0.5	1.2
	OXY30	30.9	35.8	5.5	10.5	6.1	5.1	4.2	0.2	0.5	1.3
FA	Air	29.3	36.0	5.2	11.8	5.8	4.9	5.2	0.2	0.6	1.0
	OXY21	27.7	37.0	5.1	12.1	6.1	5.1	5.2	0.2	0.5	1.1
	OXY30	28.6	37.7	5.1	11.2	5.9	5.2	4.6	0.2	0.5	1.0

To compare the influence of circulating solid matter, circulation was stopped (the airflow to EHE was stopped). The temperatures in the riser were unstable (see Figure 3). The combustion efficiency decreased (the CO level increased over the measuring range) and SO_2 concentration in flue gas increased notably (from 50 to 1500 mg/Nm^3). The ash concentration in the furnace decreased and there was not enough material to bind all the sulfur. This implies that despite the high calcium concentration in the fuel, working in a bubbling bed mode, did not ensure sufficient sulfur binding. The CFB combustion mode ensured sufficient conditions for sulfur binding, even in oxy-fuel mode.

3.2. Nitrogen Oxides Emissions

NO_x emissions remained below 200 mg/Nm^3 during all experiments (Table 4). Our experiments showed that switching to oxy-fuel combustion did not alter the NO_x emissions. The nitrogen conversion ratio to NO_x was up to 24%, similar to results from Jankowska et al. [32] with bituminous coal (20–25%). However, Pikkarainen et al. [33] measured higher nitrogen conversion ratios (28–50%). Oil shale nitrogen content remained below 0.1%. Accordingly, a high nitrogen conversion ratio to NO_x was expected (>25%) [47]. The nitrogen conversion ratio to NO_x was found to be 20–24% and the emissions were rather low.

3.3. Ashes

During the experiments, ash samples were collected from all ash flows (Figure 1). The results of chemical analysis of the ashes are displayed in Table 5. Typically for oil shale, the most abundant oxide was calcium, followed by silica, magnesium and alumina. Except for CO_2 content, chemical compositions of the ashes formed during different experiments were almost identical.

The unburnt carbon content fly ashes (0.3–4.7%) was considerably higher than in hotter ash-flows from CFB (<0.7%) (Figure 4). Together with the high CO concentration in the flue gas, it indicated re-condensation of volatiles after the coolers. Since high content of unburnt carbon in the fly ash was noticed during all the experiments, this showed that the hot zone was too short for a complete combustion of volatiles.

Mineral CO_2 content of the oxy-fuel ashes was considerably higher than in the ashes obtained in air mode (Figure 4). The difference was especially large for BA and CA. The composition and share of ash flows is different in every boiler. For oil shale CFB combustion, the share of bottom and filter ash is the largest. The BA obtained contained the most calcium and thus the effect on total CO_2 emission was considerable. Of the total carbon in the fuel, 20% was inorganic (see Table 1). It is theoretically possible to reduce the extent of decomposition of carbonate minerals to 28% in an oxy-CFB combustor firing Estonian oil shale [20]. The minimum is defined by the dolomite and sulfur content in the fuel. Limited decomposition of the carbonate minerals decreases CO_2 emissions from oil shale combustion, but increases ash production.

Oxy-fuel CFB combustion of fuels containing carbonate minerals [48–51] resulted in smaller CO_2 production due to decreased decomposition of carbonate minerals. The extent of carbonate decomposition was calculated based on the content of CaO, MgO and CO_2 in the ashes; the methodology is described more thoroughly by Arro et al. [52]. Based on the data obtained during experiments and expecting similar ash splits, such as in a utility CFB boiler [11], the average extent of carbonate minerals decomposition during regular air fired CFB experiments was 0.84, for OXY21 0.56 and OXY30 0.46. The value for utility CFB firing Estonian oil shale was 0.69 [53]. During operation in air mode, the ash calcination was more extensive than in the utility boiler, but with the oxy-fuel operation, the calcination was only partial. Figure 4 depicts that oxy-fuel ashes behaved similarly; both BA and CA contained large amounts of carbonates. The average extent of carbonate mineral decomposition of OXY30 was smaller than that of OXY21, likely because of the different thermal loads of the combustor. The measured values show that decomposition of carbonate minerals was partial, but the theoretical minimum value was not reached.

3.4. Comparison with Utility Scale

A 60 kW_{th} CFB is a relatively small device; the fuel flow rate is over 4000 times smaller than in the 250 MW_{th} utility boilers used for power production in Estonia. Nevertheless, the produced ash and flue gas are rather similar to the values obtained from industrial devices [11,53]. Pollutant emissions during experiments were also comparable to the values recorded from utility boilers (see Table 6). Emissions of nitrogen oxides were slightly higher than in utility boilers, probably due to the non-optimized secondary air inlet location. During stable CFB combustion, the sulfur oxides level in the flue gas was low. When the ash circulation was stopped (see Figure 3), the sulfur concentration in the flue gas increased to a level above typical oil shale PC boilers [45].

Table 6. Pollutant emissions from oils shale combustion, mg/Nm^3 at 6% O_2.

	SO_2	NO_x
CFB 250 MW_{th} [11]	<14	120
PC 300 MW_{th} [45]	3000	220
CFB 60 kW air	<14	141
CFB 60 kW oxy20	23	156
CFB 60 kW oxy30	<14	130

4. Conclusions

Estonian oil shale was fired in a 60 kW_{th} CFB combustor to investigate the formed flue gas and ash during air and oxy-fuel operations. The fuel was characterized by extremely high Ca-rich ash and volatiles contents. Experiments were conducted in the regular air fired CFB mode and in two different oxy-fuel modes: 21/79 O_2/CO_2 and 30/70 O_2/CO_2. The average temperature in the riser was ~740 °C; however, the temperature was 50 °C lower during the OXY21 experiment. When oxygen concentration was increased to 30%, similar temperatures as in air fired CFB were acquired. The thermal load was around 20 kW.

Produced flue gas and ash were analyzed. In air mode, the flue gas emissions for SO_2 and NO_x were <14 and 141 mg/Nm^3 @ 6% O_2, respectively; during the oxy-fuel operations, the values remained at similar levels. The chemical compositions of the oxy-fuel ashes were similar to the ashes produced in the air mode. Analysis of the collected ashes showed a decreased extent of carbonate minerals decomposition in oxy-combustion ashes. Despite decreased calcination and an apparent change in the sulfation route, there were no problems with sulfur binding. The results show that firing oil shale in an oxy-fuel circulating fluidized bed boiler could decrease CO_2 production while pollutant concentrations in the flue gas remained at a similar level compared to conventional CFB combustion. This reduces the cost of flue gas compression and further transportation and storage/utilization.

Author Contributions: L.L. is the primary author of this manuscript; the other authors participated in the experimental work, discussion and development of the ideas, and to some extent in the writing and editing of the manuscript.

Acknowledgments: This work was supported by the EU Regional Development Fund grant AR12003. The oil shale was provided by AS Viru Keemia Grupp.

Conflicts of Interest: The authors declare no conflicts of interest.

References

1. Zheng, B.; Xu, J. Carbon Capture and Storage Development Trends from a Techno-Paradigm Perspective. *Energies* **2014**, *7*, 5221–5250. [CrossRef]
2. Mathekga, H.I.; Oboirien, B.O.; North, B.C. A review of oxy-fuel combustion in fluidized bed reactors. *Int. J. Energy Res.* **2016**, *40*, 878–902. [CrossRef]

3. Stanger, R.; Wall, T.; Spörl, R.; Paneru, M.; Grathwohl, S.; Weidmann, M.; Scheffknecht, G.; McDonald, D.; Myöhänen, K.; Ritvanen, J.; Rahiala, S.; Hyppänen, T.; Mletzko, J.; et al. Oxyfuel combustion for CO_2 capture in power plants. *Int. J. Greenh. Gas Control* **2015**, *40*, 55–125. [CrossRef]
4. Anthony, E.J. Oxyfuel CFBC: Status and anticipated development. *Greenh. Gas Sci. Technol.* **2013**, *3*, 116–123. [CrossRef]
5. Scheffknecht, G.; Al-Makhadmeh, L.; Schnell, U.; Maier, J. Oxy-fuel coal combustion—A review of the current state-of-the-art. *Int. J. Greenh. Gas Control* **2011**, *5*, S16–S35. [CrossRef]
6. Neshumayev, D.; Rummel, L.; Konist, A.; Ots, A.; Parve, T. Power plant fuel consumption rate during load cycling. *Appl. Energy* **2018**, *224*, 124–135. [CrossRef]
7. Altun, N.E.; Hiçyilmaz, C.; Hwang, J.-Y.; Suat BaĞci, A.; Kök, M.V. Oil Shales in the World and Turkey; Reserves, Current Situation and Future Prospects: A Review. *Oil Shale* **2006**, *23*, 211–227.
8. Roos, I.; Soosaar, S.; Volkova, A.; Streimikene, D. Greenhouse gas emission reduction perspectives in the Baltic States in frames of EU energy and climate policy. *Renew. Sustain. Energy Rev.* **2012**, *16*, 2133–2146. [CrossRef]
9. Siirde, A. Oil Shale—Global Solution or Part of the Problem? *Oil Shale* **2008**, *25*, 201–202. [CrossRef]
10. Hotta, A.; Parkkonen, R.; Hiltunen, M.; Arro, H.; Loosaar, J.; Parve, T.; Pihu, T.; Prikk, A.; Tiikma, T. Experience of Estonian oil shale combustion based on CFB technology at Narva Power Plants. *Oil Shale* **2005**, *22*, 381–397.
11. Plamus, K.; Soosaar, S.; Ots, A.; Neshumayev, D. Firing Estonian Oil Shale of Higher Quality in CFB Boilers—Environmental and Economic Impact. *Oil Shale* **2011**, *28*, 113. [CrossRef]
12. Konist, A.; Pihu, T.; Neshumayev, D.; Külaots, I. Low Grade Fuel Oil Shale and Biomass Co-Combustion in CFB Boiler. *Oil Shale* **2013**, *30*, 294–304. [CrossRef]
13. Parve, T.; Loosaar, J.; Mahhov, M.; Konist, A. Emission of Fine Particulates from Oil Shale Fired Large Boilers. *Oil Shale* **2011**, *28*, 152–161. [CrossRef]
14. Pihu, T.; Konist, A.; Neshumayev, D.; Loo, L.; Molodtsov, A.; Valtsev, A. Full-scale tests on co-firing peat in a oil shale fired circulating fluidized bed boiler. *Oil Shale* **2017**, *34*, 250–262. [CrossRef]
15. Loo, L.; Maaten, B.; Siirde, A.; Pihu, T.; Konist, A. Experimental analysis of the combustion characteristics of Estonian oil shale in air and oxy-fuel atmospheres. *Fuel Process. Technol.* **2015**, *134*, 317–324. [CrossRef]
16. Yörük, C.; Meriste, T.; Trikkel, A.; Kuusik, R. Thermo-oxidation characteristics of oil shale and oil shale char under oxy-fuel combustion conditions. *J. Therm. Anal. Calorim.* **2015**, *121*, 509–516. [CrossRef]
17. Lei, K.; Ye, B.; Cao, J.; Zhang, R.; Liu, D. Combustion Characteristics of Single Particles from Bituminous Coal and Pine Sawdust in O_2/N_2, O_2/CO_2, and O_2/H_2O Atmospheres. *Energies* **2017**, *10*, 1695. [CrossRef]
18. Duan, L.; Sun, H.; Zhao, C.; Zhou, W.; Chen, X. Coal combustion characteristics on an oxy-fuel circulating fluidized bed combustor with warm flue gas recycle. *Fuel* **2014**, *127*, 47–51. [CrossRef]
19. Hu, G.; Dam-Johansen, K.; Wedel, S.; Peter Hansen, J. Review of the direct sulfation reaction of limestone. *Prog. Energy Combust. Sci.* **2006**, *32*, 386–407. [CrossRef]
20. Konist, A.; Loo, L.; Valtsev, A.; Maaten, B.; Siirde, A.; Neshumayev, D.; Pihu, T. Calculation of the Amount of Estonian Oil Shale Products from Combustion in Regular and Oxy-Fuel Mode in a CFB Boiler. *Oil Shale* **2014**, *31*, 211–224. [CrossRef]
21. Leckner, B.; Gómez-Barea, A. Oxy-fuel combustion in circulating fluidized bed boilers. *Appl. Energy* **2014**, *125*, 308–318. [CrossRef]
22. Rahiala, S.; Myöhänen, K.; Hyppänen, T. Modeling the behavior of limestone particles in oxy-fuel CFB processes. *Fuel* **2014**, *127*, 141–150. [CrossRef]
23. Konist, A.; Valtsev, A.; Loo, L.; Pihu, T.; Liira, M.; Kirsimäe, K. Influence of oxy-fuel combustion of Ca-rich oil shale fuel on carbonate stability and ash composition. *Fuel* **2015**, *139*, 671–677. [CrossRef]
24. Li, H.; Li, S.; Ren, Q.; Li, W.; Xu, M.; Liu, J. zhang; Lu, Q. Experimental Results for Oxy-fuel Combustion with High Oxygen Concentration in a 1MWth Pilot-scale Circulating Fluidized Bed. *Energy Procedia* **2014**, *63*, 362–371. [CrossRef]
25. Gómez, M.; Fernández, A.; Llavona, I.; Kuivalainen, R. Experiences in sulphur capture in a 30 MWth Circulating Fluidized Bed boiler under oxy-combustion conditions. *Appl. Therm. Eng.* **2014**, *65*, 617–622. [CrossRef]
26. Li, W.; Xu, M.; Li, S. Calcium sulfation characteristics at high oxygen concentration in a 1MWth pilot scale oxy-fuel circulating fluidized bed. *Fuel Process. Technol.* **2018**, *171*, 192–197. [CrossRef]

27. Glarborg, P.; Jensen, A.D.; Johnsson, J.E. Fuel nitrogen conversion in solid fuel fired systems. *Prog. Energy Combust. Sci.* **2003**, *29*, 89–113. [CrossRef]
28. Zhang, J.; Yang, Y.; Hu, X.; Dong, C.; Lu, Q.; Qin, W. Experimental Research on Heterogeneous N_2O Decomposition with Ash and Biomass Gasification Gas. *Energies* **2011**, *4*, 2027–2037. [CrossRef]
29. Mingxin, X.; Shiyuan, L.; Wei, L.; Qinggang, L. Effects of Gas Staging on the NO Emission during O_2/CO_2 Combustion with High Oxygen Concentration in Circulating Fluidized Bed. *Energy Fuels* **2015**, *29*, 3302–3311. [CrossRef]
30. Hofbauer, G.; Beisheim, T.; Dieter, H.; Scheffknecht, G. Experiences from Oxy-fuel Combustion of Bituminous Coal in a 150 kW_{th} Circulating Fluidized Bed Pilot Facility. *Energy Procedia* **2014**, *51*, 24–30. [CrossRef]
31. Duan, L.; Zhao, C.; Zhou, W.; Qu, C.; Chen, X. Effects of operation parameters on NO emission in an oxy-fired CFB combustor. *Fuel Process. Technol.* **2011**, *92*, 379–384. [CrossRef]
32. Jankowska, S.; Czakiert, T.; Krawczyk, G.; Borecki, P.; Jesionowski, Ł.; Nowak, W. The Effect of Oxygen Staging on Nitrogen Conversion in Oxy-Fuel CFB Environment. *Chem. Process Eng.* **2014**, *35*, 489–496. [CrossRef]
33. Pikkarainen, T.; Saastamoinen, J.; Saastamoinen, H.; Leino, T.; Tourunen, A. Development of 2nd Generation Oxyfuel CFB Technology—Small Scale Combustion Experiments and Model Development Under High Oxygen Concentrations. *Energy Procedia* **2014**, *63*, 372–385. [CrossRef]
34. Arro, H.; Prikk, A.; Pihu, T. Change of operation conditions of boilers heating surfaces at transition from pulverized firing of oil shale to fluidized bed technology. In Proceedings of the XXXII Kraftwerkstechnisches colloq. Nutzung Schwieriger Brennstoffe in Kraftwerken, Dresden, Germany, 24–25 October 2000.
35. James, A.K.; Thring, R.W.; Helle, S.; Ghuman, H.S. Ash Management Review—Applications of Biomass Bottom Ash. *Energies* **2012**, *5*, 3856–3873. [CrossRef]
36. Blissett, R.S.; Rowson, N.A. A review of the multi-component utilisation of coal fly ash. *Fuel* **2012**, *97*, 1–23. [CrossRef]
37. Wang, H.; Zheng, Z.-M.; Yang, L.; Liu, X.-L.; Guo, S.; Wu, S.-H. Experimental investigation on ash deposition of a bituminous coal during oxy-fuel combustion in a bench-scale fluidized bed. *Fuel Process. Technol.* **2015**, *132*, 24–30. [CrossRef]
38. Pihu, T.; Arro, H.; Prikk, A.; Rootamm, R.; Konist, A.; Kirsimäe, K.; Liira, M.; Mõtlep, R. Oil shale CFBC ash cementation properties in ash fields. *Fuel* **2012**, *93*, 172–180. [CrossRef]
39. Konist, A.; Maaten, B.; Loo, L.; Neshumayev, D.; Pihu, T. Mineral sequestration of CO2 by carbonation of Ca-rich oil shale ash in natural conditions. *Oil Shale* **2016**, *33*, 248–259. [CrossRef]
40. Loo, L.; Maaten, B.; Konist, A.; Siirde, A.; Neshumayev, D.; Pihu, T. Carbon dioxide emission factors for oxy-fuel CFBC and aqueous carbonation of the Ca-rich oil shale ash. *Energy Procedia* **2017**, *128*, 144–149. [CrossRef]
41. Markewitz, P.; Kuckshinrichs, W.; Leitner, W.; Linssen, J.; Zapp, P.; Bongartz, R.; Schreiber, A.; E. Müller, T. Worldwide innovations in the development of carbon capture technologies and the utilization of CO_2. *Energy Environ. Sci.* **2012**, *5*, 7281–7305. [CrossRef]
42. Mattila, H.-P.; Zevenhoven, R. Production of Precipitated Calcium Carbonate from Steel Converter Slag and Other Calcium-Containing Industrial Wastes and Residues. *Adv. Inorg. Chem.* **2014**, *66*, 347–384.
43. Shogenov, K.; Shogenova, A.; Vizika-Kavvadias, O.; Nauroy, J.-F. Reservoir quality and petrophysical properties of Cambrian sandstones and their changes during the experimental modelling of CO_2 storage in the Baltic Basin. *Estonian J. Earth Sci.* **2015**, *64*, 199–217. [CrossRef]
44. Shogenova, A.; Shogenov, K.; Vaher, R.; Ivask, J.; Sliaupa, S.; Vangkilde-Pedersen, T.; Uibu, M.; Kuusik, R. CO_2 geological storage capacity analysis in Estonia and neighbouring regions. *Energy Procedia* **2011**, *4*, 2785–2792. [CrossRef]
45. Konist, A.; Pihu, T.; Neshumayev, D.; Siirde, A. Oil Shale Pulverized Firing: Boiler Efficiency, Ash Balance and Flue Gas Composition. *Oil Shale* **2013**, *30*, 6–18. [CrossRef]
46. Wall, T.F. Combustion processes for carbon capture. *Proc. Combust. Inst.* **2007**, *31*, 31–47. [CrossRef]
47. Wartha, C.; Reisinger, K.; Winter, F.; Gogolek, P.; Hofbauer, H. The importance of NO Formation Characteristics for the Prediction of NO—Emissions from Grade and Fluidized Bed Combustors. In Proceedings of the 4th International Conference on Technologies and Combustion for a Clean Environment, Lisbon, Portugal, 7–10 July 1997.

48. Kolovos, N.; Georgakopoulos, A.; Filippidis, A.; Kavouridis, C. Utilization of Lignite Reserves and Simultaneous Improvement of Dust Emissions and Operation Efficiency of a Power Plant by Controlling the Calcium (Total and Free) Content of the Fed Lignite. Application on the Agios Dimitrios Power Plant, Ptolemais, Greece. *Energy Fuels* **2002**, *16*, 1516–1522. [CrossRef]
49. Fernandez-Turiel, J.-L.; Georgakopoulos, A.; Gimeno, D.; Papastergios, G.; Kolovos, N. Ash Deposition in a Pulverized Coal-Fired Power Plant after High-Calcium Lignite Combustion. *Energy Fuels* **2004**, *18*, 1512–1518. [CrossRef]
50. Gorewoda, J.; Scherer, V. Influence of Carbonate Decomposition on Normal Spectral Radiative Emittance in the Context of Oxyfuel Combustion. *Energy Fuels* **2016**, *30*, 9752–9760. [CrossRef]
51. Dai, B.-Q.; Wu, X.; De Girolamo, A.; Zhang, L. Inhibition of lignite ash slagging and fouling upon the use of a silica-based additive in an industrial pulverised coal-fired boiler. Part 1. Changes on the properties of ash deposits along the furnace. *Fuel* **2015**, *139*, 720–732. [CrossRef]
52. Arro, H.; Prikk, A.; Pihu, T. Calculation of CO_2 Emission from CFB Boilers of Oil Shale Power Plants. *Oil Shale* **2006**, *23*, 356–365.
53. Plamus, K.; Ots, A.; Pihu, T.; Neshumayev, D. Firing Estonian Oil Shale in CFB Boilers—Ash Balance and Behaviour of Carbonate Minerals. *Oil Shale* **2011**, *28*, 58–67. [CrossRef]

Paper V

Lauri Loo, Birgit Maaten, Alar Konist, Andres Siirde, Dmitri Neshumayev, Tõnu Pihu. "Carbon dioxide emission factors for oxy-fuel CFBC and aqueous carbonation of the Ca-rich oil shale ash" Energy Procedia 128 (International Scientific Conference "Environmental and Climate Technologies", CONECT 2017, 10-12 May 2017, Riga, Latvia): 144–149. doi:10.1016/j.egypro.2017.09.034

Available online at www.sciencedirect.com

ScienceDirect

Energy Procedia 128 (2017) 144–149

Energy Procedia

www.elsevier.com/locate/procedia

International Scientific Conference “Environmental and Climate Technologies”, CONECT 2017, 10–12 May 2017, Riga, Latvia

Carbon dioxide emission factors for oxy-fuel CFBC and aqueous carbonation of the Ca-rich oil shale ash

Lauri Loo*, Birgit Maaten, Alar Konist, Andres Siirde, Dmitri Neshumayev, Tonu Pihu

Department of Energy Technology, Tallinn University of Technology, Ehitajate tee 5, Tallinn 19086, Estonia

---

Abstract

Oil shale (OS) is a low-calorific-value fossil fuel. Today, Estonia’s OS usage is the largest in the world. Approximately 76 % of the electricity is produced from Ca-rich OS. Yearly, approximately 12 million tons of OS is used for power generation utilizing pulverized combustion (PC) and circulating fluidized bed combustion (CFBC) technologies that produce nearly 6 million tons of Ca-rich ash. Estonian kukersite OS consists about one third of carbonate minerals, mainly calcite. Therefore, in addition to the combustion of organic carbon, the carbonaceous minerals decompose and release additional CO_2. The extent of decomposition of carbonaceous minerals depends on combustion technology. Using oxy-fuel CFBC technology alters ash properties, including decomposition of carbonate minerals. By means of aqueous carbonation of Ca-rich ash, CO_2 can be stored safely and leakage-free for very long time.

In order to understand the changing CO_2 sequestration potential, oil shale ashes were produced at a 60 kW_{th} CFBC facility in oxy-fuel mode. The ash was treated with water and CO_2 in order to mimic the ash treatment technology currently in use in the industry. The ash bound 81 kg_{CO2}/t_{ash} it means that 6 % of the CO_2 emitted would be bound at the ash fields. Due to decreased decomposition of carbonates, when using oxy-fuel CFBC, the CO_2 specific emission of combustion would decrease by 5 % compared to regular CFBC and 19 % compared to PF. Decreased CO_2 production would result in reduced CO_2 transportation and further utilization or storage cost.

Peer review statement - Peer-review under responsibility of the scientific committee of the International Scientific Conference “Environmental and Climate Technologies”.

Keywords: oxy-fuel combustion; CO_2 mineral sequestration; CO_2 specific emissions; carbon capture and utilization; carbon capture and storage

---

* Corresponding author. Tel.: +372-6203907.
E-mail address: lauri.loo@ttu.ee

Peer review statement - Peer-review under responsibility of the scientific committee of the International Scientific Conference “Environmental and Climate Technologies”.
10.1016/j.egypro.2017.09.034

1. Introduction

Significant reductions in greenhouse gas emissions are required to slow down global climate change. More than 76 % of Estonia's electricity is produced from OS [1, 2]. OS is a solid fuel with a low heating value (8.0–9.2 MJ/kg) and a high ash content (43–53 %). Estonian kukersite OS consists for about one third of carbonate minerals, mainly calcite. During OS combustion, a considerable amount of CO_2 is produced due to the decomposition of carbonate minerals. Therefore, in addition to the combustion of organic carbon, the carbonaceous minerals decompose and release additional CO_2. OS can be utilized for energy production via pyrolysis or direct combustion. In Estonia annually 6 Mt of OS are used for shale oil production [3, 4] and 12 Mt of OS are used for power generation. Pulverized combustion [5] and circulating fluidized bed combustion technologies are in use. Implementation of CFBC has decreased environmental impact of OS combustion [6, 7], but even further decrease of CO_2 emissions is required [8]. Oxy-fuel technology promises a further decrease of environmental impact.

Oxy-fuel combustion technology is considered as one of the most promising CO_2 capture technologies [9–11] and the ash produced during oxy-fuel operation is used in this study as a starting material. The technology involves combustion of fuel in a recycled flue gas, where oxygen is added to maintain combustion. Our previous calculations and experiments [12, 13] with a laboratory scale fluidized bed reactor showed a considerable decrease of carbonaceous minerals decomposition in oxy-fuel environment. This means that CO_2 emissions decrease, but the production of the ash increases.

Vast amounts of calcium rich ash forms during OS combustion – more than 6 Mt annually [14]. Depending on the combustion technology, the ash contains up to 30 % free Ca–Mg oxides. To date more than 90 % of the OS ash hydraulically deposited [15]. Anthony et al. [16] have found that CFBC ashes exhibit considerable chemical activity which can continue for more than a year. Uibu et al. [17, 18] have studied the natural chemical processes takin place during OS hydraulic deposition. In the ash field OS CFBC ashes cement and bound approximately 8 % of the emitted CO_2 [14].

In this study, we provide CO_2 emissions from OS oxy-fuel CFBC. The analysis is based on the ashes obtained from oxy-fuel CFBC experiment in TUT. Hydraulic deposition of OS ashes were simulated and CO_2 sequestrated and emitted during the processes were calculated.

Nomenclature

q_{co_2os}	Specific emission of CO_2 for OS combustion, t_{CO2}/TJ
k_{co_2}	Extent of carbonate decomposition
ΔCO_2	The amount of CO_2 absorbed from the atmosphere, (t_{CO2}/t_{ash})
$CO_2^{treated}$	Treated ash CO_2 content, %
CO_2^{ash}	Ash CO_2 content, %
CaO^{ash}	Ash CaO content, %
M_c	Molar mass of C, 12.01 g/mol.
M_{CO_2}	Molar mass of CO_2, 44.01 g/mol.
M_{CaO}	Molar mass of CaO, 56.08 g/mol.
M_{MgO}	Molar mass of MgO, 40.30 g/mol.
TOC	Total organic carbon content, %

2. Materials and methods

2.1. Materials – oil shale and produced ash

The ashes used in the study were produced at a 60 kW_{th} CFBC test facility in Tallinn University of Technology (Fig. 1). The combustor was designed to work with oil shale, but can also handle other fuels with low calorific value. The test facility could work with regular air and with pre-set gas mixtures. The combustion process was observed at 16 points with thermal sensors and the gas composition was analyzed with FTIR analyzer.

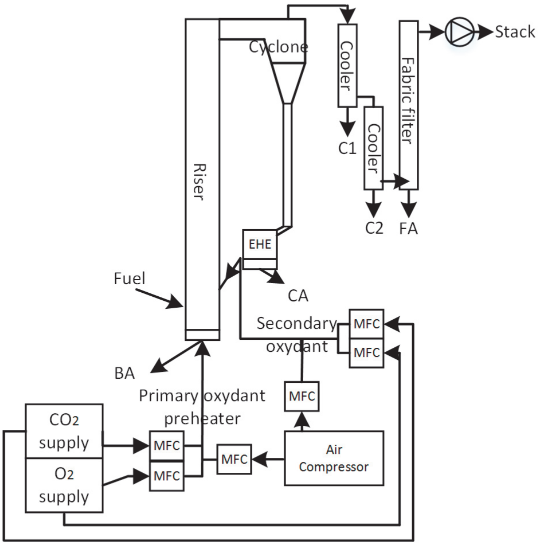

Fig. 1. Scheme of the 60 kW circulating fluidized bed (CFBC) test facility in TUT.

Ash samples were collected from 5 points. The ashes were formed during 20 % O_2 and 80 % CO_2 oxy-fuel mode and were collected from different points: bottom ash (BA), cyclone ash (CA), cooler one ash (C1), cooler two ash (C2) and filter ash (FA). The proximate and ultimate analysis results of the OS used during combustion experiments are shown in Table 1. The chemical composition of the produced ashes (Table 2) were measured with Wavelength Dispersive X-ray Fluorescence Spectrometer and Elemental Analyzer. The ashes have typically high content of calcium. OS ashes still contain carbonate minerals due to increased CO_2 partial pressure and low combustion temperature (800 °C).

Table 1. Proximate and ultimate analysis of the oil shale.

LHV, MJ/kg	Proximate analysis, wt. %				Ultimate analysis, wt. %					
Q_{net}	W_{ar}	VM_{ar}	FC_{ar}	A_{ar}	C	H	N	S	TOC	$(CO2)_{mineral}$
8.56	0.50	47.5	1.3	50.7	27.4	2.7	0.1	1.6	21.8	20.6

Table 2. Chemical composition of the oil shale ashes produced in CFBC in the oxy-fuel mode, %-wt.

Sampling point	CaO	CO_2	SO_3	MgO	Fe_2O_3	Al_2O_3	SiO_2	K_2O	Na_2O	Cl	P_2O_5	Rest
BA	44.3	29.6	6.1	7.6	2.1	2.2	6.8	0.6	0.4	0.2	0.1	0.2
CA	37.7	23.8	6.6	7.7	2.5	4.6	14.8	1.3	0.2	0.2	0.1	0.4
C1	28.8	12.3	5.7	6.1	3.9	9.1	29.2	3.4	0.3	0.3	0.2	0.5
C2	24.7	9.7	5.7	5.2	4.1	10.6	32.8	4.2	0.2	0.4	0.2	2.2
FA	24.4	8.7	5.35	4.53	4.54	10.6	32.6	4.6	0.2	0.4	0.2	3.9

A boiler is a complex reactor and solid separator. Typically, ash is extracted from several points. The ash properties and quantities differ. The ash split of experimental facility was assumed to be similar with an industrial CFBC. Plamus et al. [19] measured ash flows of OS CFBC and found that 37.4 % is bottom ash (BA), 6.9 % is removed from super- and re-heaters, 2.0 % from economizer and preheater, and the largest ash flow, 53.7 %, is removed from the filters. Similar ash split was assumed for TUT CFBC.

2.2. Methods – experiments

In order to simulate natural carbonization of calcium-rich ash on an ash field, accelerated carbonation of OS ashes was simulated in laboratory. Oxy-fuel CFBC oil shale ashes were mixed with distilled water with a solid to liquid ratio of 1/10. The solution pH increased rapidly to 12. To accelerate the natural carbonization process CO_2 was bubbled through the mixture. The solution pH was observed and kept slightly over 7.0. After half an hour the CO_2 flow was stopped, if the pH increased the experiment was continued, otherwise the solids were separated via filtering and dried at 105 °C overnight. Mineral CO_2 amount was measured in the samples with elemental analyzer using the total inorganic carbon module.

2.3. Interpretation of the analysis results

Specific emission of CO_2 (q_{co_2os}) for OS combustion is calculated using the following formula:

$$q_{CO_2OS} = \frac{\left[TOC * \frac{M_{CO_2}}{M_C} + k_{CO_2} * (CO_2)_{\min eral}\right]}{Q_{net}}, tCO_2 / TJ \tag{1}$$

The extent of carbonate decomposition (2) is calculated based on the content of CaO, MgO and CO_2 in the ashes. Arro et al. [20] found that the carbonaceous part of the Estonian OS contains on average 99.2 % of all CaO in OS, and 96.7 % of all MgO, therefore the constants are in Eq. (2).

$$k_{CO_2} = 1 - \frac{CO_2^{ash}}{0.967 * \frac{M_{CO_2}}{M_{MgO}} * MgO^{ash} + 0.992 * \frac{M_{CO_2}}{M_{CaO}} * CaO^{ash}} \tag{2}$$

If the OS ash is deposited using hydraulic deposition technology, the ash sequestrates some CO_2 from atmosphere. The amount of CO_2 absorbed from the atmosphere (ΔCO_2) during wet treatment is calculated similarly to Konist et al. [14] based on the mineral CO_2 content in the ashes (CO_2^{ash}) and in the wet treated ashes ($CO_2^{treated}$) (Eq. (3)):

$$\Delta CO_2 = \frac{CO_2^{treated} - CO_2^{ash}}{100 - CO_2^{treated} + CO_2^{ash}}, \text{ t CO}_2\text{/ t ash} \tag{3}$$

3. Results and discussion

The results of experiments are shown in Table 3. The CO_2 content in all the ashes increased. The finest filter ash bound the most CO_2 and the largest particles showed the smallest CO_2 uptake.

Table 3. CO_2 sequestrated during simulated hydraulic transportation and landfilling.

	BA	CA	C1	C2	FA	AVERAGE
CO_2, %	29.0	23.8	12.3	5.9	8.7	16.1
CO_2 after wet treatment, %	31.3	26.3	15.6	18.8	11.7	23.4
CO_2 absorbed from the atmosphere, ΔCO_2, t CO_2/t ash	0.024	0.026	0.034	0.148	0.031	0.079

Based on the CFBC oxy-fuel ash analysis and assumed ash split, the extent of carbonate decomposition was calculated (Table 4). Based on those results specific emission of CO_2 for OS CFBC oxy-fuel combustion was calculated. Compared to PC and CFBC the CO_2 output decreases 20 % and 5 %, respectively. The flue gas from CFBC and PC contains up to 20 % CO_2, but the oxy-fuel combustion residue contains up to 95 % CO_2. This eases reuse or/and transportation of the greenhouse gas.

Table 4. Oxy-fuel CFBC combustion emissions compared to CFBC [19] and PC [5].

		Oxy-CFBC	CFBC	PC
Extent of carbonate decomposition (1)	k_{CO_2}	0.46	0.69	0.95
CO_2 absorbed from the atmosphere (t CO_2/TJ)	ΔCO_2	5.5	7.8	4.7
Specific emission of CO_2 for OS combustion (t CO_2/TJ)	q_{CO2}	100.0	106.7	122.4
Specific emission of CO_2 for OS combustion + landfilling (t CO_2/TJ)		94.6	98.9	117.7
Specific emission of CO_2 for OS combustion + landfilling compared to PC (%)		80	84	100

Compared to regular CFBC, the oxy-fuel combustion system has some extra energy consumption: concentrated flow of oxygen is required, part of the flue gas has to be recycled and the flue gas is usually compressed for further processing. Escudero et al. [21] have modeled oxy-fuel CFBC power unit. According to the study, net electric efficiency of a new CFBC is 43 % and new oxy-fuel CFBC is 36 %. Based on their results specific emissions of CO_2 for oxy-fuel CFBC power production from OS is 942 kg CO_2/MWh_e. The value for CFBC is 819 kg CO_2/MWh_e, so 11 % more CO_2 per MWh_e is produced when applying oxy-fuel combustion rather than regular CFBC.

Oxy-fuel combustion simplifies CO_2 transportation and utilization. If the CO_2 produced is stored without extra cost, maximum 54 kg CO_2/MWh_e can be removed from atmosphere. The concentrated CO_2 flow could be used for precipitated calcium carbonate production. Zevenhoven et al. [22–24] have developed so-called slag2PCC technology to produce precipitated calcium carbonate from calcium-rich steel plants slags. By the means of producing PCC, CO_2 can be stored safely and leakage-free for a very long time, and at the same time a valuable product is produced.

4. Conclusions

Oxy-fuel CFBC ashes were treated with water and CO_2 to simulate hydraulic landfilling. During the process, the ashes bound on average 0.081 t_{CO2}/t_{ash}. Applying oxy-fuel CFBC technology decreases specific emission of CO_2 for OS combustion 20 % compared to PC and 5 % compared to CFBC. Then taking account all the extra energy requirements for oxy-fuel combustion (oxygen production and flue gas compression) the specific CO_2 emission for power production from OS is 942 kg CO_2/MWh_e, that is 12 % more than for regular CFBC. The flue gas of oxy-fuel combustion is concentrated flow of CO_2. This decreases cost of utilising the CO_2 for example to produce precipitated calcium carbonate.

References

[1] Siirde A. Oil Shale - Global Solution or Part of the Problem? Oil Shale 2008;25:201–202.

[2] FE032: Capacity and production of power plants, Est. Stat. (2017). Available: www.stat.ee

[3] Gusca J, Siirde A, Eldermann M, Energy Related Sustainability Analysis of Shale Oil Retorting Technologies. Energy Procedia 2015;72:216 – 221.

[4] Eldermann M, Siirde A, Gusca J. Prospects for Hydrogen Production in Oil Shale Processing Industry in Estonia: Initial Aspects of Life Cycle Analysis. Energy Procedia 2016;95:536–539.

[5] Konist A, Pihu T, Neshumayev D, Siirde A. Oil Shale Pulverized Firing: Boiler Efficiency, Ash Balance and Flue Gas Composition. Oil Shale 2013;30:6–18.

[6] Hotta A, Parkkonen R, Hiltunen M, Arro H, Loosaar J, Parve T, Pihu T, Prikk A, Tiikma T. Experience of Estonian oil shale combustion based on CFB technology at Narva Power Plants. Oil Shale 2005;22:381–397.

[7] Loosaar J, Parve T, Konist A. Environmental Impact of Estonian Oil Shale CFB Firing, in: Proc. 20th Int. Conf. Fluid. Bed Combust. Berlin: Springer; 2009.

[8] Eldermann M, Siirde A, Gusca J. Decarbonisation of Estonian Oil Shale Industry: Framework and Categories Definition. Energy Procedia 113;2017:77–81.

[9] Mathekga HI, Oboirien BO, North BC. A review of oxy-fuel combustion in fluidized bed reactors. Int. J. Energy Res. 2016;40:878–902.

[10] Stanger R, Wall T, Sporl R, Paneru M, Grathwohl S, Weidmann M, Scheffknecht G, McDonald D, Myohanen K, Ritvanen J, Rahiala S, Hyppanen T, Mletzko J, Kather A, Santos S. Oxyfuel combustion for CO2 capture in power plants. Int. J. Greenh. Gas Control 2015;4055–125.

[11] Anthony EJ. Oxyfuel CFBC: status and anticipated development, Greenh. Gases Sci. Technol. 2013;3:116–123.

[12] Konist A, Valtsev A, Loo L, Pihu T, Liira M, Kirsimae K. Influence of oxy-fuel combustion of Ca-rich oil shale fuel on carbonate stability and ash composition. Fuel 2015;139:671–677.

[13] Konist A, Loo L, Valtsev A, Maaten B, Siirde A, Neshumayev D, Pihu T. Calculation of the Amount of Estonian Oil Shale Products from Combustion in Regular and Oxy-Fuel Mode in a CFB Boiler. Oil Shale. 2014;31:211–224.

[14] Konist A, Maaten B, Loo L, Neshumayev D, Pihu T. Mineral sequestration of CO2 by carbonation of Ca-rich oil shale ash in natural conditions. Oil Shale 2016;33:248–259.

[15] Pihu T, Arro H, Prikk A, Rootamm R, Konist A, Kirsimae K, Liira M, Motlep R. Oil shale CFBC ash cementation properties in ash fields. Fuel 2012;93:172–180.

[16] Anthony EJ, Bulewicz EM, Dudek K, Kozak A. The long term behaviour of CFBC ash–water systems. Waste Manag. 2002;22:99–111.

[17] Uibu M, Uus M, Kuusik R. CO2 mineral sequestration in oil-shale wastes from Estonian power production. J. Environ. Manage. 2009;90:1253–1260.

[18] Uibu M, Kuusik R, Veskimae H. Seasonal Binding of Atmospheric CO2 by Oil Shale Ash. Oil Shale 2008;25:254–266.

[19] Plamus K, Ots A, Pihu T, Neshumayev D. Firing Estonian Oil Shale in CFB Boilers - Ash Balance and Behaviour of Carbonate Minerals. Oil Shale 2011;28:58–67.

[20] Arro H, Prikk A, Pihu T. Calculation of CO2 Emission from CFB Boilers of Oil Shale Power Plants. Oil Shale 2006;23:356–365.

[21] Escudero AI, Espatolero S, Romeo LM, Lara Y, Paufique C, Lesort AL, Liszka M. Minimization of CO2 capture energy penalty in second generation oxy-fuel power plants. Appl. Therm. Eng. 2016;103:274–281.

[22] Said A, Mattila HP, Jarvinen M, Zevenhoven R. Production of precipitated calcium carbonate (PCC) from steelmaking slag for fixation of CO2. Appl. Energy 2013;112:765–771.

[23] Eloneva S, Said A, Fogelholm CJ, Zevenhoven R. Preliminary assessment of a method utilizing carbon dioxide and steelmaking slags to produce precipitated calcium carbonate. Appl. Energy 2012;90:329–334.

[24] Mattila HP, Hudd H, Zevenhoven R. Cradle-to-gate life cycle assessment of precipitated calcium carbonate production from steel converter slag. J. Clean. Prod. 2014;84:611–618.

Curriculum vitae

Personal data

Name	Lauri Loo
Date of birth	13.03.1989
Place of birth	Estonia
Citizenship	Estonian

Contact data

E-mail	lauri.loo@ttu.ee

Education

2014–2018	Tallinn University of Technology – PhD
2012–2014	Tallinn University of Technology – MSc *cum laude* in thermal engineering
2008–2012	Tallinn University of Technology – BSc in thermal engineering
2005–2008	Viljandi C. R. Jakobson Gymnasium – high school

Language competence

Estonian	Native speaker
English	Fluent

Professional employment

01.09.2017–	Tallinn University of Technology, School of Engineering, Department of Energy Technology, early stage researcher
01.01.2017–31.08.2017	Tallinn University of Technology, School of Engineering, Department of Energy Technology, researcher
01.09.2014–31.12.2016	Tallinn University of Technology, Faculty of Mechanical Engineering, Department of Thermal Engineering, researcher
01.02.2012–31.08.2014	Tallinn University of Technology, Faculty of Mechanical Engineering, Department of Thermal Engineering, engineer

Elulookirjeldus

Isikuandmed

Nimi	Lauri Loo
Sünniaeg	13.03.1989
Sünnikoht	Eesti
Kodakondsus	Eesti

Kontaktandmed

E-post:	lauri.loo@ttu.ee

Hariduskäik

2014–2018	Tallinna Tehnikaülikool, mehhanotehnika – PhD
2012–2014	Tallinna Tehnikaülikool, soojusenergeetika – MSc (*cum laude)*
2008–2012	Tallinna Tehnikaülikool, soojusenergeetika – BSc
2005–2008	Viljandi C. R. Jakobsoni nimeline gümnaasium – keskharidus

Keelteoskus

Eesti keel	kõrgtase
Inglise keel	kõrgtase

Teenistuskäik

01.09.2017–	Tallinna Tehnikaülikool, Inseneriteaduskond, Energiatehnoloogia instituut, doktorant-nooremteadur
01.01.2017–31.08.2017	Tallinna Tehnikaülikool, Inseneriteaduskond, Energiatehnoloogia instituut, teadur
01.09.2014–31.12.2016	Tallinna Tehnikaülikool, Mehaanikateaduskond, Soojustehnika instituut, teadur
01.02.2012–31.08.2014	Tallinna Tehnikaülikool, Mehaanikateaduskond, Soojustehnika instituut, insener